MASTERARBEIT | MASTER'S THESIS

Titel | Title

Insights into hERG Channel Activators: A Literature Research on the Structure and Function

verfasst von | submitted by

Jovana Lazic BSc

angestrebter akademischer Grad | in partial fulfilment of the requirements for the degree of

Magistra pharmaciae (Mag. pharm.)

Wien | Vienna, 2024

Studienkennzahl lt. Studienblatt | Degree programme code as it appears on the student record sheet:	UA 066 605
Studienrichtung lt. Studienblatt | Degree programme as it appears on the student record sheet:	Masterstudium Pharmazie
Betreut von | Supervisor:	Assoz. Prof. Mag. Dr. Anna Weinzinger Privatdoz.

Abstract

The human Ether-a-go-go-Related Gene (hERG) potassium channel plays a crucial role in cardiac repolarization. Dysfunction of this channel can lead to severe cardiac arrhythmias, particularly Long QT Syndrome (LQTS), which is associated with an increased risk of torsades de pointes and sudden cardiac death. The high sensitivity of hERG channels to pharmacological inhibition poses a significant challenge in drug development and safety.

This thesis examines the structure, function and modulation of hERG channels with a particular focus on channel activators as potential therapeutic agents. It studies cryo-electron microscopy to elucidate the structural basis of hERG channel function and drug interactions. Additionally, docking was utilized to investigate the binding modes of various activators.

This research reveals the complex nature of hERG channel gating and the diverse mechanisms by which activators modulate channel function. There are several classes of activators, each with distinct effects on channel kinetics and voltage-dependence. The structural analysis provides insights into the molecular determinants of drug binding and channel modulation.

While computational studies offer valuable insights into activator binding, they also highlight the limitations of static docking approaches in fully capturing the dynamic nature of channel-drug interactions. This underscores the need for more advanced simulation techniques to accurately model the conformational changes associated with channel gating and drug binding.

The study emphasizes the importance of integrating structural, functional and computational approaches in understanding ion channel modulation and drug development.

Deutsche Zusammenfassung

Der humane Ether-a-go-go-Related Gene (hERG) Kaliumkanal spielt eine entscheidende Rolle bei der kardialen Repolarisation. Eine Fehlfunktion dieses Kanals kann zu schweren Herzrhythmusstörungen führen, insbesondere zum Long-QT-Syndrome (LQTS), das mit einem erhöhten Risiko für Torsades de Pointes und plötzlichen Herztod verbunden ist. Die hohe Empfindlichkeit der hERG-Kanäle gegenüber pharmakologischer Inhibition stellt eine bedeutende Herausforderung in der Arzneimittelentwicklung und Arzneimittelsicherheit dar.

Diese Masterarbeit untersucht die Struktur, Funktion und Modulation von hERG-Kanälen, mit besonderem Fokus auf Kanalaktivatoren als potentielle therapeutische Wirkstoffe. Hierfür wurden Strukturen verwendet, die durch Kryo-Elektronenmikroskopie entstanden sind, um die strukturelle Grundlage der hERG-Kanalfunktion und Wechselwirkungen mit Arzneistoffen aufzuklären. Mit der Unterstützung von Docking wurden die Bindungsmodi verschiedener Aktivatoren untersucht.

Die Forschung zeigt die komplexe Natur der hERG-Kanalschaltung und die vielfältigen Mechanismen, durch die Aktivatoren die Kanalfunktion modulieren. Es wurden mehrere Klassen von Aktivatoren, jede mit unterschiedlichen Auswirkungen auf die Kanalkinetik und Spannungsabhängigkeit, untersucht. Die Strukturanalyse liefert Einblicke in die molekularen Determinanten der Arzneistoffbindung und Kanalmodulation.

Während Computerstudien wertvolle Einblicke in die Aktivatorbindung bieten, zeigen sie auch die Grenzen statischer Docking-Ansätze auf, die dynamische Natur der Kanal-Arzneistoff-Interaktionen vollständig erfassen. Dies unterstreicht die Notwendigkeit fortgeschrittener Simulationstechniken, um die mit der Kanalschaltung und Arzneistoffbindung verbundenen Konformationsänderungen genau zu modellieren.

Diese Studie trägt zum wachsenden Wissensstand über die hERG-Kanal-Pharmakologie bei und betont die Bedeutung der Integration struktureller, funktioneller und computergeschützter Ansätze zum Verständnis der Ionenkanalmodulation und Arzneimittelentwicklung.

Acknowledgement

With profound gratitude, I would first like to express my sincerest thanks to my parents. Their unwavering support and belief in me were the cornerstone of my success. In the darkest hours, when doubt and uncertainty threatened to overwhelm me, they encouraged me and gave me the strength to carry on. Their unconditional love and trust in my abilities have always inspired me to surpass myself.

I would also like to thank my boyfriend for his constant support encouraging words, even when things did not always go smoothly. His understanding and patience, especially throughout this final phase of my studies, have been invaluable.

Special thanks go to my fellow students who have become lifelong friends throughout this academic adventure. Our shared experiences – from the heights of success to the depths of challenges – have forged an inseparable bond between us. It is an indescribable comfort to have compansions who endure the same struggles and offer unwavering support during difficult times.

With great appreciation, I would like to thank my mentor, Dr. Eva-Maria Plessl, BSc. MSc. Her tireless patience, constant availability for questions, and willingness to assist were crucial to my progress. I am particularly grateful for her expertise in various computer programs, which she generously shared, significantly enriched my work.

Last but certainly not least, my sincere gratitude goes to Ass.-Prof. Mag. Dr. Anna Weinzinger. Her decision to give me the opportunity to write my master's thesis in her department laid the foundation for this important phase of my academic career. Her continuous support and understanding were a constant source of motivation and progress.

This journey would not have been possible without the support, wisdom and encouragement of all these remarkable people. Their contributions to my personal and academic growth will forever be treasured in my heart.

Table of content

1 Introduction 1

1.1 Definition of hERG-Channel 1

1.2 Overview of the history 2

2 Structure of the hERG channel and gating 4

2.1 Molecular structure 4

2.1.1 Voltage-sensor domain 4

2.1.2 The Pore 6

2.1.3 Cytosolic N- and C-terminal domains 7

2.2 Gating 9

2.2.1 Activation 11

2.2.2 Inactivation 11

2.2.3 Deactivation 12

3 Biogenesis and Trafficking of hERG channel 14

4 Functional role and significance of hERG 16

4.1 Role in cardiac action potential 16

4.2 Arrhythmia Mechanisms and Long QT Syndrome 18

4.2.1 Inherited LQTS 19

4.2.2 Acquired LQTS 20

5 Pharmacology of the hERG-channel 23

5.1 Classification of hERG Agonists 24

5.2 Overview of hERG activators and their characteristics 26

5.2.1 RPR260243 26

5.2.2 Ginsenoside Rg3 31

5.2.3 LUF7346 37

5.2.4 ICA-105574 40

5.2.5 AZSMO-23 43

5.2.6 Mallotoxin 45
5.2.7 SKF-32802 48
5.2.8 KB130015 50
5.2.9 SB335573 52
5.2.10 PD-118057 52
5.3 Multiple mechanism 56
6 Structural Insights from Cryo-EM Studies 59
7 Cavity-Binding Activators of hERG 73
8 Discussion 85
9 List of Figures 87
10 Bibliography 93

1 Introduction

1.1 Definition of hERG-Channel

The hERG-channel stands for the abbreviation “human-Ether-a-go-go-Related Gene” channel and assumes an important part in the function of the heart. Although hERG is primarily found in cardiac muscle cells, its presence extends beyond the cardiovascular system. hERG channels have also been detected in neurons, tumor cells, smooth muscle cells, pancreatic beta cells and chromaffin cells (1). It is a part of the ether-a-go-go family of the voltage-gated potassium channel (VGK). This family divides into three subfamilies which are: ether-a-go-go Kv10, ether-a-go-go-related Kv11 and ether-a-go-go-similar Kv12 (Figure 1). The hERG-channel belongs to the Kv11 family. Furthermore, there are subclassification as Kv11.1 (hERG1), Kv11.2 (hERG2) and Kv11.3 (hERG3). hERG2 (KCNH6) and hERG3 (KCNH7) are expressed in the nervous system. This master thesis focuses on hERG1 because it is primarily expressed in the heart, where it plays a crucial role in cardiac repolarization (2) (3).

Voltage-gated potassium channels can be called by different names, such as $I_{Kr,}$ hERG or Kv11.1, depending on the context in which they are discussed. First, I_{Kr} is used to denote the native channel. Second, the term hERG specifically applies to the channel protein. Third, Kv11.1 is used when discussing fully assembled channels studied in heterologous expression systems. KCNH2 refers to the mRNA and serves as the official name for the human ether-a-go-go related gene (4).

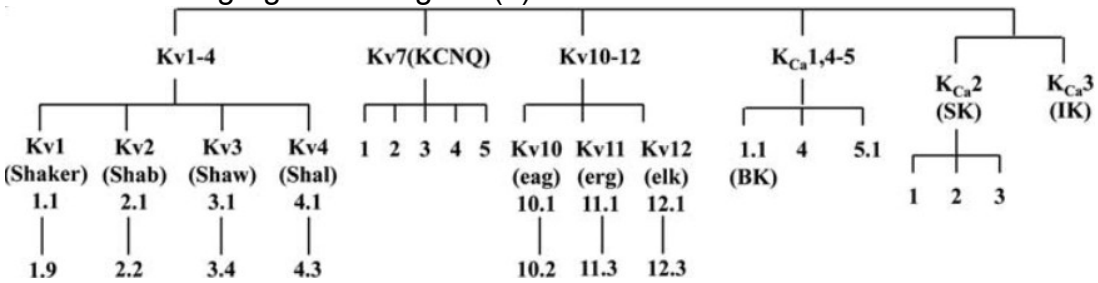

Figure 1: Overview of the classification of voltage-gated potassium channels (5)

1.2 Overview of the history

Two scientist, Hodgkin and Huxley, laid the foundation for understanding the action potential around 1950. They conducted their research using the giant axons of squid, which allowed them to explore how the excitable properties of tissues are linked to the coordinated movement of sodium and potassium ions. Today this phenomenon is called ion channels (6).

The “Shaker” potassium channel was the first to be investigated and classified. It was originally found in Drosophila melanogaster by Jan and Jan in 1987 (7). This discovery led to the identification of a large family of voltage-gated potassium (K_v) channels with similar structure and function, known as the Shaker family (4).

Two more scientist, Kaplan and Trout, found contradictions about this investigations. In the 1960 they observed that the legs of mutant Drosophila flies shake under ether anesthesia (8). Therefore they thought that this shaking is resembled the movements of Go-Go-dancers from the 1960s, leading them to coin the term “ether-a-go-go” in 1969 (4).

Noble and Tsien made another crucial discovery by identifying and characterizing the delayed rectifier K^+ current (IK) in sheep cardiac Purkinje fibers. Subsequent research revealed that I_K comprises two distinct components: I_{Kr} (rapid) and I_{Ks} (slow), each with unique properties. This finding was later confirmed in cardiac cells from guinea pigs, dogs and chickens (9).

Building on this early work, Warmke and Ganetzky made a significant discovery in 1994. They investigated a human hippocampus cDNA library using a mouse gene as a reference and compared the sequences. Their investigation showed that many genes have a similarity with eag and elk (ether-a-go-go-like). The researchers concluded that hERG is more closely related to these two genes than to the genes of the Shaker family. Due to this similarity, hERG was given the name “ether-a-go-go-related-gene” (10) (11) (12). This investigation also revealed that KCNH2 is located on chromosome 7 (4).

In 1995, Curan et al. made a crucial discover linking mutations in KCNH2 to Long QT Syndrome (LQTS), a potentially life-threatening cardiac disorder. This finding highlighted the clinical significance of hERG and sparked intense research into its role in cardiac function and drug safety (13).

Further investigations using guinea pig hearts demonstrated that the hERG gene product exhibited characteristics similar to the I_{Kr} current. Subsequently, the hERG gene was identified as the source of these channels in human cardiac tissue (9).

Studies by Beuckelmann et al. reported the presence of delayed rectifier currents in 41% of cells isolated from failing left ventricles. However, these currents were not-failing hearts. It is worth mentioning that subsequent studies have revealed that both I_{Kr} and I_{Ks} are present in normal human ventricular myocytes, but their expression and function can be altered in heart failure (9).

In the late 1990s and early 2000s, scientists realized how important hERG was for drug safety. As a result, testing drugs for their effects on hERG became required in safety checks. This change has greatly affected how pharmaceutical companies develop new medicines (14).

In 2017, a significant breakthrough was made by Wang and MacKinnon when they determined the structure of the hERG channel using cryo-electron microscopy. This achievement has greatly enhanced our understanding of the channel's function and its interactions with drugs, offering crucial insights into hERG's role in both cardiac physiology and pharmacology (1).

2 Structure of the hERG channel and gating

2.1 Molecular structure

The hERG channel consist of four alpha subunits and is scientifically a tetramer. All subunits have six transmembrane spanning alpha helical segments (S1-S6) (15). Each subunit contains a voltage sensor domain (VSD) made up of the S1-S4 helices and a pore domain (PD) formed by the S5 and S6 helices. It also includes N- and C-terminal cytosolic domains (CTD) that have regulatory functions (Figure 2) (16) (17).

2.1.1 Voltage-sensor domain

The voltage-sensor domain is formed by segments S1-S4 (Figure 3) (18). The hERG channel contains five key gating charges, which are located at regular intervals within the S4 segment. These gating charges consist of positively charged amino acids. In contrast, the S2 and S3 segments contain acidic amino acids, which contribute negative charges. The interactions between the positive and negative charges creates electrostatic attraction, forming salt bridges. These salt bridges contribute to the stabilization of the hERG channel structure (19).

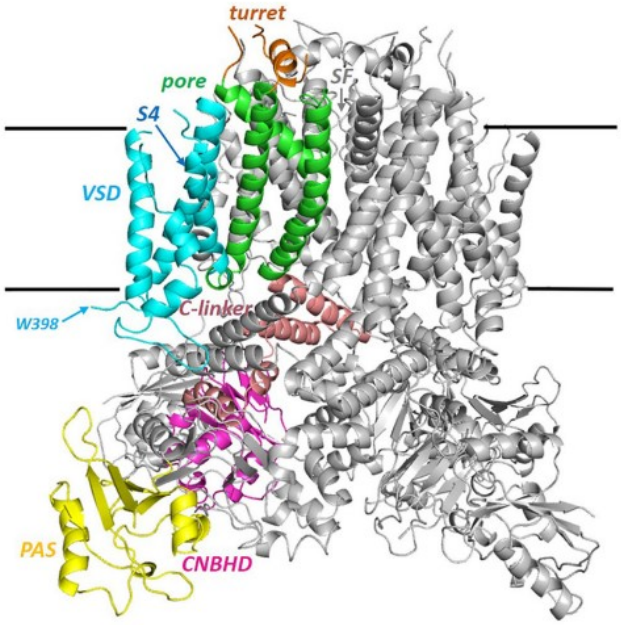

Figure 2: Side view of the full hERG cryo-EM structure (20)

Upon depolarization, the positive charges in the S4 segment are electrostatically attracted, leading to a movement of this segment. This conformational change then transfers the signal, ultimately resulting in the opening of the channel (19). Specifically, helix S4, which carries five positively charged residues, senses the voltage change and moves up or down across the membrane, transmitting the motion to the pore domain that, in turn, closes or opens the channel to ion passage (17).

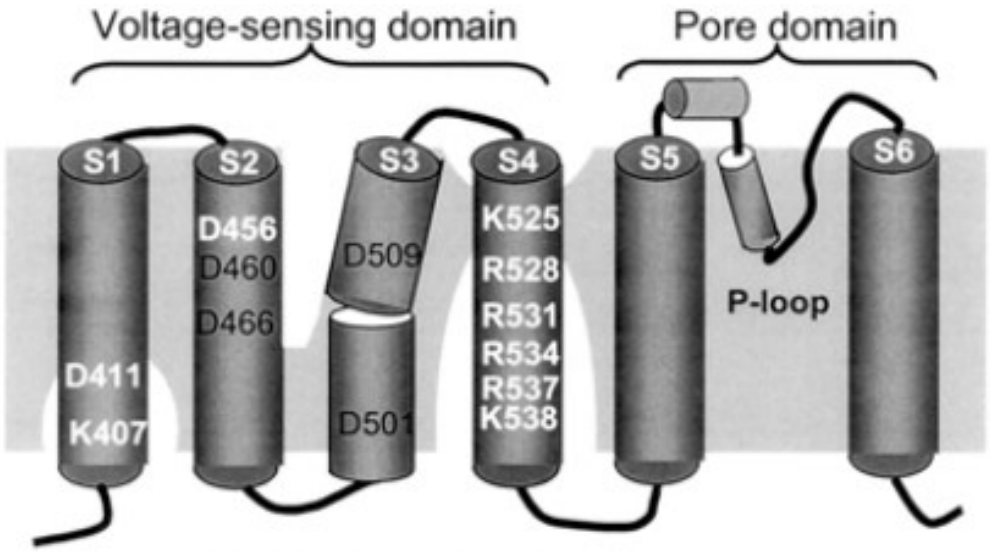

Figure 3: Structure of the voltage sensor domain, illustrating the distribution of positive and negative charges across the individual segments (19)

2.1.2 The Pore

The hERG channel contains an **asymmetric** pore structure that undergoes dynamic conformation changes as the channel transitions between its closed and open states. The asymmetric pore domain is surrounded by the four segments and contains S5-S6 helices, with a S5-P-loop in the middle. The S5-P-loop is known as a selectivity filter and is located in the narrow part of the pore, where it regulates the passage of potassium ions through the channel (Figure 4) (18) (21) (22).

The central cavity of the pore is filled with water molecules and surrounded by the S6 transmembrane helices, which play a crucial role in opening and closing the pore, acting as the “gates” that control access to the ion conduction pathway (18) (21) (22). Notably, the hERG pore cavity is smaller compared to other potassium channels, with a radius of almost 6 Å at a key location within the pore-forming region. This unique feature contributes to the channel’s distinctive properties (1) (20).

A glycine at position 648 enables large conformational changes in the S6 helices, facilitating the transition between closed and open states. The voltage sensor domain transmits an electromechanically coupled signal to the pore, which subsequently opens the channel, facilitating the selective and regulated flow of potassium ions (1) (18) (21) (22).

The intracellular region is also important for regulating ion flow through the open channel. Recent structural studies have captured the hERG channel in its open state, which may represent a pre-inactivated open state. This is particularly significant for understanding the channels unique gating properties, including its rapid inactivation (18) (21) (22) (20). Importantly, the pore region is not only crucial for ion conduction but also plays a vital role in drug binding (20).

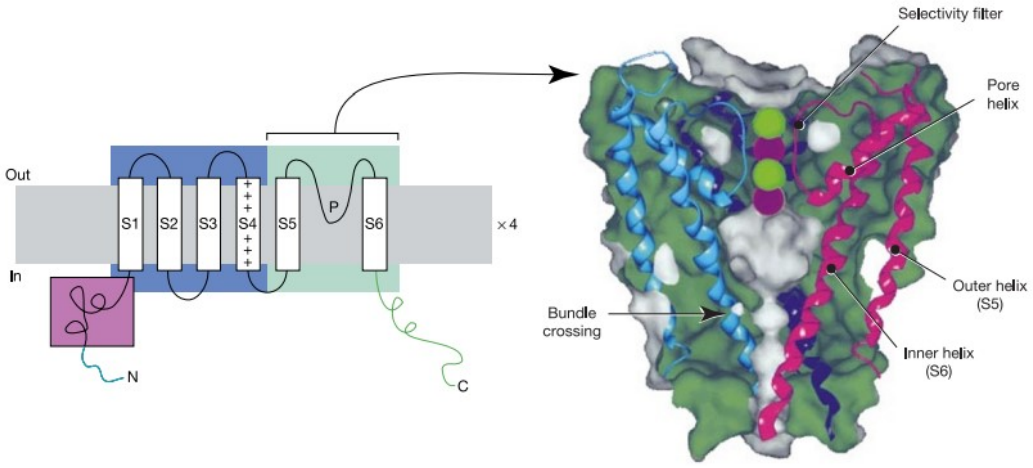

Figure 4: Structure of the hERG channel with a detailed depiction of the pore domain (21)

2.1.3 Cytosolic N- and C-terminal domains

The hERG protein is distinguished by its unique intracellular N- and C-terminal domains. The N-terminal cytoplasmic region consists of an eag-domain with a PAS (Per-Arnt-Sim) domain. This PAS domain is covered by a short sequence containing an amphipathic helix, known as the N-Cap. The C-terminus is constructed from both a C-linker region and a cyclic nucleotide-binding homology domain (CNBHD) (1) (23) (24).

These cytosolic domains play crucial roles in channel function, particularly in gating mechanisms. The N-terminal eag-domain is essential in regulating voltage-dependent gating, especially deactivation. Intriguingly, the eag-domain can regulate gating even when it is not covalently attached to the channel, suggesting a complex mechanism of inactivation (25).

Interactions between the PAS and CNBH domain are responsible for the deactivation of the channel. An intrinsic ligand within the CNBHD, consisting of amino acid residues 860-862, binds to the PAS domain, leading to slow deactivation. Point mutations or deletion of one of the cytosolic domains can accelerate the deactivation kinetics (25) (26) (27).

Structural insights into these functional interactions have been gained through Förster resonance energy transfer (FRET) experiments. These studies

suggest that the N- and C-terminal regions lie in close proximity to each other, with two quadratic planes separated vertically by almost 8 nm. This spatial relationship aligns with a structural model inspired by hyperpolarization-activated cyclic nucleotide-gated (HCN) channels, where the CNBHD is positioned beneath the channel pore region. The C-linker/CNBD region of hERG is suspended below the transmembrane domains, with the N-terminus positioned at the top and nearby switch domains oriented towards each other, facilitating important interdomain interactions (28).

The critical role of these cytosolic domains in hERG channel physiology is further emphasized by the fact that mutations in the eag domain have been linked to Long QT Syndrome Type 2 (LQTS). These mutations disrupt the regulation of gating, highlighting the importance of these domains not only for normal channel function but also in the context of disease (25).

2.2 Gating

The unique feature of hERG potassium channels is their extremely slow activation and deactivation kinetics. This means that the channels open and close gradually in response to changes in membrane potential (Figure 5, 6). In contrast, the inactivation and recovery from inactivation of hERG channels occur very quickly and are highly voltage-dependent (29) (30). This rapid C-type inactivation is a key aspect of the channel's functionality, contributing to inward rectification (4).

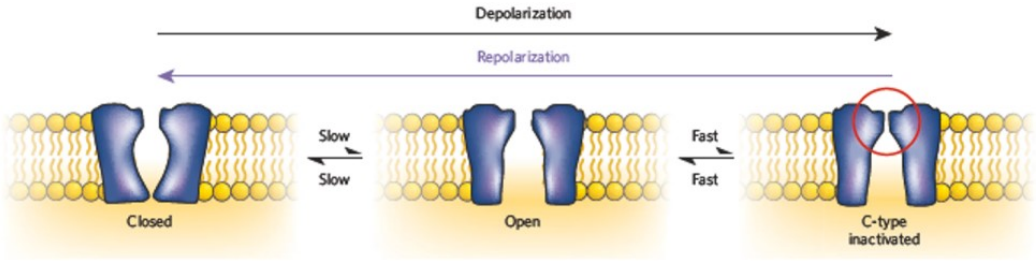

Figure 5: Conformation changes during the channel transitions between close and open (22)

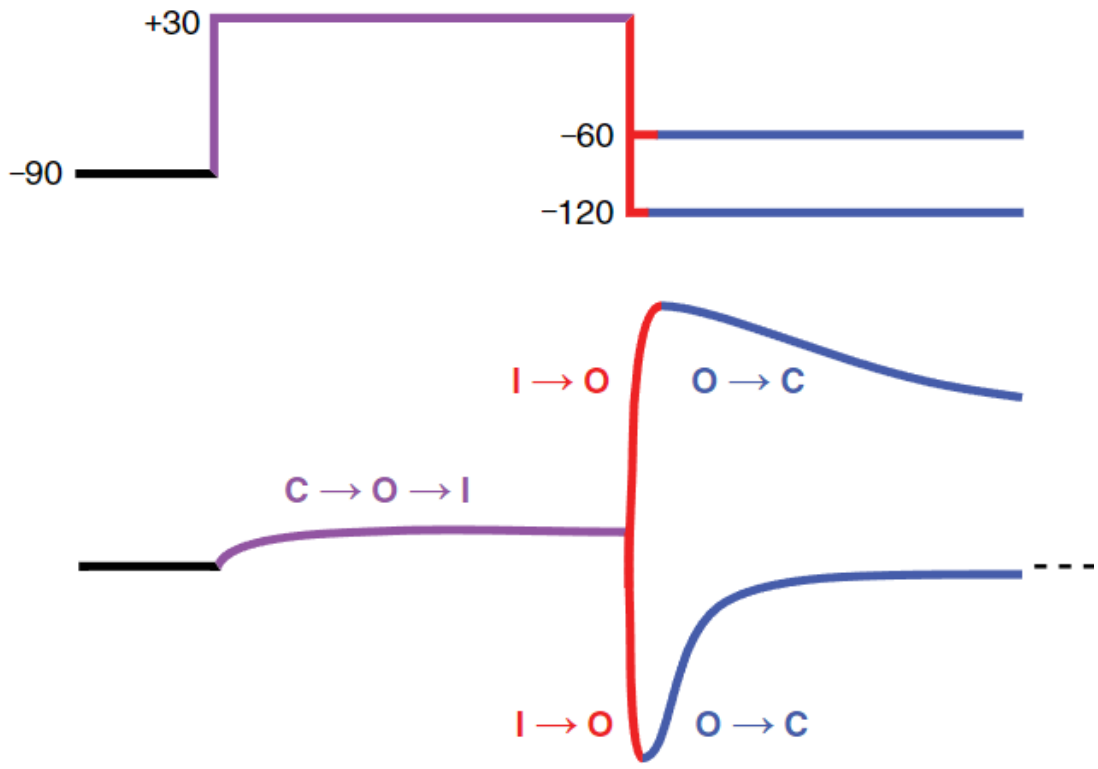

Figure 6: Transitions between the different states, C--> closed, O--> open, I--> inactivate (4)

The cytoplasmic and transmembrane regions of the hERG channel interact to precisely regulate the channels opening and closing kinetics (4). Due to the rapid voltage-dependent inactivation, hERG channels display inward rectification. Throughout the depolarization of the cell membrane, hERG channels slowly open (Figure 7). However, they rapidly become inactivated, resulting in minimal outward ion flow during the early part of an action potential (4) (18) (29) (30). At the start of repolarization, as the membrane voltage begins to return to its resting potential, these channels quickly recover from their inactivated state. This recovery causes a second, larger change in current: a flow of potassium ions that peaks at about -40 mV. This movement of potassium helps bring the membrane potential back to its resting state after the action potential (4) (18) (29) (30).

These distinctive gating properties of the hERG channel, including its slow activation and deactivation coupled with rapid inactivation and recovery, are critical for the channels role in cardiac action potential repolarization and the maintenance of normal heart rhythm. The closing of the channels is a relatively slow process, making them key determinants for the termination of the plateau phase and the timing of cardiac action potential repolarization, which is essential for preventing arrhythmias (18) (4) (29) (30) (31).

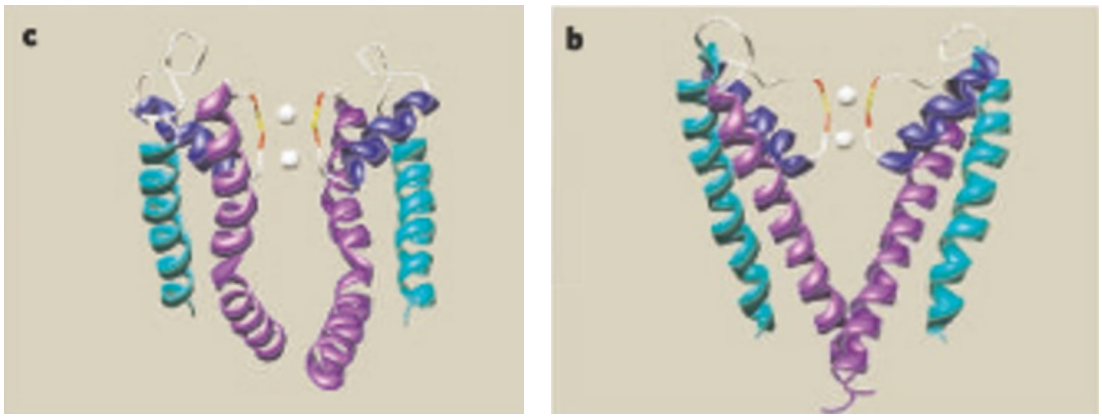

Figure 7: Left: Crystal structure in an open state (22); Right: Crystal structure in a closed state (22)

2.2.1 Activation

The activation gate of the hERG channel is dependent on the movements of the voltage sensor (32). As previously noted, the activation of the hERG channel is very slow compared to the activation speed of other K_v ion channels, taking 10 to 100 times longer to activate (29) (33). The reason for this slow activation is the delayed movement of the S4 segment, which serves as the voltage sensor (33) (34). One potential explanation for the slow S4 movement is that the voltage sensor may be missing a positive charge compared to other K_v channels (35).

The kinetics of the voltage sensor movement are also influenced by the amino acid composition of the S4 segment itself, as well as the negatively charged amino acids in the other transmembrane segments. The formation of salt bridges between the positively charged residues in the S4 segment and the negatively charged residues in S1-S3 may further contribute to the slow voltage sensor kinetics (35).

The S4-S5 linker is thought to play an important role in coupling the voltage sensor movement to the opening of the activation gate. During depolarization, the movement of the voltage sensor causes the S4-S5 linker to interact with the S6 segment, leading to the opening of the activation gate (36).

2.2.2 Inactivation

Generally, two different mechanisms of K_v channel inactivation are recognized. On the one hand, there is fast N-type inactivation and on the other hand, there is a slow C-type inactivation. N-type inactivation, induced by the N-terminus, closes the inner mouth of the channel pore, thereby blocking ion flow. In contrast, C-type inactivation is ended by the N-terminal domain, which also ends the N-type inactivation in Shaker. The C-type inactivation in Shaker is cancelled by a mutation in the pore helix (Thr449Val) (22).

The inactivation of hERG channels follows the C-type mechanism, but it is faster than the C-type inactivation in Shaker channels. This process is affected by the Ser631Val mutation, analogous to the Thr449Val mutation that eliminates C-type inactivation in Shaker channels. The S4 transmembrane

segment serves as a voltage sensor for both activation and inactivation, with different regions for the respective processes. While N-type inactivation is mediated by the N-terminal domain, which occludes the inner mouth of the channel pore, C-type inactivation involves structural changes in the outer mouth of the pore, which block the conduction pathway. These molecular rearrangements occur in hERG channels, despite their inactivation being governed by the slow C-type mechanism, which is a critical feature for normal heart function (22).

2.2.3 Deactivation

The deactivation of hERG occurs as slowly as their activation, with the N-terminus playing a crucial role in this process (23). The closing of the hERG channel is regulated by various molecular interactions between its structural components. Notably, the interaction among three key regions – the N-terminal Cap domain, the PAS domain and the intracellular cyclic nucleotide binding homology region – plays a crucial role in determining the deactivation rate of the hERG channel (37). A critical molecular determinant of this slow deactivation is a three-dimensional hydrophobic nexus involving these domains (38).

Experimental studies have shown that deletion of the N-terminal tail, the entire PAS domain, or most of the N-terminus can accelerate the deactivation of hERG channels. These findings suggest that the N-terminus affects deactivation by interacting with other channel structures like the S4-S5 linker (37) (39). The S4-S5 linker is thought to participate in different state changes, including deactivation (40). On the other hand, during repolarization, as the voltage sensor returns to its original position, the S4-S5 linker helps close the S6 segment and deactivate the channel (36).

Furthermore, the transmembrane regions of the hERG channel have also been found to impact deactivation kinetics. Neutralizing the charges in specific transmembrane segments can speed up the deactivation process (41) (42). Extracellular factors, such as acidification, can also influence deactivation by affecting voltage sensor relaxation (43).

In summary, the slow deactivation of hERG channels is regulated by the complex interplay between the N-terminal domains and the transmembrane regions of the channel. Disrupting these interactions, either through deletions or charge neutralizations, can lead to faster deactivation kinetics (40) (43).

3 Biogenesis and Trafficking of hERG channel

The process of creating the hERG protein begins in the cell nucleus, where the hERG gene is transcribed into mRNA. This mRNA is then carried to the cytoplasm, where it is translated into protein at the endoplasmic reticulum (ER). Once the hERG protein is formed, chaperones like Hsp70, Hop and DNAJA2 help it fold correctly and assemble into tetramers. Hsp90 is crucial for ensuring the protein folds properly and matures by preventing the buildup of misfolded intermediates and guiding them through the secretory pathway (44).

If the hERG channels are misfolded or non-functional, chaperones such as Hsp40 and Hsc70 identify and target them for degradation. The chaperone protein Hop plays a crucial role in hERG channel processing. It serves a dual function. Firstly, in conjunction with DNAJA2, it facilitates the release of hERG channels from Hsc70. Secondly, Hop aids in recruiting Hsp90 to the hERG protein. Hsp90 is significant because it prevents the clumping of misfolded proteins and promotes the proper maturation of the hERG channel. This intricate interplay of chaperone proteins ensures the correct folding and processing of hERG channels, which is essential for their normal function (Figure 8) (44).

Chaperones help correctly folded hERG proteins reach the Golgi apparatus, where they undergo a crucial process called glycosylation. This step is important for stabilizing the proteins and ensuring they work properly on the cell surface (44). After glycosylation, the channels are packaged into vesicles and sent to the plasma membrane, where they are integrated into the lipid bilayer, allowing them to function correctly (4) (44) (45).

However, the formation of hERG channels can be disrupted by various factors, such as genetic mutations or pharmacological agents. For example, specific point mutations like G601S and T473P have been shown to impair the proper trafficking of hERG channels. Similarly, certain substances can interfere with

hERG protein folding, a notable example is arsenic trioxide. Furthermore, the maturation and export of hERG channels from the endoplasmic reticulum can be hindered by compounds such as Pentamidine. These examples illustrate the diverse mechanisms through which hERG protein function can be compromised, highlighting the complexity of maintaining normal channel activity (44).

Throughout its synthesis and processing, the hERG protein undergoes rigorous quality control (QC) mechanisms in the endoplasmic reticulum. These QC processes serve to either rectify protein folding issues or stop further progression of improperly folded proteins. In cases of persistent misfolding, the cell responds by upregulation chaperone production to aid in proper protein conformation. However, if chaperone are unable to rectify the folding errors, the cell initiates other strategies. Specifically, misfolded hERG proteins are labeled by CHIP (Carboxyl terminus of Hsc70 interacting protein) and ubiquitin, marking them for degradation. This targeted breakdown occurs in the proteasome, a cellular structure dedicated to protein disposal. This multilayered quality control system ensures that only correctly folded and functional hERG proteins progress through the secretory pathway, maintaining cellular homeostasis and proper channel function (44).

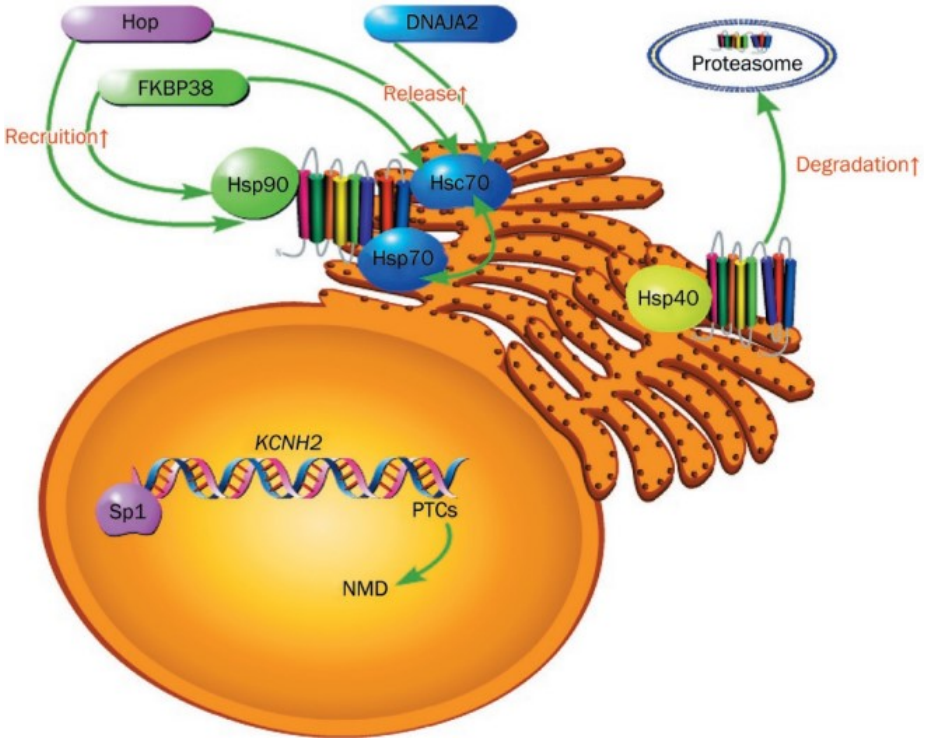

Figure 8: Cellular control mechanisms of hERG channel production (44)

4 Functional role and significance of hERG

4.1 Role in cardiac action potential

For cardiac muscle cells in the ventricles to function properly, they require precise regulation of electrical activity. The heart action potential is the electrical signal that stimulates the contraction of these muscle cells and consists of five different phases. The phase zero represents depolarization, which occurs due to the rapid influx of sodium ions. This influx increases the membrane potential and excites the cell. Phase one, known as transient repolarization, involves the efflux of potassium ions, leading to a rapid return to less positive charges. During the second stage of the action potential, known as the plateau phase, the cells electrical charge stays fairly steady. This stable period is mainly due to calcium ions entering the cell through specific openings called L-type calcium channels. At the same time, proteins that exchange sodium and calcium ions also plays a part in keeping this balance. The inward currents during this phase are balanced by early contributions from delayed rectifier currents, resulting in the characteristic flat plateau observed in the ventricular action potential (29) (46) (12).

After that, phase three begins, which is the repolarization phase where the cell's membrane potential returns to its resting state. During this phase, the delayed rectifier potassium current is essential and is made up of two main parts: I_{Kr} (the fast component) and I_{Ks} (the slow component). These currents repolarize the cell and terminate the action potential. The final phase is the refractory period, which involves a recovery phase after the action potential has ended (Figure 9). This phase is particularly important because it ensures that cardiac muscle cells temporarily do not respond to new electrical signals, thereby preventing the heart from beating too rapidly in succession (29) (46) (12).

As previously mentioned, hERG is a specific type of potassium channel responsible for the I_{Kr} current. Particularly during phase three, hERG plays a vital role by generating a recurring current after the cardiac action potential has

concluded. The hERG channels are activated in response to membrane depolarization. Inactivation of hERG leads to significant recombination, resulting in initially low current flow. As the channels recover from inactivation and repolarization resumes, they transition to a relaxed state, allowing the current flow to increase again (46).

The distinctive kinetics of hERG, with slow activation and deactivation but very rapid voltage-dependent inactivation, are compatible with its specialized function in cardiac repolarization (18).

Pharmacological treatment of arrhythmias often targets hERG channels using class III antiarrhythmic. The disruption of hERG channel function, whether due to genetic mutations or medication effects, can significantly alter the hearts electrical rhythm. This interference often results in a prolonged cardiac action potential, manifesting as Long-QT-Syndrome. These issues can have serious consequences. They can slow down the heart's electrical reset, make the QT intervals on an ECG longer and increase the risk of a dangerous heart rhythm called "Torsade de Pointes". In the worst cases, this can even cause sudden cardiac arrest (46).

When developing new medicines, scientists face a big hurdle: some drugs that are not meant to affect heart rhythm can still block the hERG channel. This makes it tricky to create safe medications (46).

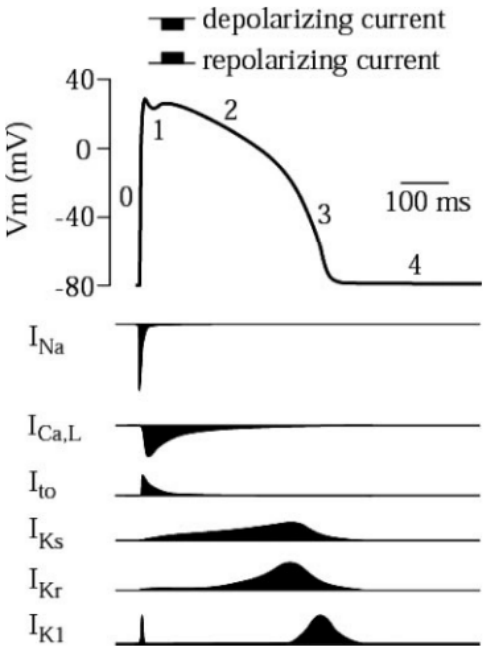

Figure 9: Top: Cardiac action potential with the different phases; Bottom: Individual ion currents with their respective time courses (47)

4.2 Arrhythmia Mechanisms and Long QT Syndrome

As mentioned in the previous paragraph, changes in the hERG gene can cause a condition called Long QT Syndrome (LQTS). On an electrocardiogram (ECG), a widened QT interval is observed, which gives rise to the name “Long QT Syndrome”. The prolonged QT interval shows that the hearts electrical system is taking longer to reset, specifically in the ventricles. This delay increases the risk of Torsade de Pointes (TdP), a specific type of polymorphic cardiac ventricular tachycardia (12) (48).

LQTS can be either inherited (congenital) or acquired. Most inherited cases are due to genetic mutations that affect heart ion channels: mutations that reduce the function of I_{Ks} (LQT1) or I_{Kr} (LQT2) or mutations that increase the function of I_{Na} (LQT3). Acquired LQTS usually happens due to drugs that block the I_{Kr} channel (48).

Torsade de Pointes is characterized by polymorphic ventricular tachycardia, a condition where the heart beats rapidly and irregularly. It often results from a prolonged electrical recovery phase in the heart, which shows up as a prolonged QT interval on an electrocardiogram (ECG). On an ECG, Torsade de Pointes is marked by a shifting electrical axis of the heart, creating a wave-like pattern that changes direction. This is identified as a twisting of the QRS complex around the isoelectric line (12).

The onset of Torsades de Pointes in Long QT Syndrome is driven by a prematurely triggered ventricular complex (PVC) that interacts with an electrically unstable area, leading to re-entrant circuits and persistent arrhythmias. New research has clarified that PVCs are not directly caused by early afterdepolarizations (EADs) as once assumed. Instead, they are triggered by sharp voltage gradients, which develop in localized regions where the action potential duration is significantly extended due to LQTS (48).

While Torsade de Pointes can be serious, it is not always fatal. Patients can sometime return to a normal sinus rhythm. LQTS is a serious condition affecting the heart's repolarization process, which can lead to dangerous ventricular arrhythmias and potentially sudden cardiac death. Torsade de Pointes is often one of the first signs of LQTS (13) (22) (49).

4.2.1 Inherited LQTS

LQTS has two main types: inherited and acquired (drug-induced). Inherited LQTS is mostly autosomal dominant, though there are rare autosomal recessive types like Jervell and Lange-Nielsen syndrome. While Nakano and Shimizu identified three key ion channels related to inherited LQTS (KCNQ1, hERG and SCN5A) recent research have found at least 15 different genes involved. However, mutations in KCNQ1 (LQT1), KCNH2 (hERG, LQT2) and SCN5A (LQT3) still account for about 75% of genotype-positive LQTS cases (50) (51).

One of these genes, called hERG, is responsible for a type of LQTS known as Type 2 and has over 500 identified mutations. These inherited mutations can disrupt normal hERG channel function in various ways, often leading to dominant-negative effects on the I_{Kr} current (49) (50). Loss-of-function mutations can cause serious cardiac arrhythmias by altering channel trafficking, gating or both. Some mutations affect voltage sensitivity, while others alter channel kinetics, which can change the duration of the hearts action potential (52) (53) (54).

The mutations are classified into four main groups based on their cellular effects. The first group involves disorders of transcription and translation. The second group pertains to inadequate protein trafficking. The third group is characterized by abnormal channel opening and closing kinetics associated with loss-of-function mutations. Finally, the fourth group involves altered channel permeability (55) (56).

Many hERG mutations (Figure 10) are missense-mutations, which lead to misfolding of the individual subunits of the channel and subsequent degradation via the ubiquitin-proteasome pathway (52) (53) (54). It is important to note that some rare mutations can cause a gain of function. These mutations

enhance repolarization and shorten the action potential. Such changes are referred to as Short QT Syndrome (57) (58).

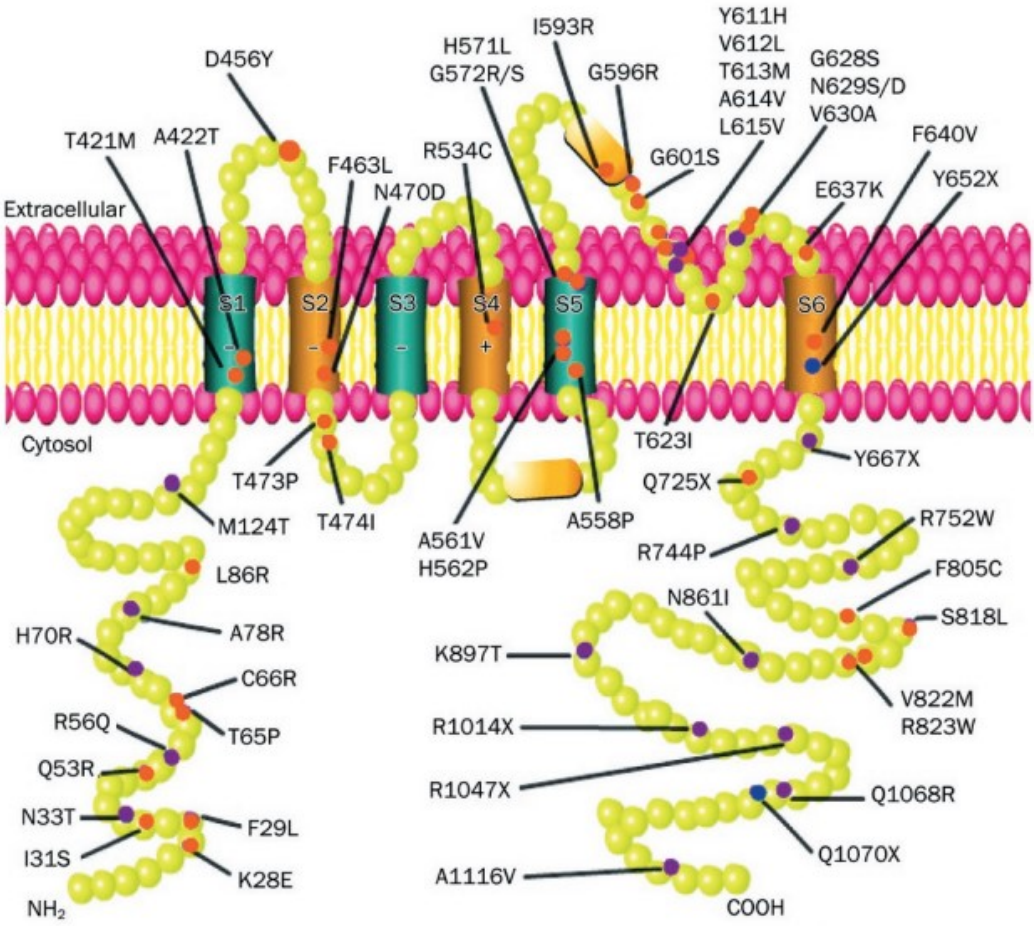

Figure 10: Overview of LQT2 mutations; Yellow: Represents amino acids; Purple, orange and blue dots show various mutations (44)

4.2.2 Acquired LQTS

Acquired LQTS, commonly referred to as drug-induced LQTS, is caused by medications that interfere with hERG channel function, leading to a reduction in the potassium current I_{Kr}. While this form of LQTS is more prevalent than the inherited type, precise comparative statistics are not well-established (59) (60).

However, it is known that certain structural determinants of the drugs, such as specific molecular configurations, can increase their propensity to block hERG

channels. The unique gating properties of these channels also play a significant role in how drugs bind and affect channel function (18) (61).

It is crucial to note that not all hERG channel-blocking drugs necessarily cause LQTS. The risk is influenced by various factors, including dosage, drug metabolism and individual patient characteristics. Several classes of medications have been associated with acquired LQTS including but not limited to certain antiarrhythmics, antibiotics and antipsychotics (60) (62).

As acquired LQTS can be life-threatening, regulatory agencies now mandate very extensive hERG testing in preclinical drug development. A major source of information on the potential effects of medicines on the QT interval (Figure 11, 12) and also a widely applied screening tool for new drug safety, is an *in vitro* risk assays. These assays have led to the development of automated analysis methods for establishing bioanalytical techniques (18) (22).

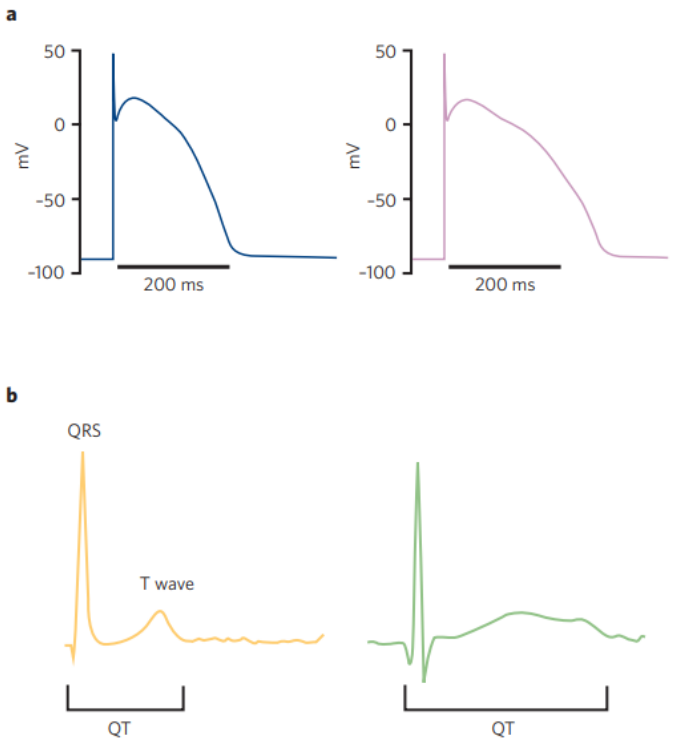

Figure 11: Image (a, left): a normal action potential in humans, (a, right): a prolonged action potential simulated by reducing hERG current by 80%; Image (b, left): standard ECG recording for one cardiac cycle, (b, right): irregular ECG recording showing a prolonged QT interval (22)

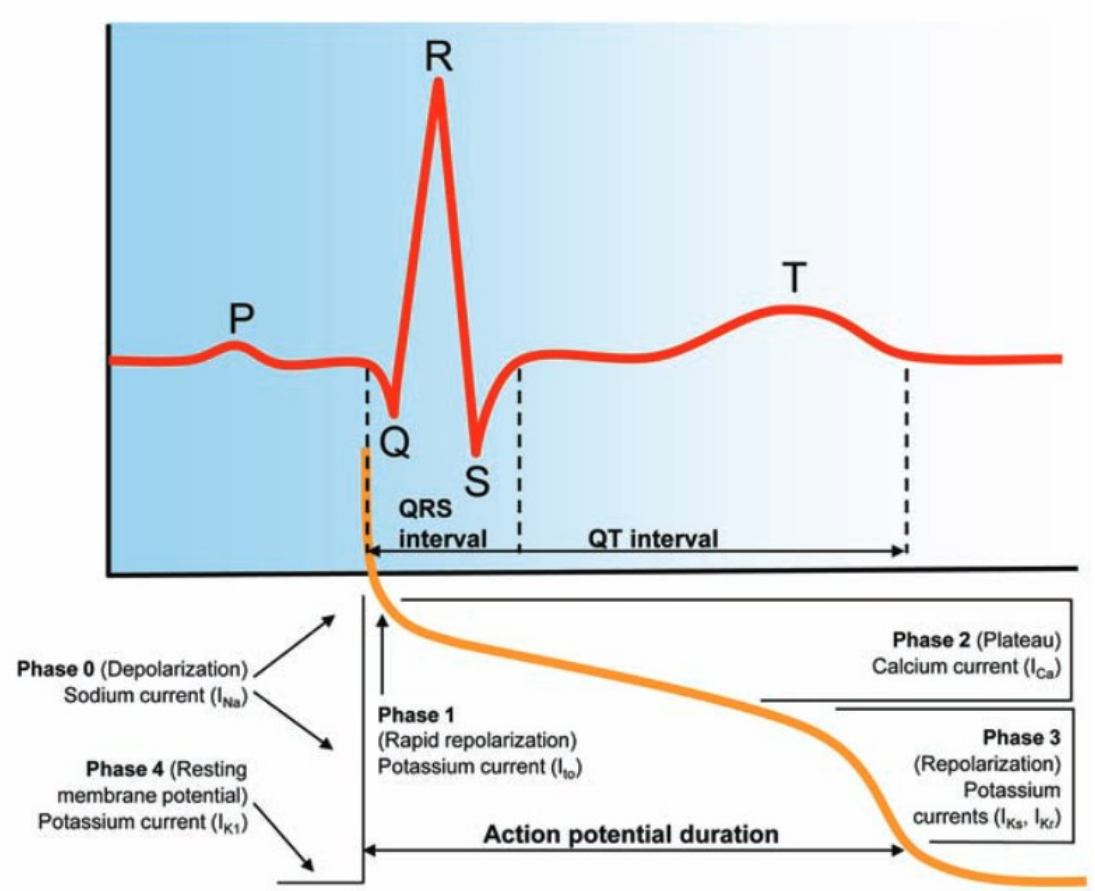

Figure 12: A single heartbeat depicted by an electrocardiogram and the corresponding cardiac action potential trace (5)

5 Pharmacology of the hERG-channel

Since their discovery, hERG channels have been a major focus because they play a vital role in cardiac repolarization and are linked to various drug-induced arrhythmias (4). The hERG channel controls a rapid potassium current, known as I_{Kr}, which is crucial for the hearts electrical activity. This current helps coordinate the synchronized repolarization of heartbeats, ensuring the heart maintains its regular rhythm. The precise regulation of I_{Kr} through hERG channels is fundamental to normal cardiac action potential repolarization and consequently to overall cardiac function (63).

To date, it remains unclear why so many structurally diverse compounds block the hERG channel. This promiscuous drug binding has led to the withdrawal of several blockbuster drugs from the market due to their potential to cause life-threatening arrhythmias, such as Torsades de Pointes (TdP) (63). Therefore, it is crucial to test new drugs for hERG channel inhibition early in the lead optimization process (52) (5).

Although the hERG channel is blocked by many classes of drugs, it possesses unique binding properties, which have been demonstrated through alanine-scanning mutagenesis. Four amino acids have been shown to play a crucial role in determining how effectively drugs block the hERG channel. Two of these amino acids are the polar residues threonine (Thr) at position 623 and serine (Ser) at position 624, located at the base of the pore helix. The other two amino acids are tyrosine (Tyr) at positon 652 and phenylalanine (Phe) at position 656 in the S6 segment. These last two are not found in other K_v channels, contributing to hERGs unique pharmacological profile (22) (64).

The unique arrangement of these four amino acids contributes to the central cavity of the channel, creating a high-affinity drug binding site. The presence of an aromatic amino acid at the position 652 is crucial for the effective inhibition by specific drugs such as Cisapride and Terfenadine. This demonstrates that a specific chemical interaction, known as a cation-π interaction, plays a key role in this process (22).

5.1 Classification of hERG Agonists

While scientists have identified a substantial array of hERG channel antagonists, Harchi noted in his study that there are currently 20 known agonists, which are categorized into different types based on their mechanisms. Fundamentally, these agonists are classified in four types. Agonists that do not fit neatly into one of these categories typically exhibit multiple mechanisms of action (2).

The four main types of hERG agonists are (Figure 13):

1. Type one agonists: These primarily enhance hERG current by slowing the closure of the channels activation gate (deactivation) but may also cause a modest reduction in the channels ability to inactivate. Examples include RPR260243, Ginsenoside Rg3 and LUF346 (31) (2).
2. Type two agonists: These act mainly through a rightward shift in the voltage dependence of inactivation. Examples include ICA-105574, AZSMO-23, NS3623 and MC450 (2).
3. Type three agonists: Also known as “facilitators”, these negatively shift the voltage dependence of activation. Examples include Mallotoxin, SKF-32802 and KB130015 (2).
4. Type four agonists: Also known as “pore modifiers”, these increase the open probability of the channel. Examples include SB-335573 and PD-118057 (2).

Uncategorized hERG activators, such as ITP-2, HW-0168, LUF7244, ML-T531, A-935142, PD-307243, NS1643 and VU0405601 (Figure 14), either exhibit multiple mechanisms or cannot be easily classified. Further studies are needed to better understand these activators and their specific mechanisms of action (15) (31) (2).

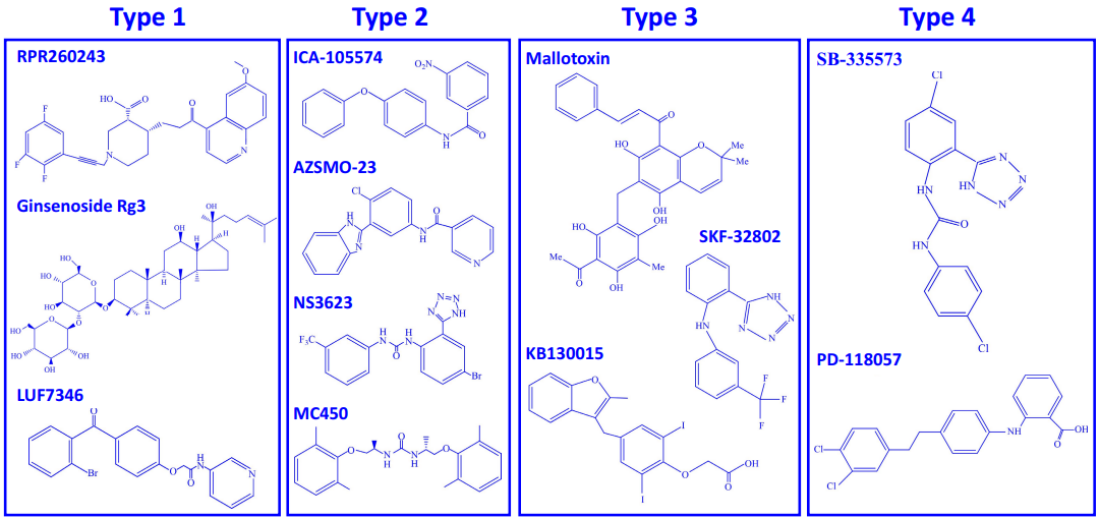

Figure 13: Chemical structure of agonists classified by their mechanisms (2)

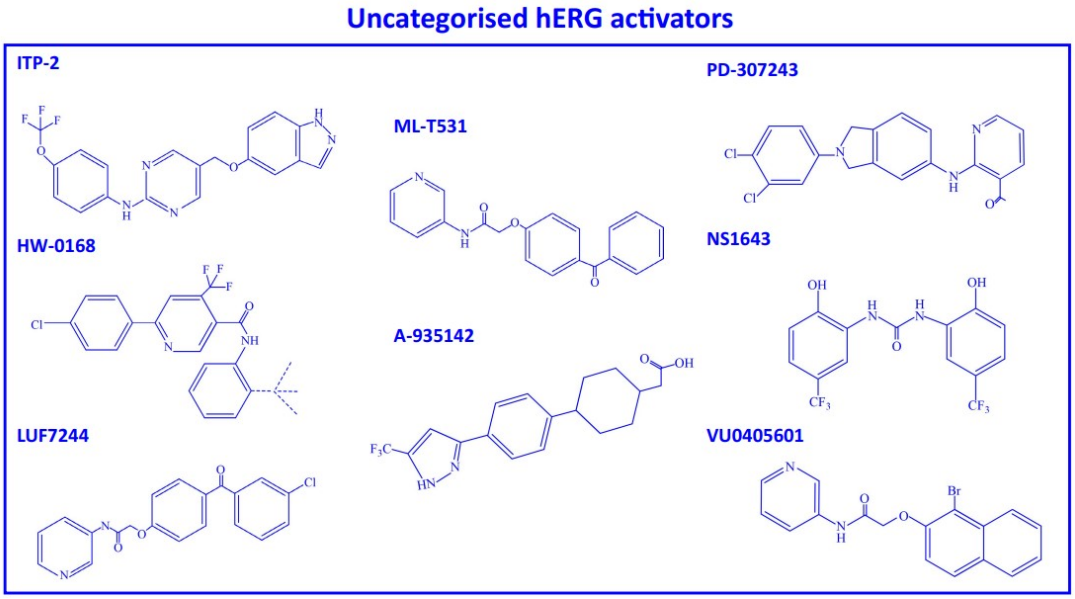

Figure 14: Chemical structure of agonists with uncategorized mechanisms (2)

5.2 Overview of hERG activators and their characteristics

5.2.1 RPR260243

As previously mentioned, activators are classified into different types. RPR260243 is recognized as the first hERG channel activator. Specifically, RPR260243 is chemically known as [3R, 4R)-4-[3-(6-methoxy-quinolin-4-yl)-3-oxo-propyl]-1-[3-(2,3,5-trifluoro-phenyl)-prop-2-yn-1-yl]-piperidine-3-carboxylic acid] (18). The activator RPR260243 is known for prolonging the deactivation rate of hERG channels (18).

Mechanism of Action

RPR260243 operates in a temperature- and voltage-dependent manner over a concentration range of 1 to 30 µM. Its primary effects include prolonging hERG channel deactivation with minimal impact on hERG current amplitude and negligible alteration of steady-state activation parameters or channel inactivation processes (18) (65).

As shown in Figure 15, RPR260243 binds to specific residues in the hERG channel.

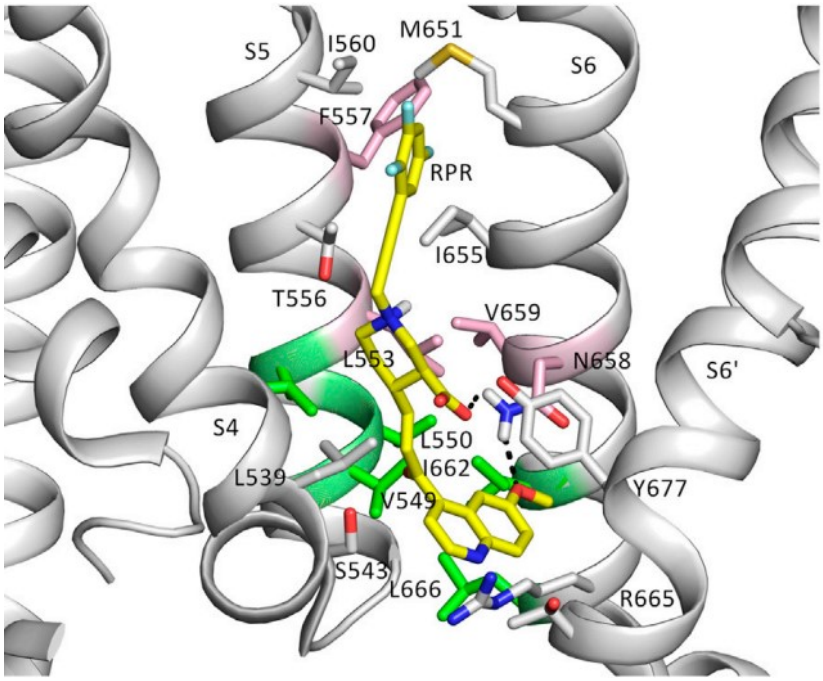

Figure 15: Binding residues of RPR260243; Yellow: RPR260243; Pink: Prolongation of deactivation; Green: Attenuation of deactivation (66)

Electrophysiological Effects

RPR260243 demonstrates significant effects on cardiac electrical activity at varying concentration. These effects have been studied using different experimental models, including zebrafish and guinea pig hearts (18) (66) (65).

In zebrafish whole hearts, the changes induces by RPR260243 at a concentration of 30 µM are visualized using the potentiometric dye RH237. At this concentration, RPR260243 causes several alterations in cardiac electrical activity. On the one hand, it shortens the action potential duration and decreases triangulation of the action potential waveform. On the other hand, it increases the steepness of the electrical restitution curve and extends the post-repolarization refractory period (18) (66) (65).

Detailed analysis of action potentials recorded after the fourth stimulus in the cycle, comparing the same heart with and without RPR260243, reveals a targeted reduction in the duration of the late repolarization phase. This effect is particularly evident in the preferential shortening of late-phase repolarization (65).

Quantitative measurements in zebrafish hearts show that the mean action potential duration (ADP) at 90% repolarization decreases significantly from 132 ± 4 ms in control conditions to 111 ± 2 ms in the presence of 30 µM RPR260243. However, the APD at 30% repolarization remained largely unchanged, indicating a selective modulation of the action potential morphology. This selective shortening of late-phase repolarization results in a notable decrease in the triangulation index (Figure 16), a common predictor of cardiac arrhythmogenicity, from 74 ± 3 ms in control conditions to 45 ± 3 ms with RPR260243 (67).

At a lower concentration of 5 µM, RPR260243 demonstrates different effects in guinea pig hearts. These include the enhancement of T-wave amplitudes, extension of the PR interval and reduction in the duration of the QT interval (18) (66) (65).

Figure 17 illustrates the electrophysiological effects of RPR260243 on hERG channel currents, showing its impact on current deactivation and persistent current components (68).

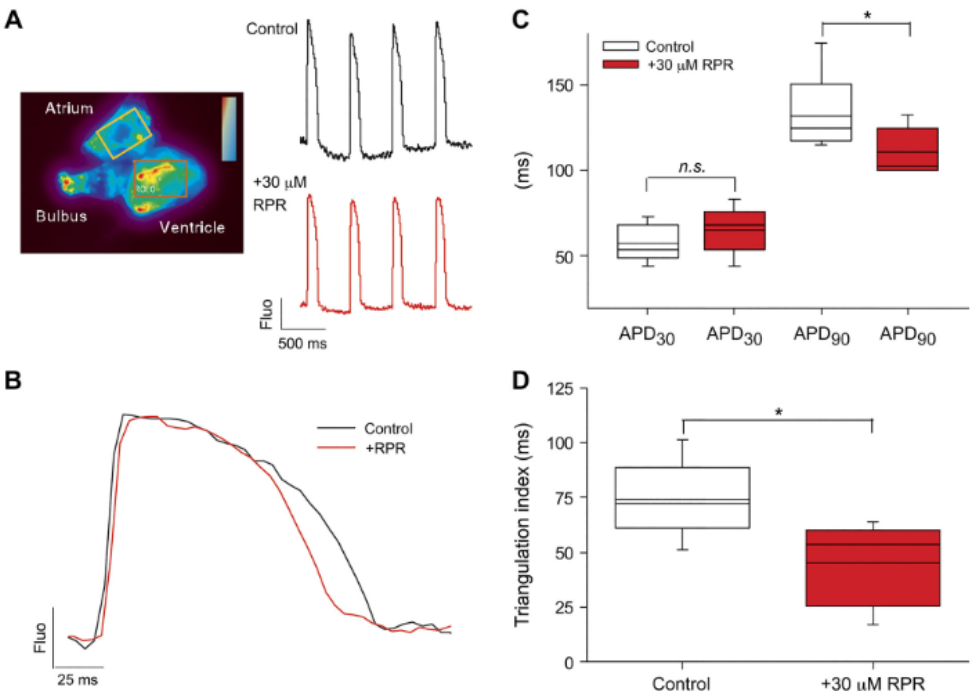

Figure 16: Research was conducted with and without RPR260243. The results using the potentiometric dye RH 237 are represented by red for high and blue for low signal intensity (A). The difference is evident in B, which shows that RPR shortened the ADP. Picture C illustrates a boxplot of the impact of RPR260243 on the ADP measured at 30% and 90% repolarization. Effects on the Triangulation index are shown in D (65).

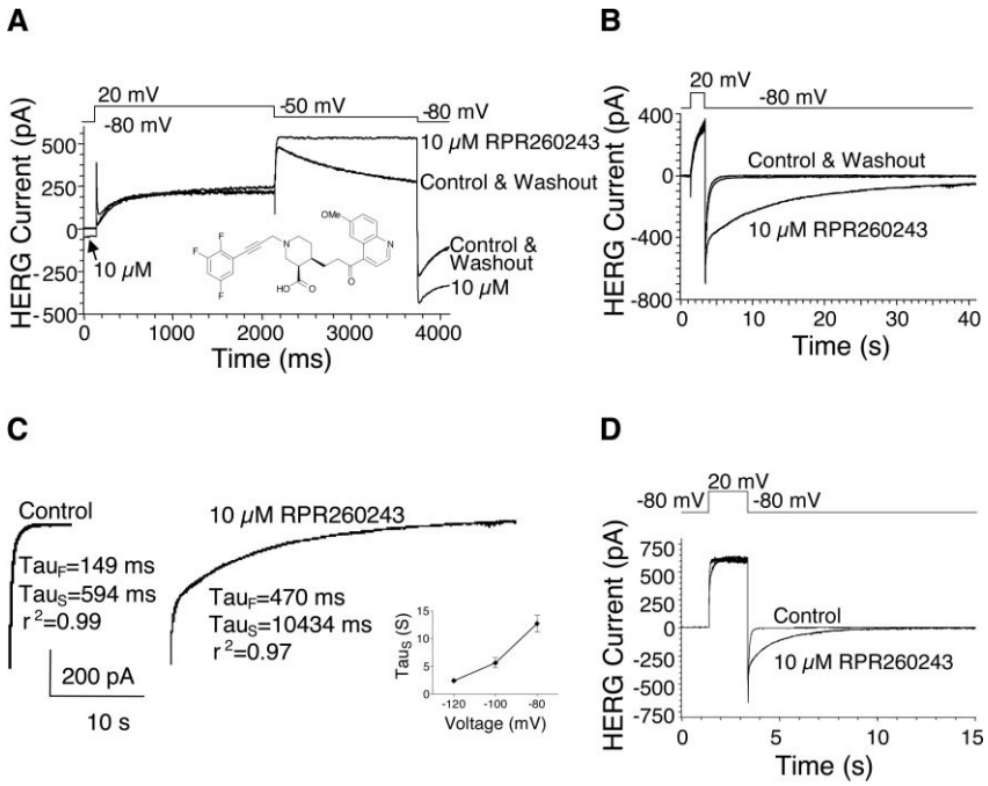

Figure 17: RPR260243 effects on hERG currents: Slow deactivation, produces persistent currents at room temperature (A, B) and 37°C (D). Effects are reversible and voltage-dependent (C). Chemical structure shown in A (68).

Selectivity and Interactions

RPR260243 exhibits a high degree of specificity in its action. Research has shown that it does not significantly interact with either cardiac sodium channels or KCNQ1/KCNE1 potassium channels. This selective behavior is particularly noteworthy because these ion channels, like hERG, are also associated with Long QT Syndrome. The compounds ability to target hERG channels without affecting these other important cardiac ion channels underscores its potential therapeutic value (18). Additionally, it acts as a weak inhibitor of cardiac L-type Ca^{2+} channels with the potency of inhibition linked to specific amino acid residues in the channel structure (31) (65) (65).

The mechanistic understanding of RPR260243s action is further enhances by insights into its interaction with specific amino acids within the hERG channel. The presence of threonine at position 556 in hERG enhances the effectiveness of RPR260243, while an isoleucine at the corresponding positon in rERG3 introduces an additional blocking effect. This single amino acid difference

illustrated the complexity of channel interactions and the importance of molecular structure in pharmacological activity (18) (65).

Therapeutic Potential

RPR260243 shows promise in managing certain forms of Long QT Syndrome, particularly Type 2 caused by mutations affecting hERG channel deactivation. Its ability to enhance protective currents without significantly increasing hERG current during the action potential suggests a nuanced approach to preventing arrhythmias while minimizing the risk of excessive action potential shortening (65).

Limitations and Considerations

Despite its promising profile, several limitation and considerations must be acknowledged. At higher concentrations, RPR260243 may lead to undesirable changes in cardiac action potentials. While it is highly selective for hERG channels, its weak inhibition of L-type Ca 2+ channel may have unintended consequences that warrant further investigation. Most studies conducted thus far have been in vitro or ex vivo, highlighting the need for more comprehensive in vivo studies to fully understand the compounds effects within complex physiological systems. Careful dosing is crucial to avoid excessive shortening of action potential duration, which could lead to Short QT Syndrome. Similar to other hERG agonists, RPR260243 could potentially induce excessively short action potential duration and refractoriness, creating a substrate for reentry based arrhythmias (65).

5.2.2 Ginsenoside Rg3

Ginsenoside Rg3 is an active compound found in Panax ginseng, a traditional herbal remedy widely used in East Asian medicine. It is classified as a type 1 hERG channel activator. Unlike other hERG activators such as RPR260243, Ginsenoside Rg3 is effective at much lower concentrations, with an activation threshold as low as 0.4 μM. It can activate the channels at more negative voltages and at a concentration of 3 μM, it doubles the current through the channels (31) (69).

Mechanism of Action

The mechanism by which Ginsenoside Rg3 activates hERG channels involves its interaction with specific binding residues located at the voltage sensor of the channel. In the S1 segment, the binding residue is Y420, while in the S2 segment, there are two binding residues: L452 and F463. Finally, in the S4 segment, the binding residues are I521 and K525. This specific interaction profile suggests that Ginsenoside Rg3 may have a unique mechanism of action compared to other hERG channel activators, potentially allowing it to activate the channels at more negative voltages (2) (70).

The regulatory impact of Ginsenoside Rg3 on hERG channels become more pronounced as its concentrations increases. Even at lower levels, this compound demonstrates a notable ability to modulate channel function. As the concentration rises, Rg3 effect on the tail current becomes particularly striking. It prolongs the currents duration, effectively slowing down the process of hERG channel deactivation. This relationship between concentration and effect underscores the potent and nuanced influence Ginsenoside Rg3 exerts on these crucial ion channels (69).

Ginsenoside Rg3 impact on hERG channels extends beyond its direct effects, as its breakdown products also influence channel function in diverse ways. The metabolite Protopanaxadiol (PPD) does not directly affect the channel but can counteract Rg3 actions by inhibiting its effects. Conversely, Compound K (CK) slows down hERG channel deactivation, resulting in a substantial, long-lasting tail current. Protopanaxatriol (PPT), another metabolite, has the opposite effect, speeding up the channels deactivation process. These varied

interactions highlight the complex nature of Ginsenosid Rg3 influence on hERG channel activity (69).

Moreover, specific metabolites of Ginsenoside Rg3, like PPD, can counteract its influence on hERG channels by preventing the Rg3-mediated delay indeactivation. This antagonistic action indicates an intricate interaction between Ginsenoside Rg3 and its metabolites, potentially influencing its overall therapeutic effectiveness (69).

As the Figure 18 shows, Compound K (CK) primarily influences the deactivating-tail current of hERG channels, which occurs at the end of repolarization. It does not significantly affect the main hERG current or the initial tail current during this phase (69).

CKs main effect is to slow down the deactivation of hERG channels, causing the current to persist longer. This means the channels remain open for an extended period, allowing more potassium ions to flow out. As a result, the current does not decay normally in the presence of CK but instead stays elevated, leading to a large, persistent outward current (69).

The effect of CK on the persistent deactivating-tail current is concentration-dependent. Higher concentrations of CK result in a stronger effect with an EC50 of 16.6 μM, indicating that CK is quite effective at prolonging channel activity (69).

Additionally, CK causes a leftward shift in the activation curve of hERG channels. This shift allows the channels to open at more negative voltages than usual, making them easier to activate even at lower voltages (69)

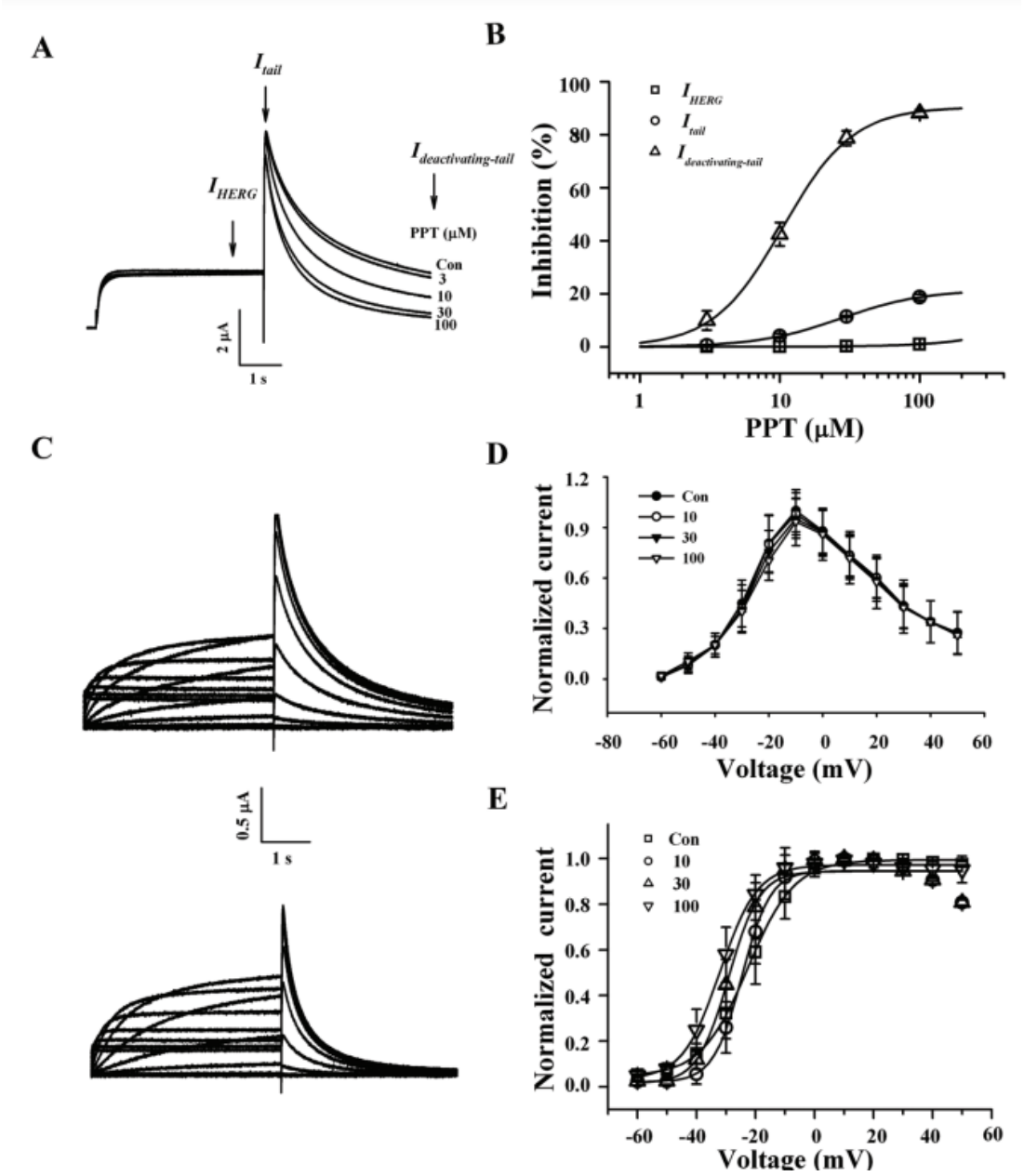

Figure 18: Impact of Compound K on hERG K+ Channel Currents (69)

Protopanaxatriol (PPT) (Figure 19) primarily affects the deactivating-tail current of hERG channels, which occurs at the end of repolarization. Unlike Compound K, PPT does not significantly impact the main hERG current or the initial tail current (69).

PPT accelerates the deactivation of hERG channels, causing the tail current to decay faster. This results in the channels closing more quickly, reducing potassium ion flow. The effect is concentration-dependent with an IC50 of 10.6 μM, indicating PPTs effectiveness in shortening the current duration (69).

Unlike CK, PPT does not shift the activation curve, meaning it does not make the channels easier to activate at lower voltages. Instead, it mainly affects how quickly the channels close (69).

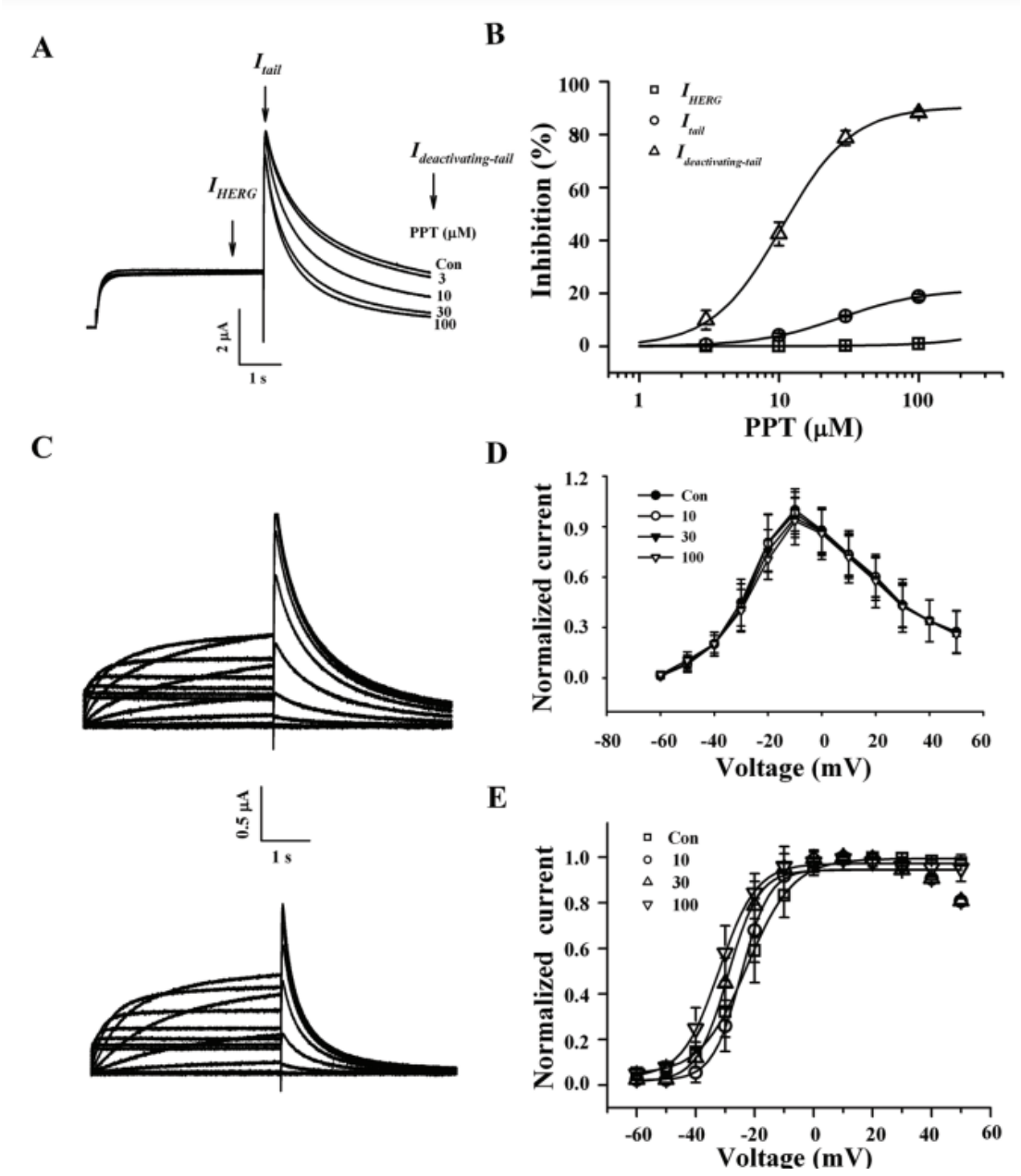

Figure 19: Impact of Protopanaxatriol on hERG K+ Channel Currents (69)

Protopanaxadiol (PPD) (Figure 20) alone has minimal effect on hERG channel activity, including the main current, tail current and deactivating-tail current. However, in the presence of Ginsenoside Rg3, PPD counteracts Rg3 effects

by blocking its enhancement of the deactivating-tail current. This results in the channels closing faster than they would with Rg3 alone (69).

The antagonistic effect of PPD on Rg3 is concentration-dependent, shifting the concentration response curve of Rg3 to the right. PPD does not alter the activation curve, meaning it does not change the voltage at which hERG channels open. It only reverses Rg3 effect on prolonging channel opening (69).

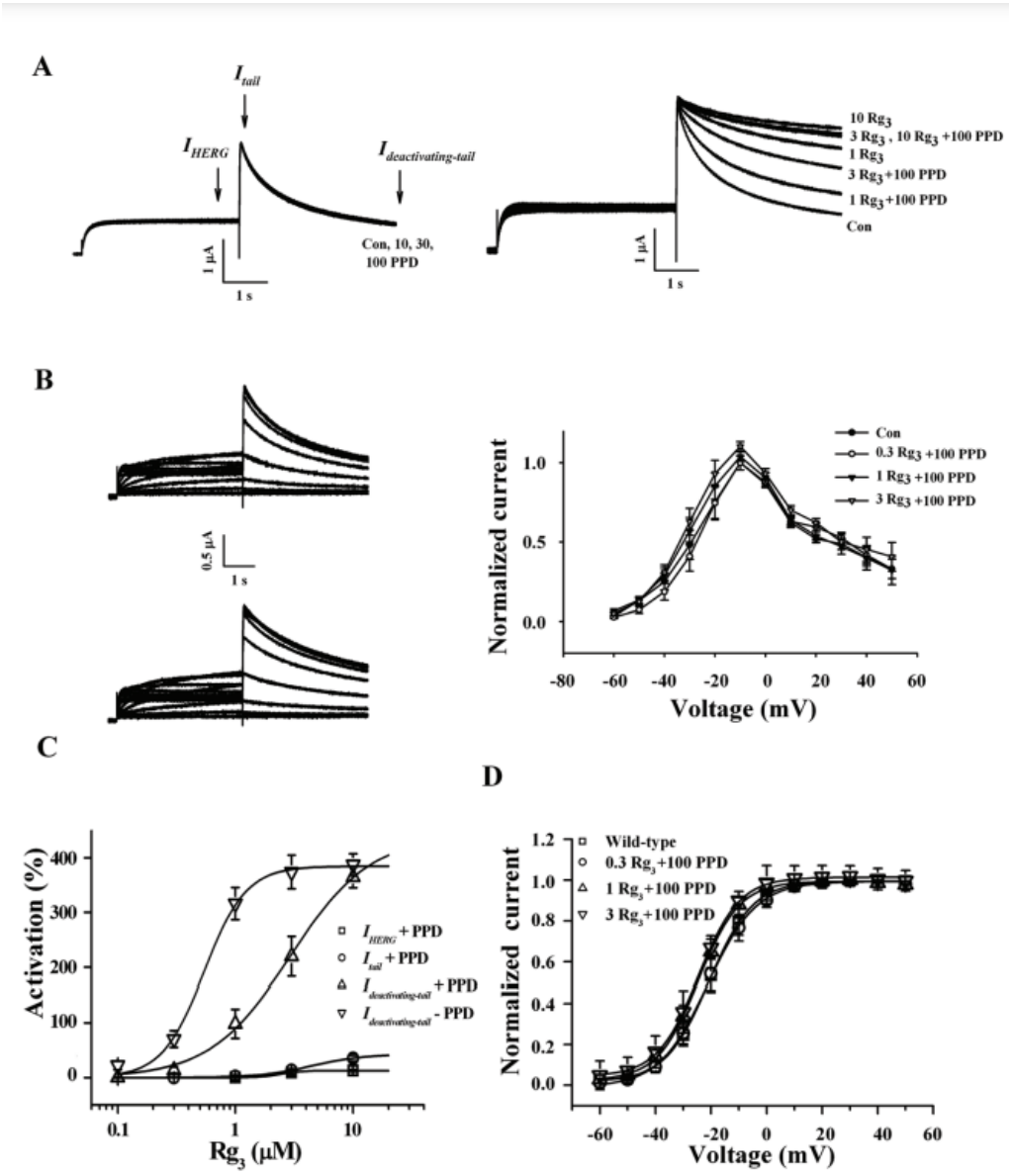

Figure 20: Impact of Protopanaxadiol (PPD) on hERG channels (69)

Effects on other ion channels

While RPR260243 does not affect other channels, Ginsenoside Rg3 influences additional ion channels such as KCNQ1 and KCNQ1/mink (31).

This broader spectrum of activity may contribute to its diverse pharmacological effects, including its potential role in regulating cardiac rhythm and function (69).

Antitumor Properties

In addition to its effects on ion channels, Ginsenoside Rg3 has shown strong antitumor properties in both in vitro and in vivo studies. It can be utilized either alone or in combination with other chemotherapeutic agents to enhance therapeutic efficacy. One of the key mechanisms by which Ginsenoside Rg3 enhances the efficacy of chemotherapy is by promoting apoptosis and slowing down cell growth (71). For example, it has been found to make cancer cells more sensitive to chemotherapy by influencing various signaling pathways, such as the PI3K/AKT pathway, which is critical for cell survival and proliferation (72) (73).

Clinical applications and efficacy

Ginsenoside Rg3 has been investigated for its potential in treating various cancers, including lungs, prostate and gastric cancers. Studies have demonstrated that it seems to make cancer cells more sensitive to drugs they have become resistant to, which could make chemotherapy work better. For example, in lung cancer studies, Ginsenoside Rg3 has shown some promising results. It appears to boost the effectiveness of drugs like Osimertinib by making cancer cells less stem-like and more likely to die off. Researchers have also discovered that Ginsenoside Rg3 can enhance the efficacy of Gefitinib, a widely used medication for lung cancer (72) (74).

Cardioprotective Effects

Research has also uncovered that Ginsenoside Rg3 offers protective benefits for the heart. It helps shield heart muscle cells from damage caused by oxidative stress by activating the Nrf2-antioxidant response pathway. This activation leads to the upregulation of various antioxidant enzymes, which in turn reduces oxidative damage and improving cardiac function. Moreover, Ginsenoside Rg3 has been reported to improve endothelial function and

reduce vascular contraction, which may further contribute to its cardioprotective properties (75) (76).

5.2.3 LUF7346

Mechanism of Action

LUF7346 is identified as a type 1 activator of hERG channels. It exerts its effects primarily by slowing the deactivation of I_{Kr} channels and positively shifting the steady state inactivation curve of these channels. These actions help in managing the therapy for both acquired and inherited long QT syndrome (77).

Comparison with other activators

In contrast to RPR260243, LUF7346 shows a more pronounced reduction in hERG channel inactivation. Despite this stronger effect on inactivation, LUF7346 has not been linked to a higher risk of causing arrhythmias. This favorable safety profile may be attributed to LUF7346s minimal impact on other types of ion channels, especially when compared to the broader effects of RPR260243 (2).

Effects on I_{Kr} current

Although the available research does not offer a complete picture of how LUF7346 interacts with all ion channels, some insights have been gained. The I_{Kr} current was studied using HEK293 cells to investigate the effects of LUF7346. Experiments with a concentration of 3 µM of the LUF7346 activator unfortunately showed no changes that affected the I_{Kr} current directly. However, a shift in the inactivation point was observed. This influences the I_{Kr} current in that it remains active over an extended voltage range. LUF7346 also slowed down the deactivation speed of the current. Nevertheless, LUF7346 enhances the I_{Kr} current by shifting the inactivation process and delaying deactivation (77).

Pharmacological Profile of LUF7346

Figure 21 provides an overview of the activity of the activator LUF7346. Image A shows the chemical structures of compounds LUF7243, LUF7244, LUF7344 and LUF7389. Illustration B demonstrates that LUF compounds significantly increased the binding of [3H] Dofetilide. It shows a comparison between the absence and presence of 10 and 50 µM of the LUF compounds after 6 minutes of dissociation. The graphics in C present the effects of LUF7346 on activation, inactivation and deactivation of the hERG channel. The activation and inactivation curves for I_{Kr} in D demonstrate that LUF7346 shifts the inactivation of the channel. Finally, E clearly shows that the time constants of deactivation were prolonged by LUF7346 (77).

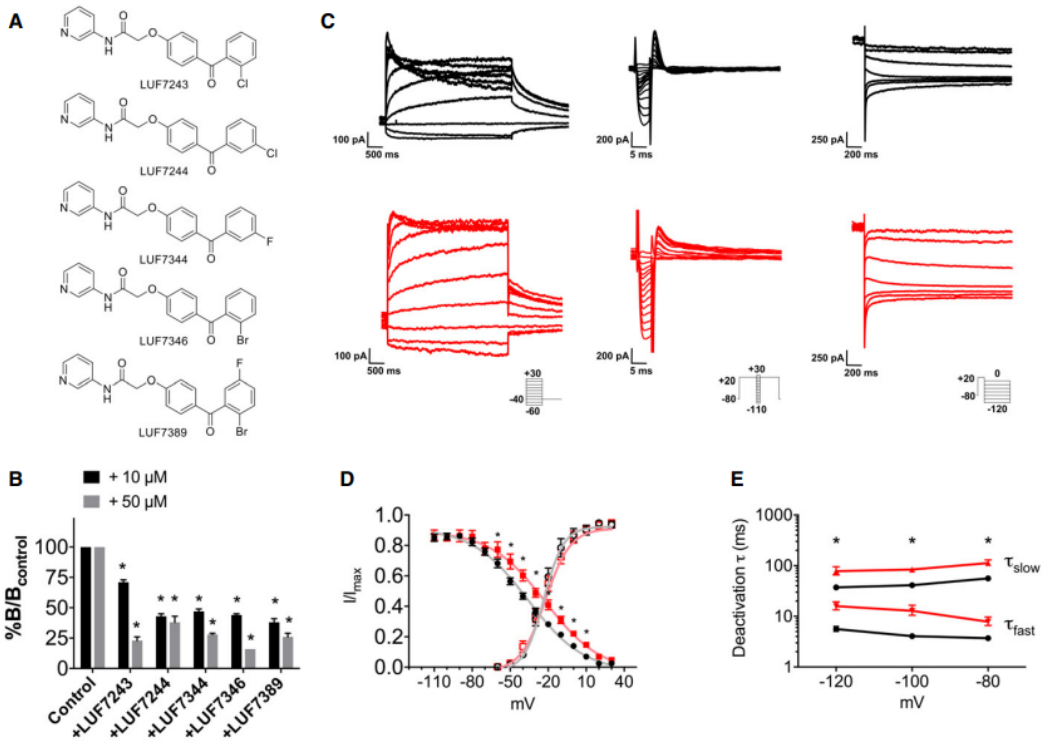

Figure 21: This Figure from Sala et al. shows the effect of the allosteric modulator LUF7346 on the IKr current in HEK293-hERG cells (77)

Impact on other ion channels

Studies have shown that when applied at a concentration of 10 µM to HEK293 cells, LUF7344, a structurally similar compound, did not influence the function of either I_{Kir} or I_{Na} channels. Furthermore, experiments using canine heart

muscle cells demonstrated that the same concentration of LUF7346 had no substantial impact on Ica-L currents (78).

Genetic studies

A study by Sala et al. used cardiomyocytes derived from various genetic hiPSC lines. The cell lines were as follows:

1. LQT1R594Q/JLNSR594Q with different mutations in the KCNQ1 gene
2. LQT2N996I/LQT2corr with different mutations in the KCNH2 gene
3. LQT1R190Q/LQT1corr with different mutations in the KCNQ1 gene
4. hESCWT/hESCLQT2N996I with different mutations in the KCNH2 gene

The cell lines responded differently to the experiment. The QT interval had varying lengths depending on the cell line. On one hand, JLNSR594Q showed a longer QT interval than LQT1R594Q, while on the other hand, the QT interval in LQT2N996I was longer than in LQT2corr. The wild type demonstrated that genetics have a significant influence on the QT interval (77).

Potential therapeutic applications

LUF7346 holds potential as a treatment for both inherited and acquired types of LQTS. An experiment utilizing matched pairs of induced pluripotent stem cells (iPSCs) carrying the LQT2-linked KCNH2 mutation c.A2987T (N996I) demonstrated LUF7346s ability to counteract the LQTs characteristics. Moreover, in this same cellular model, LUF7346 successfully restored proper channel activity in cases where QT prolongation had been artificially induced by drugs (2).

Future research Directions

Given these properties, LUF7346 emerges as an intriguing candidate for additional research, particularly in the context of treating inherited and drug-induced forms of LQTS. Nevertheless, a comprehensive understanding of its possible therapeutic applications and safety considerations requires more detailed and extensive investigations (2) (77) (78).

5.2.4 ICA-105574

Mechanism of action

This activator is classified as a type 2 hERG channel activator. ICA-105574 exerts its effects by interacting with a specific area of the hERG channel, a hydrophobic pocket. It is located underneath the selectivity filter, between two subunits that form the pore region with residue F557, located at the S5, being a key interaction partner. By binding to this site, ICA-105574 alters the channels behavior, promoting a state where ion can flow more freely and reducing the likelihood of the channel entering its non-conductive inactivated state (79).

Effects on channel function

It affects both voltage gated inactivation and at higher concentrations channel activation. ICA-105574 induces a significant change in the voltage-dependent inactivation of the channel, moving it 180 mV towards more positive voltages. This alteration leads to a tenfold enhancement of outward current under normal physiological conditions. When present in high amounts, this activator can also affect the channels activation process, causing it to occur at more negative potentials (18) (77).

Potency and effectiveness

ICA-105574 stands out for its strong effectiveness, reaching half of its maximum impact at a concentration as low as 0.43 μM, which highlights its potency. At its highest effect, the drug boosts the current by 5.5 times, demonstrating its powerful ability to activate the hERG channels (80).

Impact on current-voltage relationship

What makes ICA-105574 particularly interesting is how it affects the current voltage (I-V) relationship. It reshapes the typical bell-shaped curve, altering the way the channel responds to voltage. At a concentration of 2 μM, this effect becomes even more pronounced, causing a noticeable shift in the voltage curve (80).

Physiological effects

In guinea pigs hearts, ICA-105574 leads to a shortening of the action potential, which can be counteracted by E-4031, known hERG channel blocker (18) (77).

Concentration dependent effects

Figure 22 shows that ICA-105574 affects hERG currents in a concentration dependent manner. This became evident when an experiment using 0.3, 1 and 3 µM showed increasing activation. The maximum effect was achieved at 3 µM. The Figure 22 B illustrates the voltage-current relationship at a concentration of 2 µM, where currents through the membrane were measured a various voltages. Without ICA-105574, the currents show no change. Meanwhile, a concentration of 2 µM visibly enhances the currents. In the diagram below, the measured currents at different voltages were compared (80).

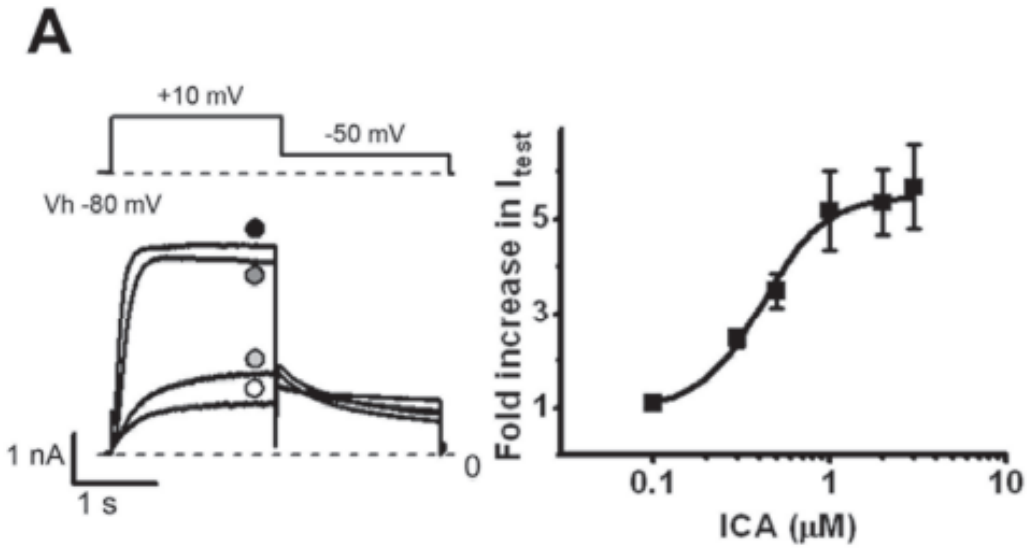

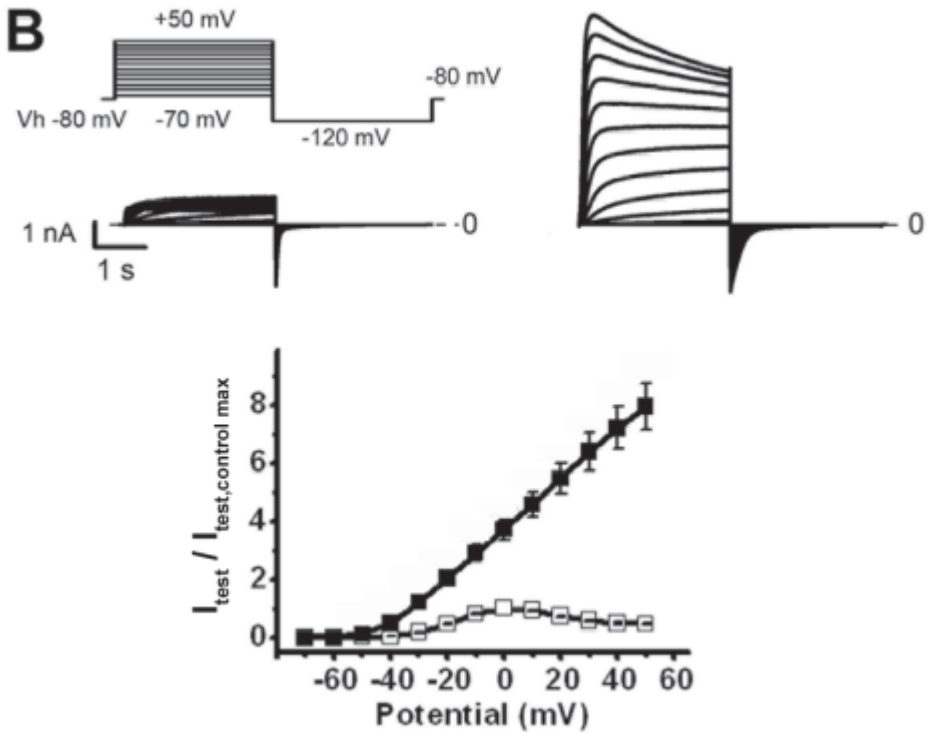

Figure 22: Effect of ICA-105574 on hERG currents in HEK293 cells (80)

Limitations

Although lower concentrations of ICA-105574 successfully activate hERG channels, higher doses can cause negative side effects, limiting its therapeutic range (81) (82).

When used in higher doses (3 µM or more), ICA-105574 might shorten the hearts action potential too much. This over-correction could potentially result a short QT syndrome, which might increase the chances of a dangerous heart rhythm problem known as ventricular fibrillation (83) (84).

5.2.5 AZSMO-23

Mechanism of action

AZSMO-23 (N-[3-(1H-benzimidazol-2-yl)-4-chloro-phenyl] pyridine-3-carboxamide) is classified as a type 2 hERG channel activator, which induces a shift in the voltage dependence of inactivation. Its activator activity is enhanced in the presence of the F656T mutation. However, when the Y652A mutation is present, AZSMO-23 functions as a blocker. While AZSMO-23 has a similar mechanism of action to ICA-105574, the shift in voltage dependence of inactivation induced by AZSMO-23 is only 74.5 mV, compared to the 180 mV shift caused by ICA-105574 (2) (83).

Effects on various Ion Channels

An important consideration is that AZSMO-23 exhibits a lack of specificity for hERG channels. The compound demonstrates diverse effects on various ion channels. For example it inhibits hKv4.3-hKChIP2.2, hCav3.2 and hKv1.5 channels. In contrast, it activates hCav1.2/ β2/α2δ channels (85).

Experimental Observations

An experiment conducted by Manniko et al. reveals the effects of AZSMO-23 on the hERG channel. Figure 23 A illustrates the current levels before and after a 5-minute treatment with AZSMO-23. This graph shows the pre-pulse current at various voltages following the treatment, highlighting a significant change in the channels behavior. Meanwhile, Figure 23 C displays the tail current in comparison to the control. It is clear that the impact on the tail current is less pronounced than the notable changes observed in the pre-pulse current (83).

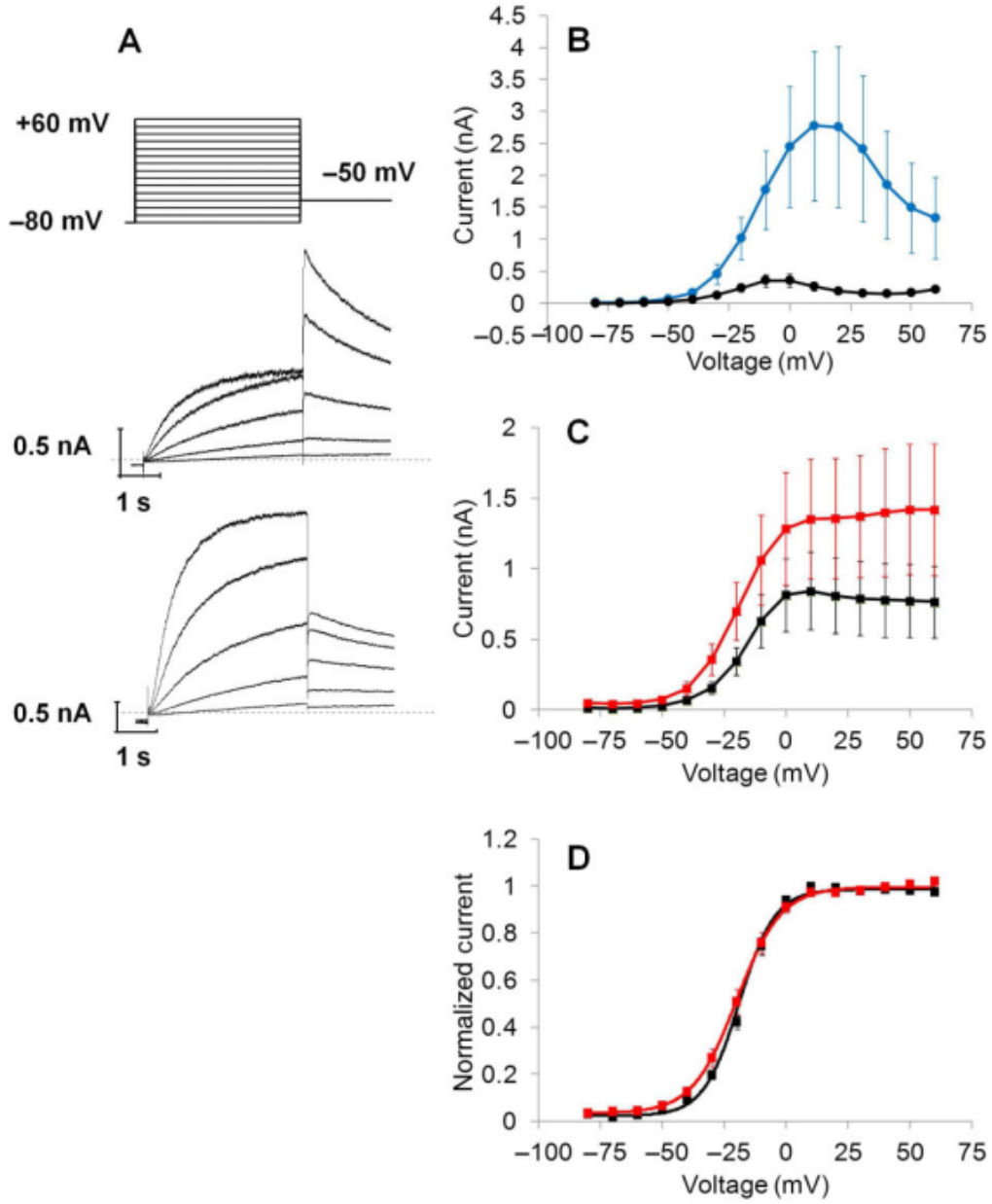

Figure 23: AZSMO-23 effects on the hERG channel (85)

5.2.6 Mallotoxin

Classification

Mallotoxin, a natural compound extracted from Mallotus phillippinensis, is a potent enhancer of hERG1 channel function. Its distinctive mode of action sets it apart from other hERG activators and is a member of the type 3 category of hERG channel activators. The alkaloid Mallotoxin shifts the voltage at which the channels typically open, leading to an increase in current strength. This mechanism allows Mallotoxin to increased hERG channel activity under normal cellular conditions (31) (86).

Effects on voltage sensitivity

Mallotoxin alters the voltage sensitivity of hERG channels. When applied at a concentration of 10 μM, it causes the activation threshold to shift by about 24 mV towards more negative potentials. This change enables the channels to become active at lower membrane voltages compared to their usual operating range (18).

Impact on channel kinetics and current

According to Zeng et al., Mallotoxin not only shifts the activation curve but also modifies channel kinetics. It speeds up the process of channel opening and delays channel closing. These effects together significantly boost the hERG current. Research has demonstrated that when exposed to Mallotoxin at a concentration of 2.5 μM, hERG channels exhibits an increase in potassium ion flux. Simulating cardiac action potentials, the total amount of potassium ions flowing through these channels was observed to increase by about five times compared to normal conditions (18).

Unique properties and potency

The special property of Mallotoxin is that it does not substantially change the voltage dependence of channel inactivation, setting it apart from type 2 activators. Mallotoxin exhibits exceptional potency, reporting EC50 values of 0.34 μM for step current and 0.52 μM for tail current. These values indicate that Mallotoxin is considerably more potent than many artificially synthesized hERG activators (18).

Experimental Findings

In Figure 24, an experiment conducted by Zeng et al. using the compound Mallotoxin at a concentration of 2.5 µM in CHO cells is shown. They applied a 2-second pulse at +20 mV, followed by another 2-second step at -50 mV to measure the tail current. This process was repeated every 10 seconds.

Panel B in Figure 24 shows that Mallotoxin reaches a maximum effect after approximately 500 seconds, which is blocked upon the addition of Dofetilide, a known hERG blocker. The final result, as illustrated in C, is that Mallotoxin increases the current, but this effect can be washed out when Mallotoxin is removed (86).

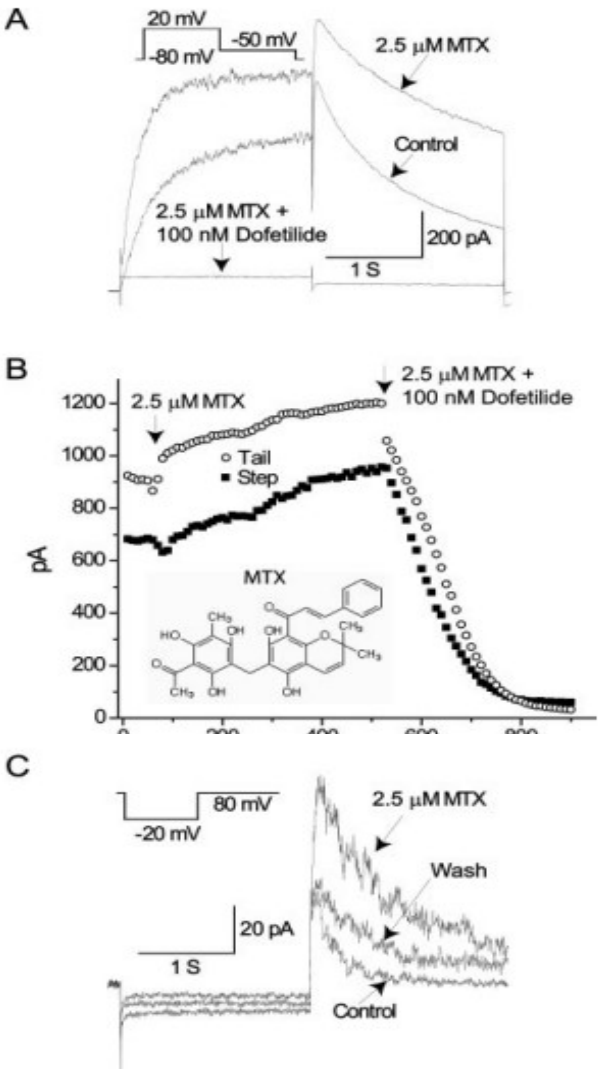

Figure 24: Mallotoxin enhances hERG channel currents; Dofetilide blocks this effect. The effect is reversible in inside-out patch experiment (86).

Dose effects and lowered activation potential

The findings also revealed that Mallotoxins effects are concentration-dependent as Figure 25 shows. Higher doses of Mallotoxin resulted in a more pronounced impact on the channel. Intriguingly, Mallotoxin also lowered the threshold at which the channel becomes active. Under normal conditions, the channel reaches peak activity at +30 mV. However, in the presence of 10 µM

Mallotoxin, this value shifted to +10 mV, indicating that the channel become more active at lower voltages (86).

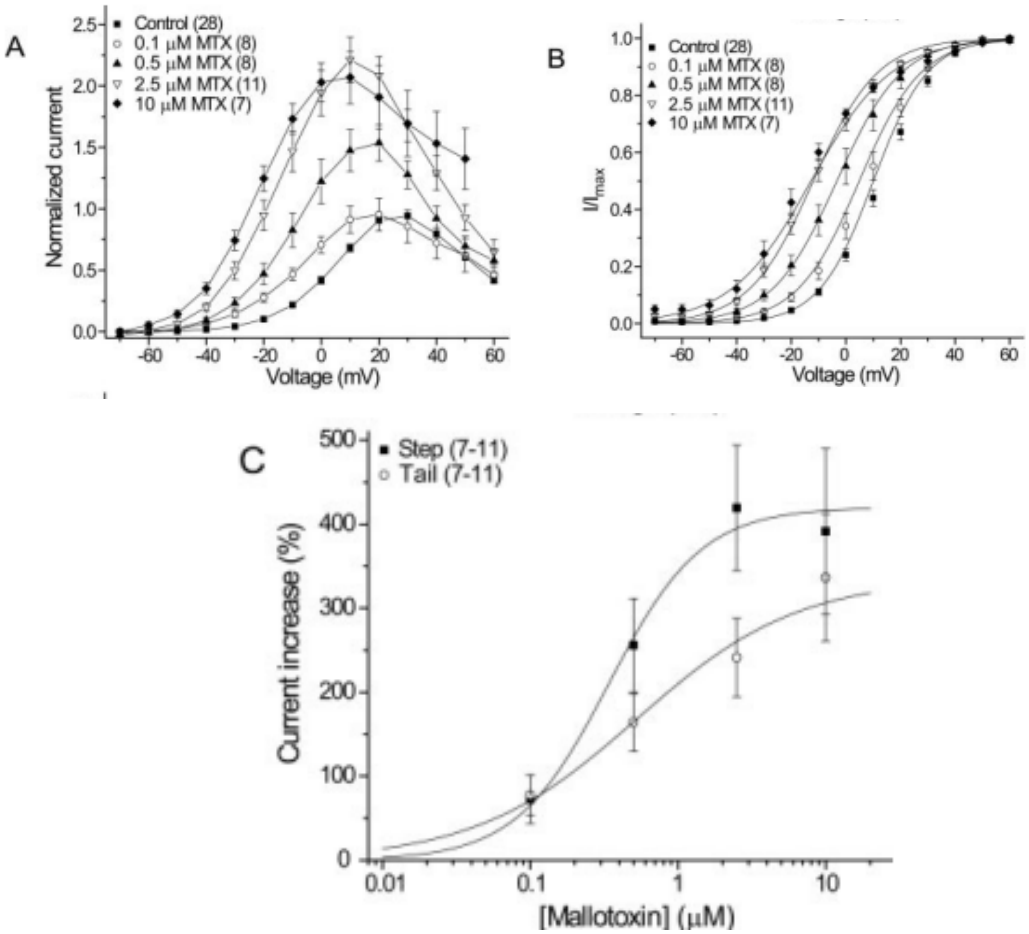

Figure 25: Overview how Mallotoxin enhances hERG channel acitivity by making the channels open at lower voltages and increasing current flow with the effect increasing as the concentration of Mallotoxin rises (86)

5.2.7 SKF-32802

Mechanism of action

SKF-32802, a type 3 activator, is characterized by its ability to shift the voltage dependence of channel activation towards more negative potentials (2) (87).

This activator interacts strongly with the selectivity filter of the hERG channel. Unlike some other hERG activators, SKF-32802 exhibits similar affinity for both the closed and open states of the channel. This characteristic sets it apart from type 1 and type 2 activators, which typically affect deactivation rates or inactivation gating (2) (87).

Electrophysiological Effects

SKF-32802 causes a reduction in activation time while leaving deactivation and inactivation unchanged. The reduction of the activation occurred from 371.1 ms to 135.6 ms, which significantly enhance the channels responsiveness during cardiac action potentials (87).

Impact on Channel Activity

SKF-32802 is capable of raising the plateau of the voltage-activation curve resulting in an enhancement of the channel activity (Figure 26). Figure 27 B illustrates the leftward shift of the activation curve induced by SKF-32802 (87).The key interactions partners for SKF32802 within the hERG channel are T623, S624, Y652 and F656 (87). Additionally, it is also known as a weak inhibitor of I_{Na} and for the L-type calcium channel (2).

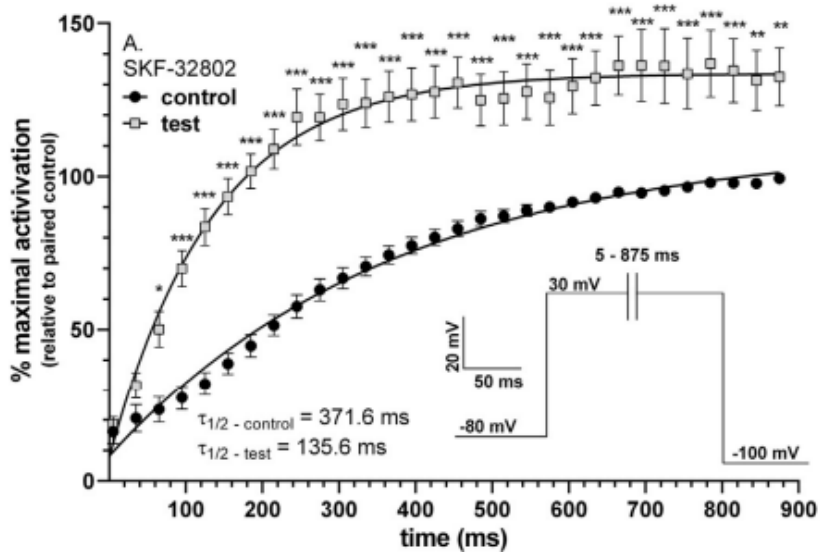

Figure 26: Representation of the activation kinetics of SKF-32802 (87) Comparison of voltage dependence of activation samples for SKF-32802 (B) and its corresponding control (A) (87)

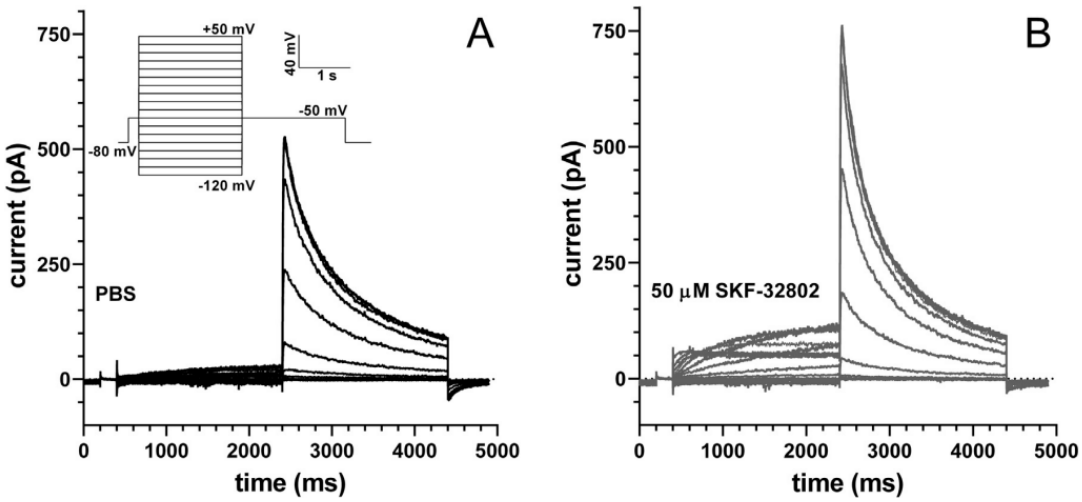

Figure 27: Comparison of voltage dependence of activation samples for SKF-32802 (B) and its corresponding control (A) (87)

5.2.8 KB130015

Voltage Dependence and Activation

KB130015 causes a negative shift in the voltage dependence of channel activation, allowing hERG channels to open at more hyperpolarized membrane potentials. It activates the channels more rapidly, specifically accelerating activation at -20 mV by 3.8 times faster. The deactivation is also accelerated by KB130015, but this effect is not as pronounced as the activation (31) (88).

Unlike Mallotoxin, KB130015 enhances the current through the channels at voltages below 0 mV. Specifically, at a concentration of 10 µM, the channels open at a voltage of -16 mV, whereas under normal circumstances, this would occur at a higher voltage (31) (88).

Concentration-Dependent Effects

KB130015 shows an enhancement of the current at higher concentrations. At 10 µM, the current reaches 264 % of its original value. At a concentration of 30 µM, the current is first enhanced and then slowly decreases. This confirms that KB130015 both activates and blocks the channel (Figure 28) (88).

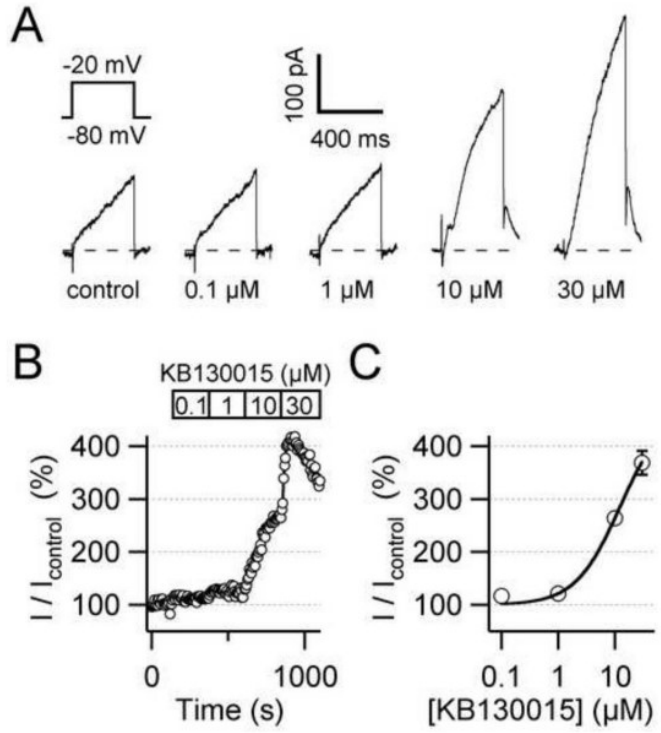

Figure 28: Illustration of activation and blocking by KB130016 and the concentration dependent effect (88)

Independence from Inactivation Mechanism

The experiment by Gessner et al. confirmed that KB130015 exerts its effect independently of the inactivation mechanism, which was demonstrated using a mutant hERG1-S620T (Figure 29) (88).

Mutants were utilized to demonstrate the independence from the inactivation mechanism. The mutants S631A and S620T slightly attenuated the blocking effect of KB130015 but the activating effect of KB130015 remained intact (88).

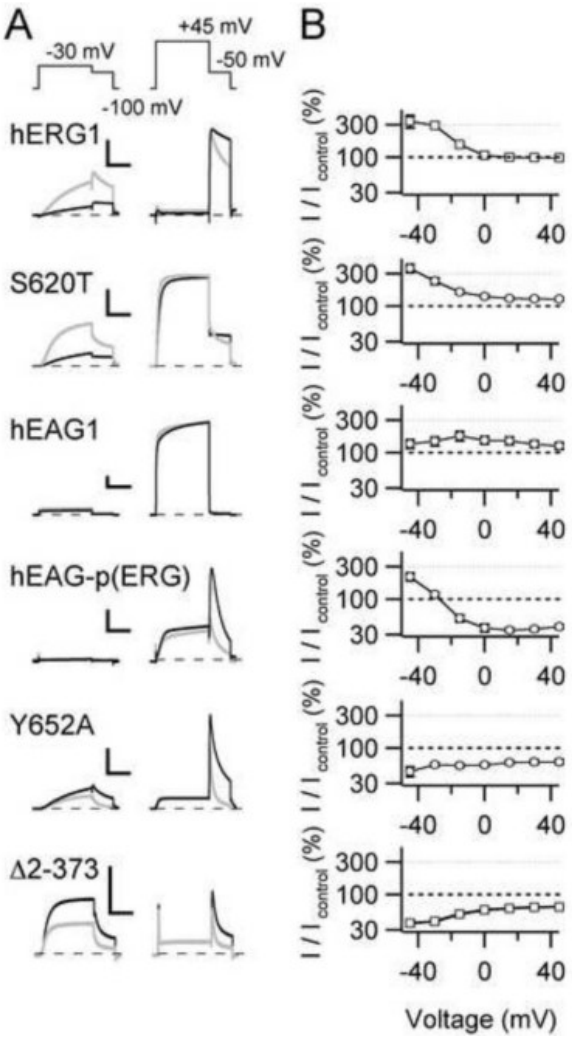

Figure 29: Overview that the activation of hERG1 channels by KB130015 depends on hERG1 gating (88)

Role of Specific Amino Acids

An experiment involving the Y652A mutation showed that this amino acid in the pore of the hERG1 channel is crucial for activation by KB130015. With this mutation, the enhancement of the current by KB130015 was completely

prevented but the channel continued to be blocked. This leads to the conclusion that the amino acid Y652 plays an important role in the binding of KB130015 and the opening of the channel (88). Gessner et al. propose that KB130015 my bind to a site outside the pore, similar to the mechanism suggested for RPR260243. They hypothesize that this binding site is accessible from the intracellular side when the channel is closed, and that the interaction with Y652 might be essential for linking KB130015 binding to channel activation (88).

5.2.9 SB335573

SB335573 is a type 4 hERG channel activator known for its strong interaction with the selectivity filter. It is distinguished by its equal affinity for both the open and closed states of the channel, facilitated by a hydrogen bond between the tetrazole nitrogen and the sidechain –OH. Additionally, it forms hydrogen bonds with S649 and M645 on a neighboring subunit. Similar to SKF-32802, a type 3 hERG activator, SB335573 acts as a weak blocker of the L-type calcium channel and the I_{Na} (2).

5.2.10 PD-118057

Mechanism of Action

PD-118057 is a hERG1 activator that increases the probability of channel opening allowing more current to pass through the channels. Unlike some other activators, PD-118057 enhances the current through the hERG channel without affecting its voltage-dependent gating mechanisms (31) (89).

Specificity and Effects on hERG Channels

In HEK293 cells, PD-118057 has been shown to double the current without altering the probability of the channels opening and closing. Notably according to Sanguinetti, PD-118057 does not affect other cardiac currents, making it relatively specific to hERG channels (31).

Experimental Studies

Researchers conducted experiments to examine the effects of PD-118057 on hERG channels. In one study, they used a concentration of 3 μM to investigate how PD-118057 affects the voltage-dependent activation of the hERG channel. HEK293 cells expressing different versions of the hERG channel were used and comparisons were made with and without the drug. These comparisons are visible in panels A-F of the Figure 30. Figures 30, G and H depict the current-voltage relationship, illustrating the channels open probability. The final figure shows the tail currents of the channels with the Boltzmann function applied for better understanding (89).

In another experiment, researches compared PD-118057 with Thapsigargin, a drug that works differently, to test how the two drugs react in normal and

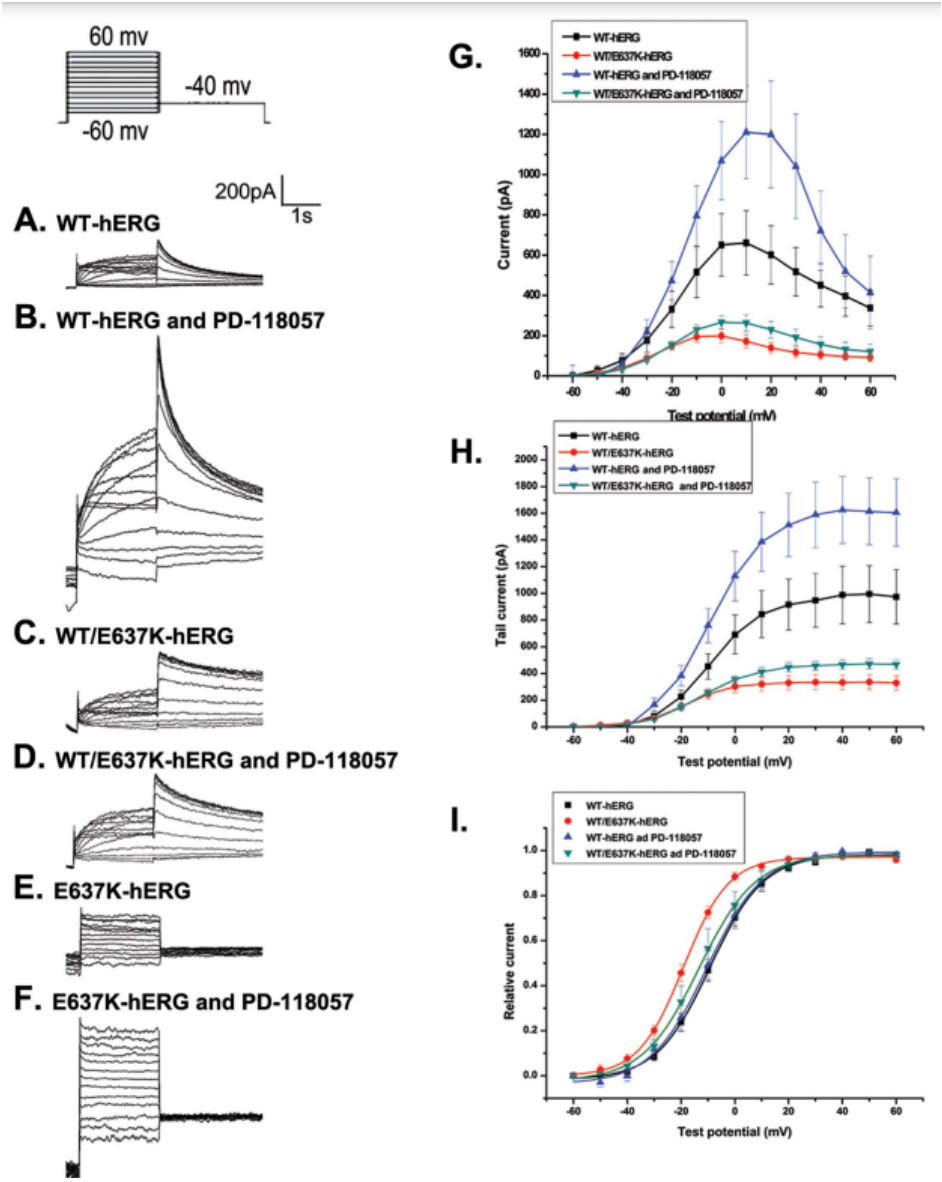

mutated hERG channels (89).The physiological effects of PD-118057 are significant. It contributes to the shortening of the action potential and QT interval, which could have important implications for treating certain cardiac conditions (31).

Figure 30: Figure from Mao et al. shows the effect of PD-118057 on the voltage-dependent activation of the hERG channel (89)

Compound	Effect on hERG1 channel				
	Slows rate of deactivation	Positive shift in V-dependence of inactivation	Negative shift in V-dependence of activation	Increases open probability (P_o)	EC_{50} (cell type)
RPR260243	+++	+			*n.d. (~3 µM)(CHO)[4]
Ginsenoside Rg3	+++		+		0.4 µM(X. o.)[17]
ICA-105574	+	+++	+		0.5 µM(HEK)[47]
Mallotoxin	+		++	+	0.4 µM(CHO)[22]
KB130015	+		++		12 µM(HEK)[23]
PD-118057		+		++	n.d. (~10 µM)(HEK)[24]
PD-307243		+		+	n.d. (~2 µM)(CHO)[27]
NS1643		+/-	++		10.4 µM (X. o.)[30]
NS3623		+		+	79 µM(X. o.)[48]
A-935142	+	+	+		n.d. (>20 µM)(HEK)[26]

Figure 31: Figure from Sanguinetti, M. gives an overview of the mechanisms of hERG1 channel agonists (31)

5.3 Multiple mechanism

Several hERG channel agonists exhibit multiple mechanisms of action. These activators demonstrate the complexity of hERG channel modulation and offer potential advantages in therapeutic applications (31).

The agonist, A-935142, caused a +15 mV shift in the V0.5 for inactivation, increased the rate of activation, and decreased the rate of deactivation. This is consistent with a -9 mV shift in the V0.5 for activation (31).

PD-307243 reduced the inactivation rate and increased the hERG tail current by 3.4 times at a concentration of 10 μM, without affecting the activation or deactivation rates of the channels (31).

NS1643 led to a maximum increase in hERG1 current by 300% at 10 μM, accelerated the activation rate, and shifted the V0.5 for activation by -27 mV. This shift develops gradually over time and is observed in oocytes only at much higher drug concentrations. NS1643 also shifts the activation curve of ERG2 and ERG3 channels to the left. Additionally, NS1643 slows the inactivation rate, either without a shift in CHO cells or with a positive shift in the V0.5 for inactivation in oocytes (31).

In awake guinea pigs, NS3623 shortened the QTc interval by 30% and normalized the QT interval prolonged by E4031. NS3623 also increased the QRS duration and slowed cardiac conduction at 10 μM in isolated guinea pig hearts perfused using the Langendorff method, an effect reversed by the I_{Kr} blocker E4031 (31).

Comparative Study

The compounds Dofetilide, Terfenadine and Verapamil were fitted to the experimental data and tested for accuracy. The left side of the Figure 32 shows how the drugs act over time based on 10 voltage pulses (82).

Dofetilide differs from Terfenadine and Verapamil as it remains “trapped” in the channels. All models except Model 0α were able to explain the data well (Figure 33). Model 0α could not show any change in current because it only considered conductance and not dynamics. In contrast, Terfenadine and

Verapamil are less “trapped”, which means that the current recovered between pulses, indicating drug unbinding. Only certain models were successful for Terfenadine, whereas all simple trapping models were excluded for Verapamil (82)

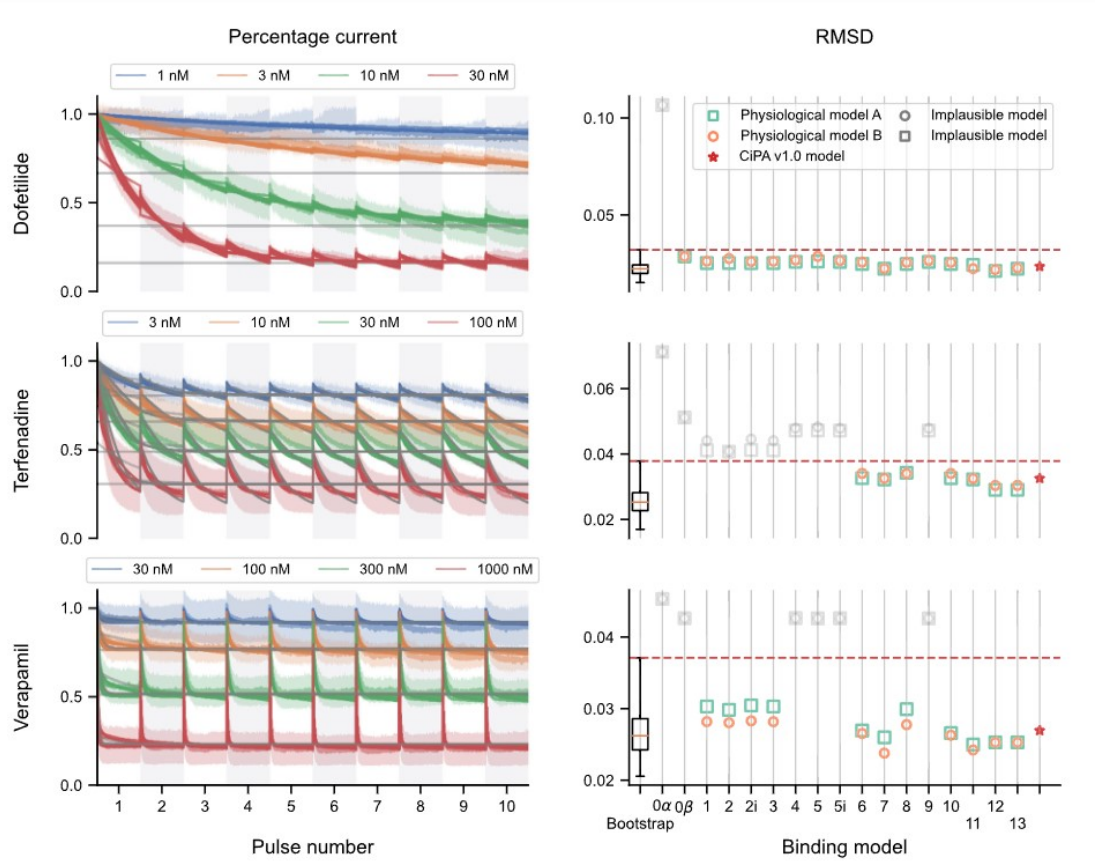

Figure 32: Calibration of the binding models and their RMSDs for Dofetilide, Terfenadine and Verapamil including comparison of the percentage current data with the calibrated models and the RMSD of the bootstrap samples compared to the reference model CiPA v1.0 (82)

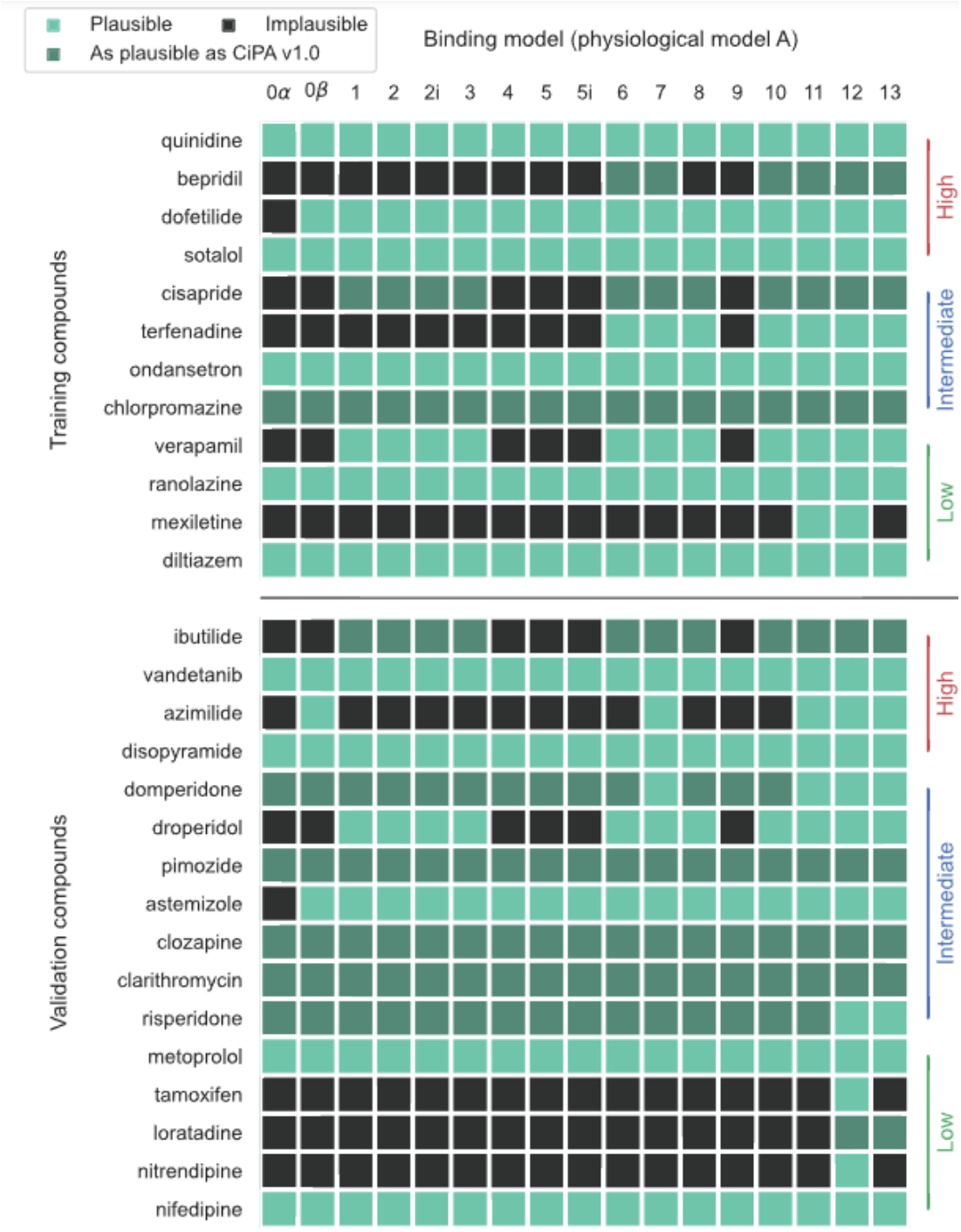

Figure 33: Overview of the binding models that were used (82)

6 Structural Insights from Cryo-EM Studies

Cryo-EM Structure of the Open Human Ether-a-go-go-Related K+ Channel hERG by Wang W. and MacKinnon R.

hERG is a highly senstive protein. Antibiotics, antimalarials, gastroprokinetic agents, antihistamines, antiarrhythmics as well as antipsychotics are inhibited by hERG, which indicates a high sensitivity to a wide range of substances. A justification for the high sensitivity could be the “central cavity” in the ion conduction pathway of hERG (1).

The study by Wang and MacKinnon determined the structure of the hERG potassium channel at 3.8 Å resolution using cryo-electron microscopy. A modified hERG construct (hERGT) was used in which certain amino acid sequences were removed to prevent aggregation during purification (Figure 34) (1).

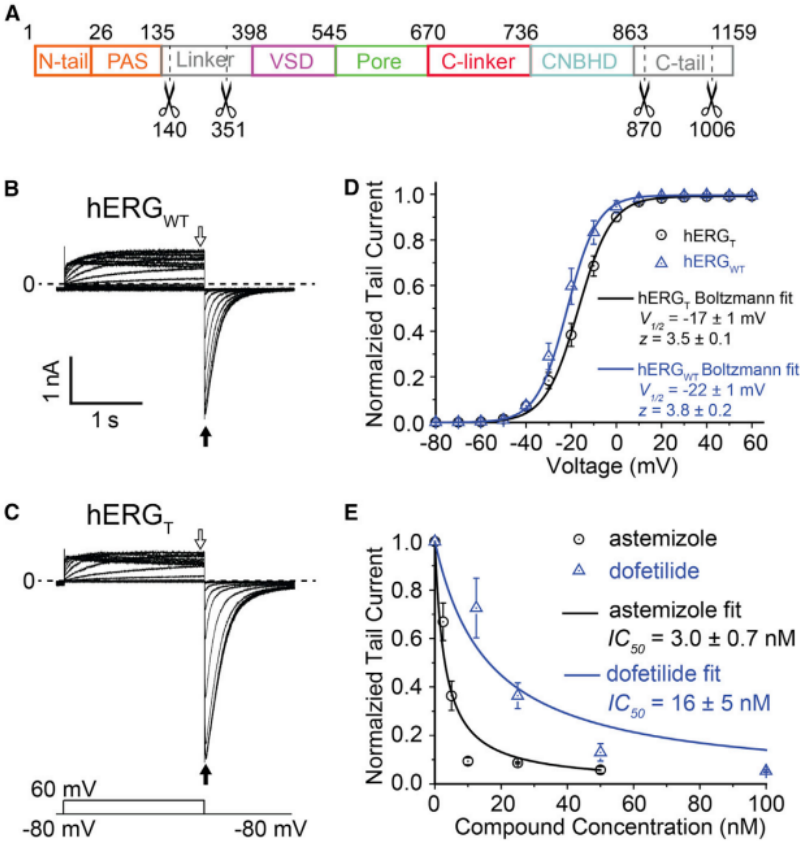

Figure 34: (A): The hERGT construct removes certain amino acid residues from the hERG primary structure to facilitate cryo-EM structure determination at a 3,8 Å resolution. (B): Voltage recordings show the electrical properties of wild type hERG (hERGWT) in transfected HEK293T cells. (C): Similar voltage recordings for the modified hERGT construct demonstrate its electrophysiological properties. (D): The normalized tail current curves show differences in voltage sensitivity and activation between hERGWT and hERGT. (E): Dose-response curves demonstrate the response of the hERGT cahnnel to the drugs astemizole and dofetilide, including IC50 values (1).

The hERG channel was expressed in HEK293S GnTI-cells at 37C and 5 % CO2. Electrophysiological measurements were performed in HEK293T cells. For the potassium concentrations, the bath solution contained 20 mM K+, while the pipette solution contained 120 mM K^+. Astemizole and dofetilide were used as test substances to study inhibition of the channel (1).

The structure in Figure 35 shows the channel in an open state with depolarized voltage sensor. An unusually small central cavity surrounded by hydrophobic pockets could explain the high sensitivity to many drugs (1).

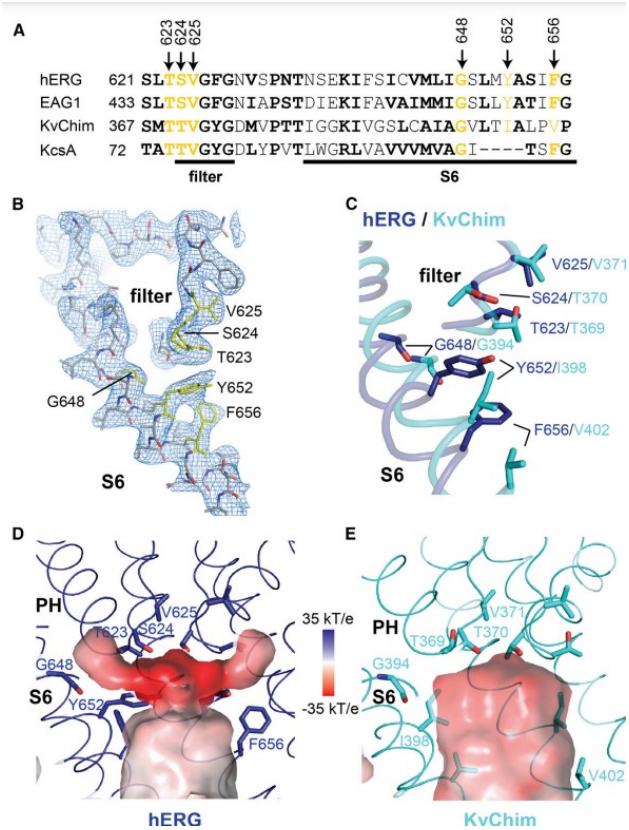

Figure 35: (A): The sequence alignment shows conserved amino acid residues and those associated with drug binding, with relevant residues highlighted in yellow. (B): The EM density map of the putative drug binding site is displayed as a blue mesh, while the molecular model shows the relevant residues in yellow. (C): The overlay of hERG and KvChim shows the position of drug-binding related residues near the central cavity. (D): The inner molecular surface around the central cavity of hERG is represented in terms of electrostatic potential, with relevant residues highlighted. (E): The inner molecular surface of KvChim is represented similarly to that of hERG to illustrate structural similarities (1).

A subtle structural difference in the selectivity filter may be related to rapid inactivation. The voltage sensors are not domain-swapped but packed against their own pore subunit. The study provides insights into the mechanism of voltage sensor activation and the causes of hERGs drug sensitivity (1).

Comparative analysis of various potassium channel structures revealed a nuanced but significant deviation in hERGs selectivity filter. The arrangement of the F627 side chain within the GFG sequence of hERG differs from the usual position of the corresponding phenylalanine or tyrosine in other K^+ channels. This distinctiveness could be related to hERGs exceptionally rapid inactivation (1).

To test this hypothesis, a mutant (S631A) of the hERG channel with slowed inactivation kinetics was analyzed (Figure 36). Interestingly, the selectivity filter of this mutant showed a configuration similar to that of other potassium channels. This observation supports the hypothesis that the specific positioning of F627 in the wild type could be related to the process of rapid inactivation (1).

These findings suggest that the observed structure of wild-type hERG might represent an inactivated state, which is manifested by the unusual arrangement of the phenylalanine in the GFG sequence (1).

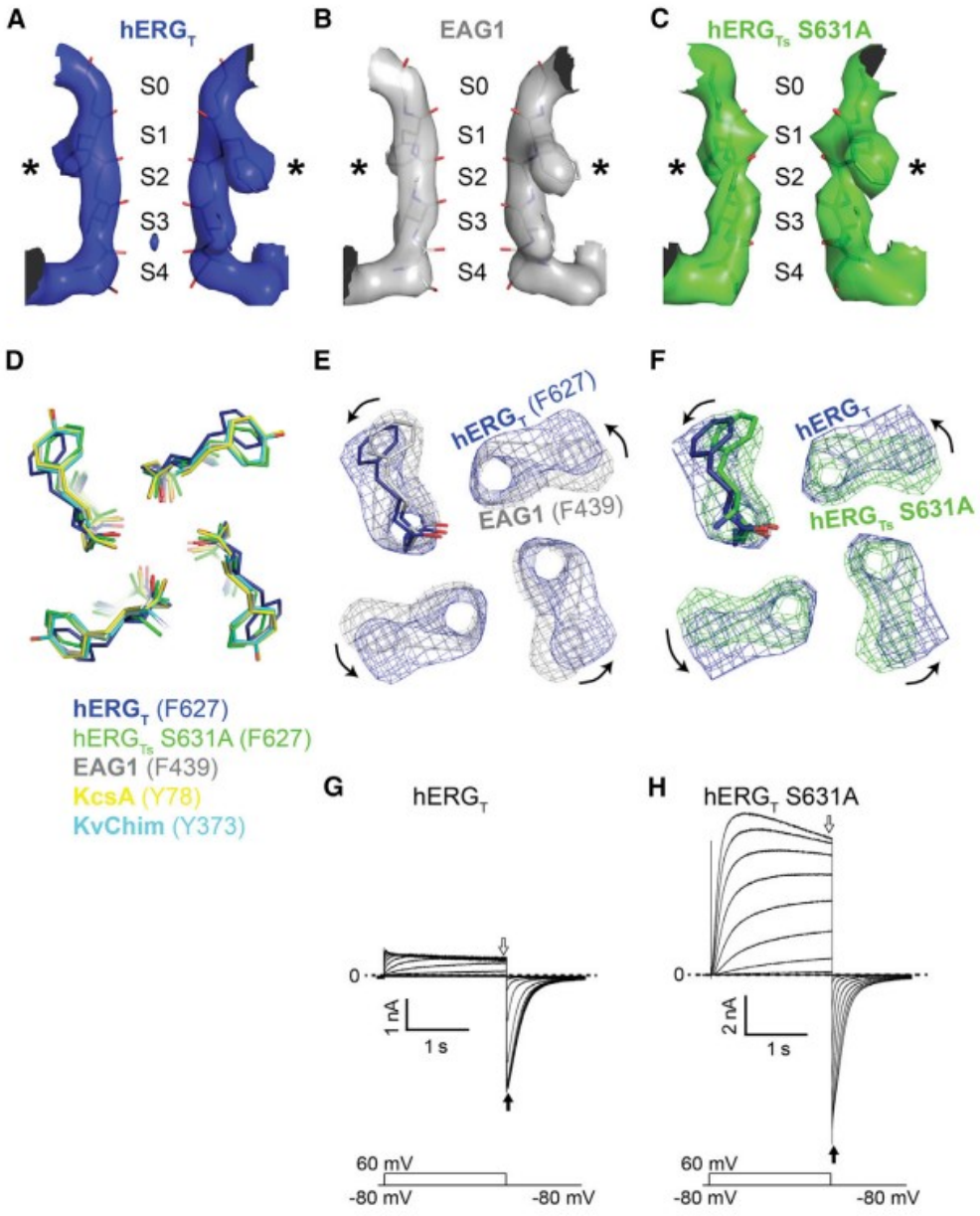

Figure 36: (A-C): The side view of the cryo-EM density maps shows the selectivity filters of hERGT, EAG1 and the non-inactivating mutant hERGTs S631A, highlighting the positions of the aromatic residues. (D): The overlay of the aromatic residues in the selectivity filter illustrates the differences between hERGT, hERGTs S631, EAG1, KcsA and KvChim. (E): The density maps of F627 in hERGT and F439 in EAG1, viewed from the extracellular side, show a counterclockwise rotation of the residue. (F): The overlay of the density maps and models of F627 in hERGT and hERGTs S631A highlights the structural differences between the two variants. (G-H): Representative whole-cell voltage

recordings demonstrate the electrical properties of hERGT and the non-inactivating mutant hERGT S631A in HEK293T cells (1).

Potassium dependent structural changes in the selectivity filter of HERG potassium channels by Lau, C. H. Y et al.

hERG potassium channels have a uniquely rapid inactivation kinetics. The study determined structures of both the conducting and non-conducting selectivity filter of hERG (Figure 37) (90).

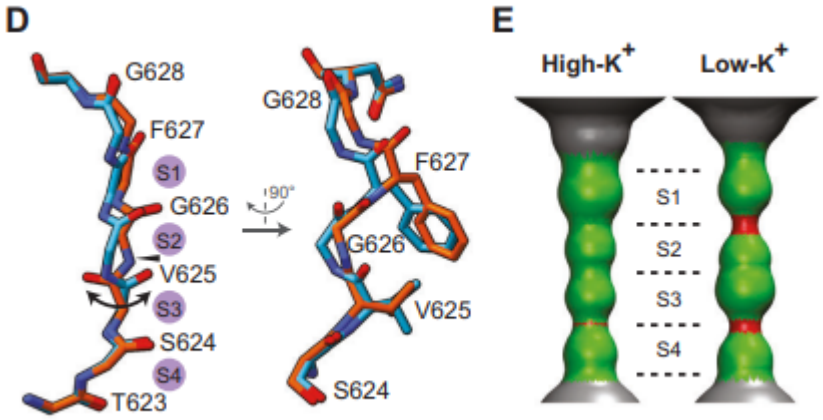

Figure 37: Figure from Lau et al. shows (D): The overlay of structures shows that a low K+ concentration, the backbone of F627/G628 and the V625 carbonyl experience significant displacements. (E): The selectivity filter profile shows an expansion at V625 and constrictions at S624 and G626 at low K+ concentration compared to the high-K+ structure (90).

In the conducting state, the selectivity filter exhibits a cylindrical shape. Conversely, in the non-conducting state, the valine backbone carbonyls are oriented away from the central axis of the channel (90).S620 on the pore helix plays a central role through different interactions in the various states, stabilizing different parts of the filter via interactions (Figure 38) (90).

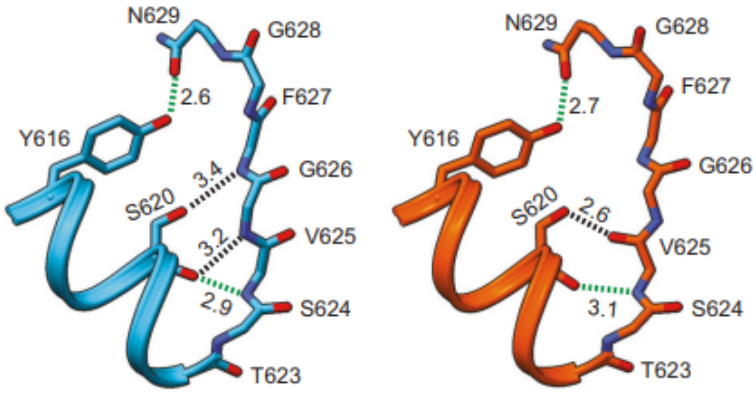

Figure 38: Figure from Lau et al. represents the structures with high (blue) and low (orange) K+ concentrations exhibit different hydrogen bonding patterns, particularly regarding the interactions of the S620 side chain (90).

At high K+ concentration (300 nM), the filter shows a cylindrical shape with inward-facing carbonyl groups. At low K+ concentration (3 mM), when the hERG channel is inactivated, the V625 carbonyl groups are rotated outwards. MD simulations show that ion conduction occurs with inward-facing V625 carbonyls but not with outward-facing ones. At high K+, S620 coordinates interactions with F627/G626 amides and at low K+, with flipped V625 carbonyl (Figure 39) (90).

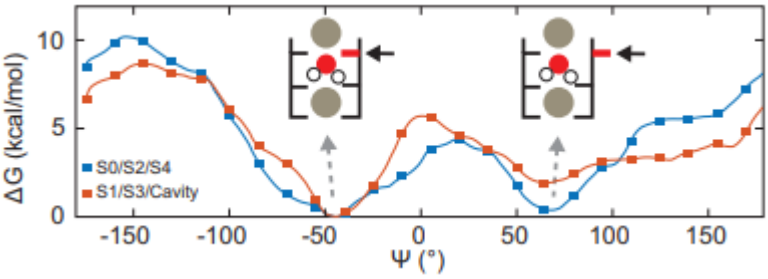

Figure 39: Figure from Lau et al. demonstrates: The free energy profile derived from umbrella sampling of the V625-Gly626 linkages Ψ angle rotation reveals energy minima at Ψ= -50° and +70° for V625 backbone carbonyls pointing towards and away from the central axis, respectively, when ions are held in S0/S2/S4 (blue) or S1/S3/cavity (orange) configurations (90).

The energy barrier for V625 carbonyl rotation is significantly lower at 4-5 kcal/mol compared to KcsA. S620-Y616 interaction enables free rotation of the

V625-G626 peptide bond and acts as a catalyst for state transition (Figure 40) (90).

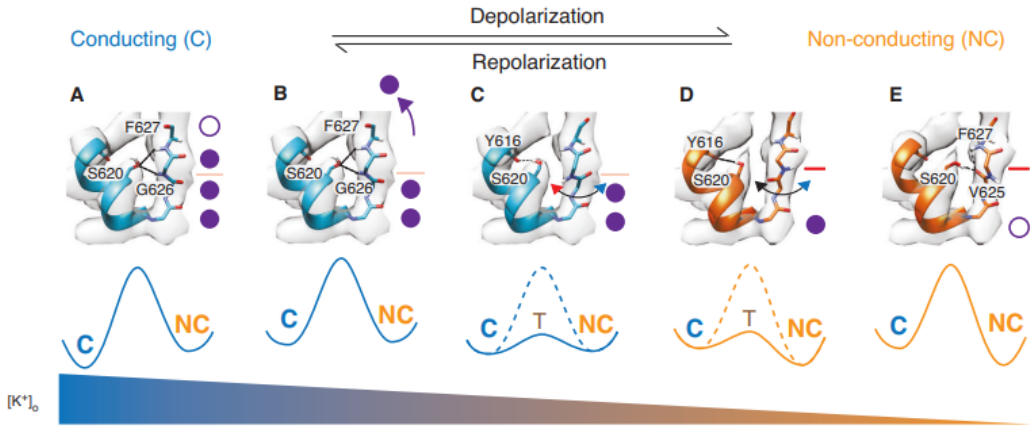

Figure 40: Figure from Lau et al. shows: Illustration of the transition between conducting and non-conducting states of the hERG potassium channel selectivity filter using cryo-EM maps and protein structures. It depicts a five-stage process, from the conducting state where S620 interacts with F627/G626 amides, through a transition state where S620 interacts with the Y616 backbone, to the non-conducting state where S620 interacts with the flipped V625 backbone carbonyl. Energy diagrams accompany each stage, showing the relative energies of conductive, transition and non-conductive states. The figure also demonstrates changes in energy barriers for ion movement and shows how potassium concentration influences the flavored state of the channel (90).

Cryo-EM Structure of K+-Bound hERG Channel Complexed with the Blocker Astemizole by Asai, T. et al.

The structure of the hERG channel was determined in 2017 using cryo-EM, identifying four deep hydrophobic side pockets as potential binding sites for inhibitors (Figure 41). New cryo-EM structures show the K+ bound hERG channel with and without astemizole (91).

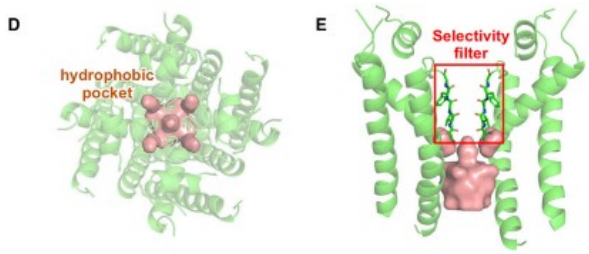

Figure 41: These show the hydrophobic pockets of the hERG channel that are potential binding sites for inhibitors (91).

The modified hERG gene (hERGT) was expressed in HEK cells and retains ion channel activity as well as astemizole binding capability. The binding affinity of astemizole to hERGT was determined using AS-MS and is comparable to the wild-type hERG channel (Figure 42) (91).

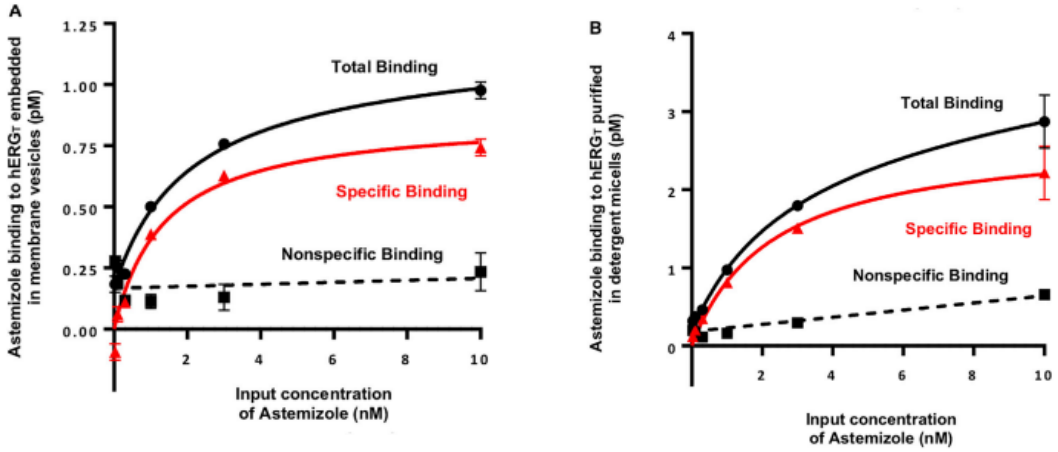

Figure 42: These display the binding affinity curves of astemizole to hERGT, demonstrating its comparability to the wild-type hERG channel (91).

Cryo-EM analyses provided important insights into the structure of the hERG channel under various conditions. In the presence of K^+, a resolution of 3.9 Å

was achieved, with two K^+ ions identified in the selectivity filter. When examined with astemizole and K^+, the resolution improved to 3.5 Å. In this case, three K^+ ions were observed in the selectivity filter and additional densities were seen in the hydrophobic pockets, suggesting the binding of astemizole (Figure 43, 44) (91).

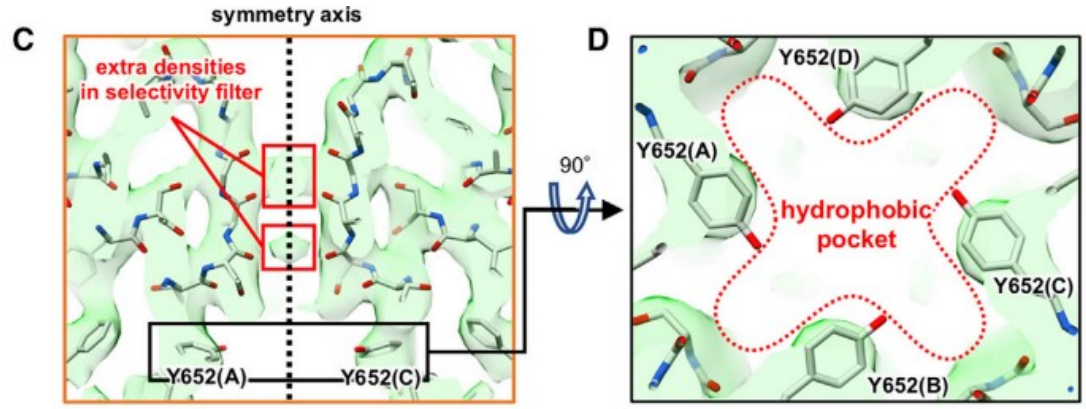

Figure 43: These show the cryo-EM structure of the hERG channel with K+ ions in the selectivity filter (91).

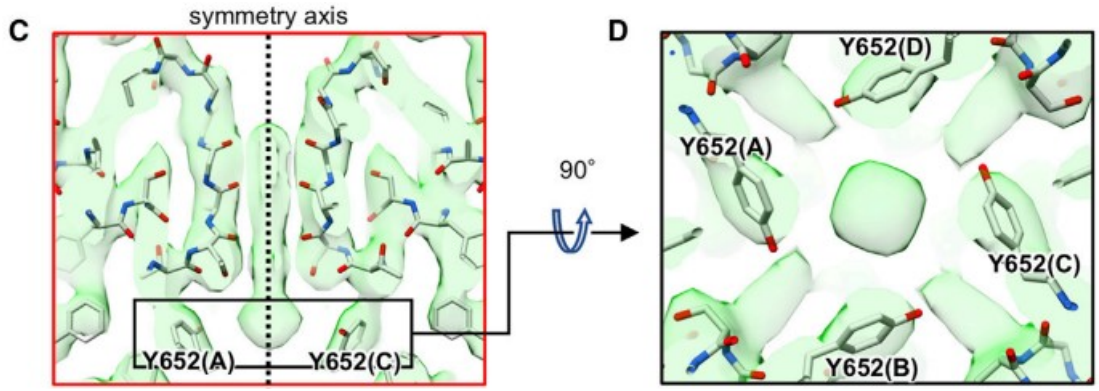

Figure 44: These illustrate the structure with astemizole and K+, showing the additional densities in the hydrophobic pockets (91).

The proposed inhibition mechanism of astemizole on the hERG channel consists two main components (Figure 45). First, astemizole blocks the selectivity filter of the channel, directly interrupting the potassium ion current. Second, astemizole prevents the removal of the potassium hydration sphere in the selectivity filter. This leads to the potassium ions being unable to shed their hydration shell, which is necessary for normal ion transport through the channel. Through this dual action, astemizole effectively inhibits the potassium ion current through the hERG channel (91).

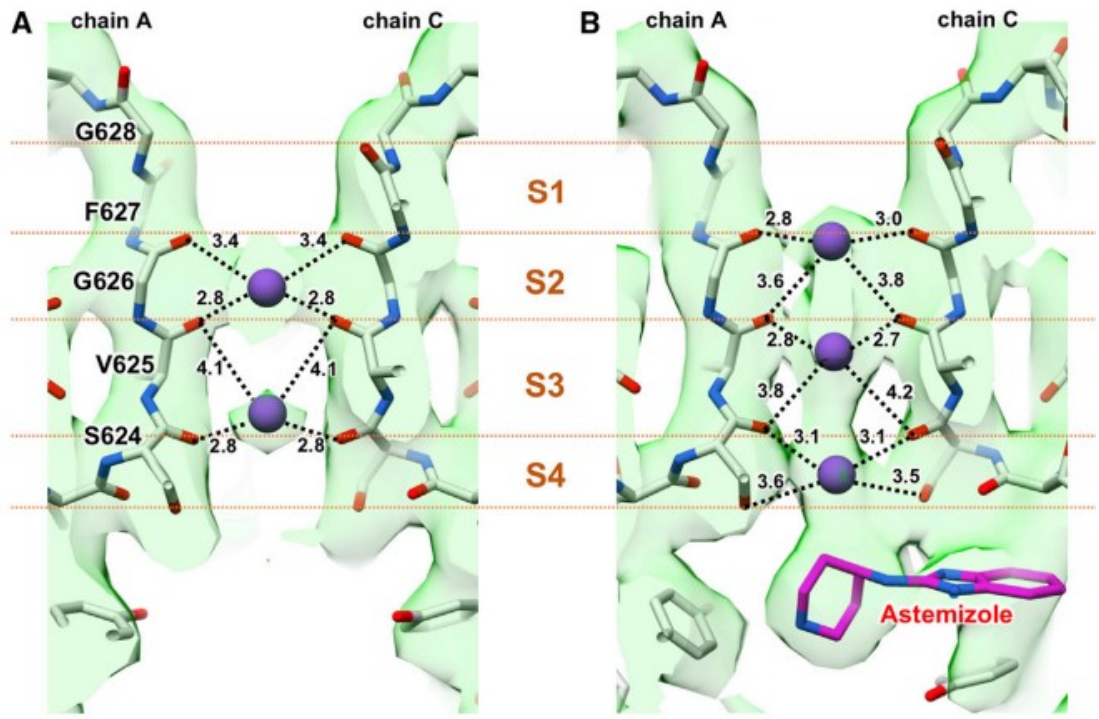

Figure 45: These provide a close-up view of the selectivity filter with and without astemizole, helping to visualize the proposed inhibition mechanism (91).

Improved higher resolution cryo-EM structures reveal the binding modes of hERG channel inhibitors by Miyashita, Y. et al.

The study by Miyashita et al. focuses on the structural analysis of the hERG potassium channel and its interaction with inhibitors, which is of great importance for drug safety. The researchers overcame previous challenges in structural analysis by employing alternative detergents and optimized image processing methods, addressing issues such as preferred particle orientation and limited resolution (92).

Using digitonin as a detergent, they successfully conducted a structural analysis of hERGT assuming asymmetry (C1 symmetry), achieving a high-resolution structure of 3.27 Å (Figure 46). This approach allowed for both top and side views of the particles and revealed a clear transmembrane domain. The final hERGT map was reconstructed from 254,567 particles, with the protein model including residues K407 to R665, excluding some loops connecting transmembrane helices due to unclear maps (92).

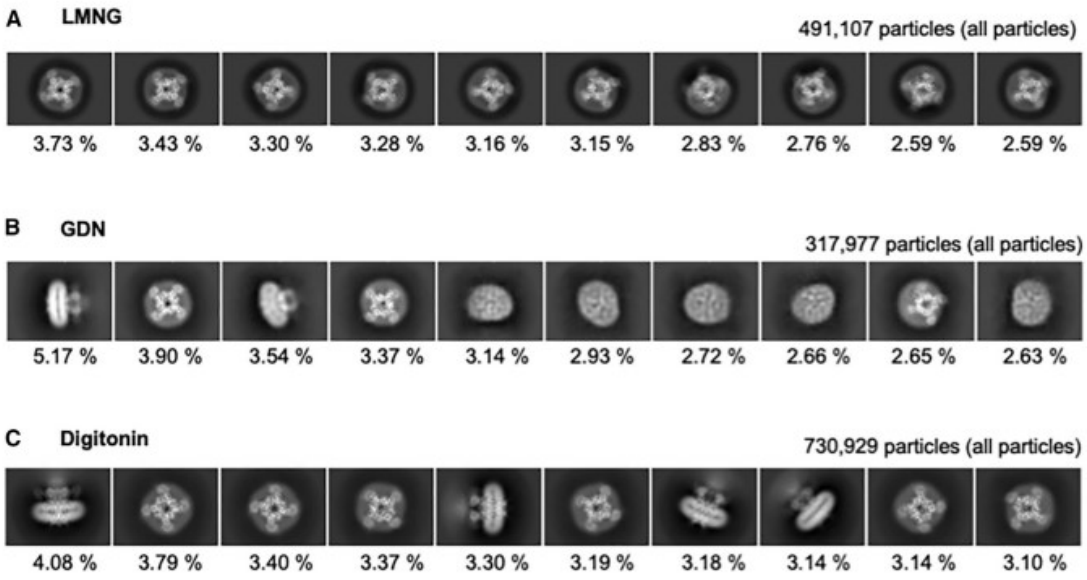

Figure 46: Comparison of hERG particles in different detergents (92)

The study examined hERGT structures with and without bound inhibitors focusing on astermizole, E-4031 and pimozide. While the overall protein structure remained largely unaffected by inhibitor binding, significant changes were observed in the amino acid Y652. Without astemizole, Y652 displays a symmetrical arrangement but the drugs binding disrupts this symmetry and

alters the orientation of the Y652 side chains, suggesting its potential role in drug binding (Figure 47) (92).

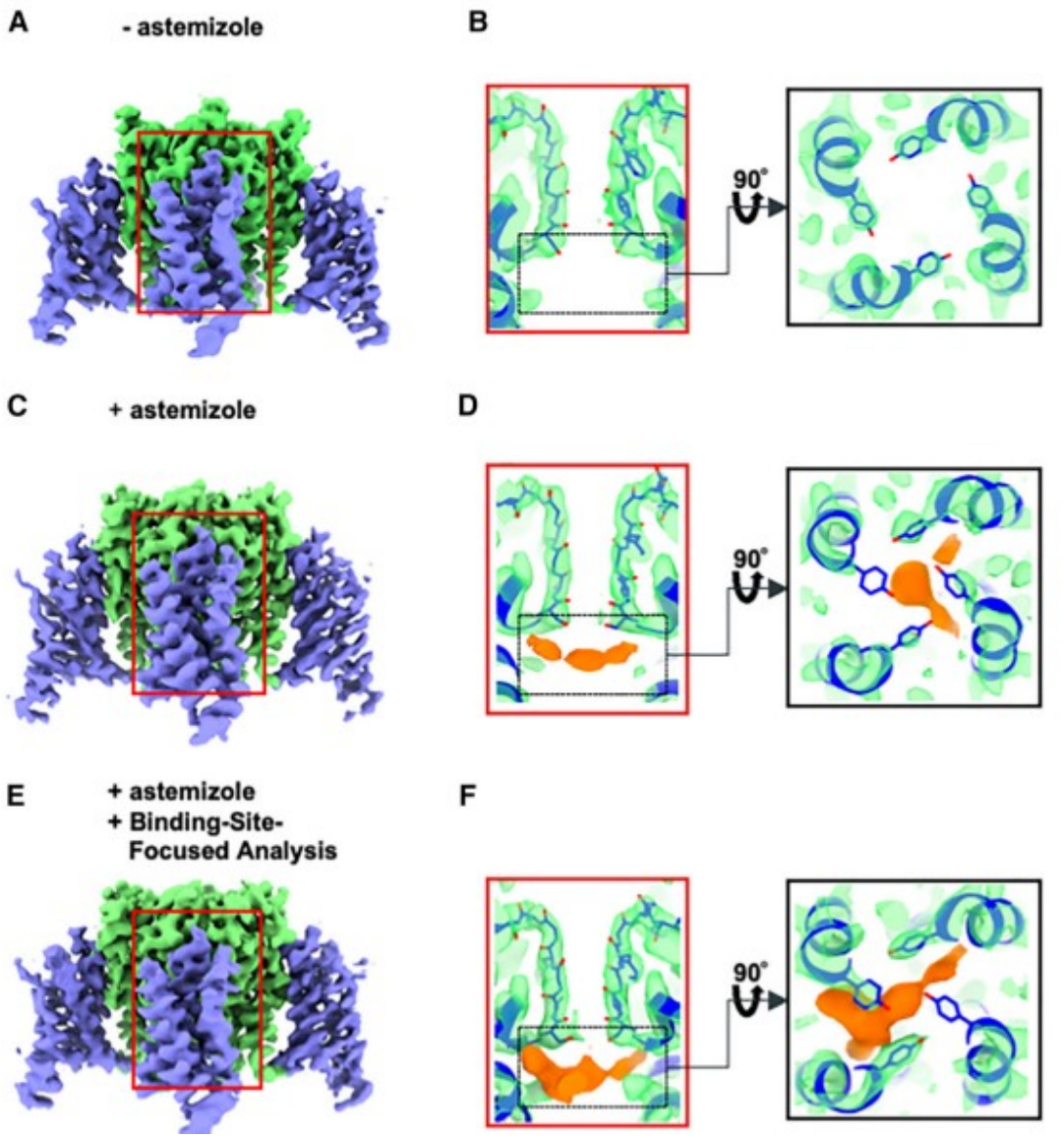

Figure 47: Showing the structures of the transmembrane domain of hERGT with and without bound astemizole, including overview and close-up images of the selectivity filter in different states (92).

All three inhibitors share a common binding mechanism. Located at the center of the cavity, piperidine blocks the selectivity filter through its positive electrostatic potential, thus inhibiting potassium ion transport. The binding is stabilized by complex interactions, including hydrogen bonds, hydrophobic interactions and electrostatic focus (92).

For astemizole, the researchers identified two possible binding models, both exhibiting similar binding energies (Figure 48). These models demonstrate complex interactions with the protein, including specific hydrogen bonds and hydrophobic interactions with various amino acid residues (92).

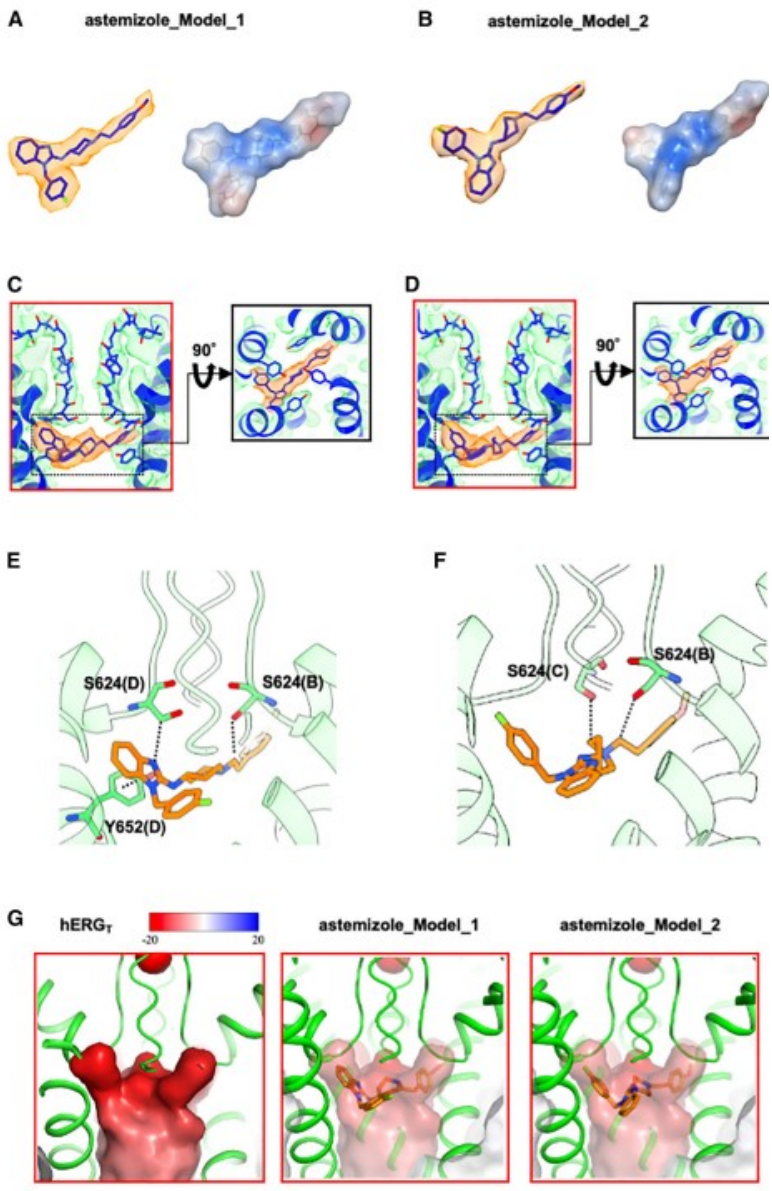

Figure 48: This figure likely shows the binding modes of astemizole, including the two possible binding models and the role of piperidine (92).

E-4031 and pimozide, two clinically relevant hERG inhibitors, were found to bind similarly to astemizole in the central cavity below the selectivity filter (Figure 49). The study emphasizes the importance of charge distribution and electrostatic interactions for the binding positon and strength of all three inhibitors (92).

Comparison of the four subunits analyzed under C1 symmetry revealed nearly identical structures, suggesting that the obtained C1-hERGT exhibits C4 symmetry. This finding provides valuable information about the overall structure and symmetry of the hERG channel (92).

These findings provide a detailed understanding of the binding and inhibition mechanisms of hERG inhibitors, which could significantly contribute to predicting and avoiding cardio toxic side effects in future drug development (92).

Figure 49: This image illustrates the similarities and differences in how E-4031 and pimozide interact with and bind to the hERG channel (92).

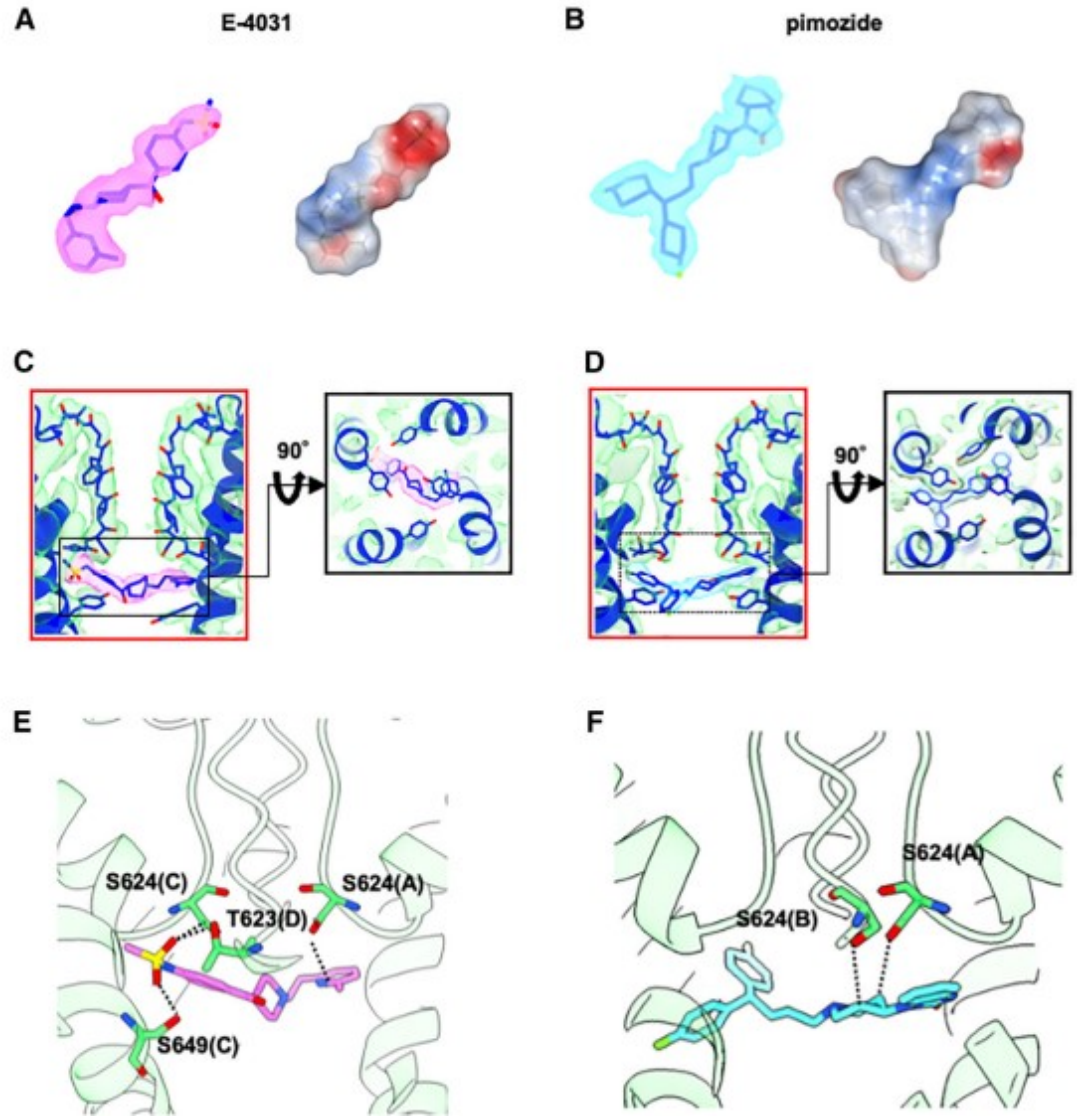

7 Cavity-Binding Activators of hERG

Since molecules bind under different conditions to the hERG channels, this is of great interest for future studies towards the search of activator molecules. For this study, we focused on investigating whether we can find a difference between the activated and inactivated state identified by Lau et al. when it comes to the binding site of the activators. It is known from experiments that a low potassium concentration leads to the inactivated state. To achieve the structures in the two different states, Lau et al. made use of this and obtained two structures, one with a low potassium concentration (inactivated state) and one with a high concentration (activated state). Interestingly, they saw a distinct electron density at position S4 of the filter for the low potassium concentration. We therefore placed an ion at this exact position to investigate whether this specific condition will have an influence on the docking of the compounds binding close to the selectivity filter. Aligning the two structures showed barely any other distinction, except for the interactions within the filter itself.

Methods

In our experiment, we docked the activators ICA105574, SKF32802, LUF7346, AZSMO23, KB130015 and SB335573 along with their derivatives to the hERG protein in both the activated and inactivated states. The molecules were built using MolView v2.4. We employed the GOLD software from the Cambridge Crystallographic Data Centre (CCDC) for docking (93). For each state, 100 runs were performed. Since we knew the most important binding residues, we limited our docking to this site. For ICA105574 as well as LUF7246 and their derivatives, we limited the search for a binding site to a radius of 1 nm around residue F557. This included the important residues within the cavity (Y652 and F656) as well as the filter (for detailed results and the best docking score see Figure 50). For SKF32802 we chose T623, S624, Y652 and F656. For AZSMO23, we utilized the residues Y652 and F656 as binding sites. In the case of SB335573, the residues S624, S649, M645 and Y652 were used. We allowed the program to set the most bulky residues as flexible, meaning they could rotate and adapt different states in order to find the best binding poses.

In the inactivated state, we additionally inserted an ion based on the observed density in the S4 position of the selectivity filter of the channel (1).

Results and Discussion

Figure 50 shows the detailed docking results of each best score for ICA105574, SKF32802, LUFs, AZSMO-23, KB130015 and SB335573 in both states. The results confirm that the activators can bind at the known binding sites identified by mutational studies (84) (87) (94). Interestingly, the ion inserted in the S4 segment did not significantly affect the binding of the activators.

Figures 51-53 present all obtained docking results for each compound in the activated and inactivated state. All investigated molecules were successfully docked in the binding site identified by experiments. However, we cannot clearly differentiate the binding possibilities between the two states.

While the derivatives have modified substituents, potentially leading to suboptimal conformations around the filter and affecting their ability to stabilize the ion, our current docking model cannot explain why they show a different effect on the hERG channel. As, for example, some of the ICA derivatives do not show any activity or even a slight block (84), one might expect they would adopt a different binding pose, not bind to this side at all, and/or bind to a side in the cavity as most hERG channel blockers do. But Figures 51 show that they can all bind to this pocket between the two subunits, in the same manner as ICA105574 – with the different substituents facing towards the pore, beneath the filter. Therefore, we cannot explain their different effects on the channel.

Since ICA105574 inhibits channel inactivation, one would expect that it binds to the activated state (79). However, from our results we could not determine a difference between the bindings of ICA105574 to the activated or inactivated state.

SKF-32802 binds the hERG channel in its open or closed state (87). Therefore, one would expect a difference in binding when it comes to the inactivated state. However, our docking results do not show this (Figures 50, 53). All important

binding residues can interact with the compound in both states (87). We further cannot distinguish between the active compound binding and its derivatives, which are blockers (see Figures 53). They can all bind to the same site identified as the activators binding site in our docking studies. We cannot determine what makes a blocker and what an activator by analyzing our results.

LUF7346 and LUF7757 bind to the activated state and highly reduce the inactivation of the channel (94). One would therefore conclude that they might prohibit a stable binding of the ions to the S4 site or change the filter conformation. However, we cannot see any difference between bindings to the activated or inactivated state (see Figure 50). Also, the derivatives are blockers. As for ICA105574 and its derivatives, all LUF-like compounds can bind to the same binding site and we cannot distinguish a blocker from an activator in our results.

AZSMO23 causes a shift in the voltage dependence of inactivation (83). It is therefore expected to bind to the activated state, making it harder for the channel to inactivate. However, as for the others, we do not see a difference in binding of the molecule to the activated or inactivated state (see Figures 50, 54).

Donovan et al (87) determined that SB-335573 acts by increasing the open probability of the channel. It therefore should stabilize the open state of the channel. In our docking studies, we cannot determine a difference between the bindings of SB-335573 to the activated or inactivated state (Figures 50, 54).

There might be several reasons for our results when it comes to not capturing any differences between the states: 1) The captured structures are rather similar. An alignment to the pore (including S5, p-helix, selectivity filter and S6) shows an RMS of 0.58 Å. Therefore, one might argue that it is expected that the binding site will be accessible in both states. Since the ion in the S4 site of the selectivity filter was a distinctive feature of the inactivated state, we did include it and one therefore might expect a difference in binding. This however did not show. The docking programs take ions into account, but each program to a different amount. Therefore, a different docking program might show

different results. 2) One might further argue that binding of a molecule might induce another conformational change in the hERG channel itself that might lead to the different effects and can therefore not be explained by looking at only a few different captured states of the protein.

To gain a deeper understanding of the binding mechanisms and state dependency, further research is necessary. Potential approaches could include advanced simulation techniques or experimental structural analysis.

Activated state **Inactivated state**

A ICA105574, 84.2530

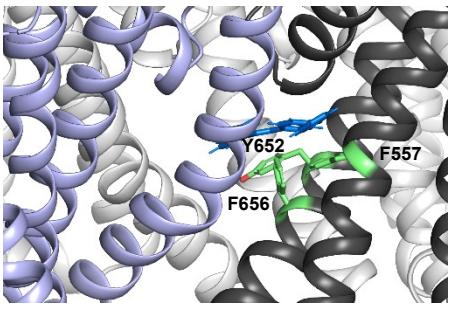

B ICA105574, 74.8249

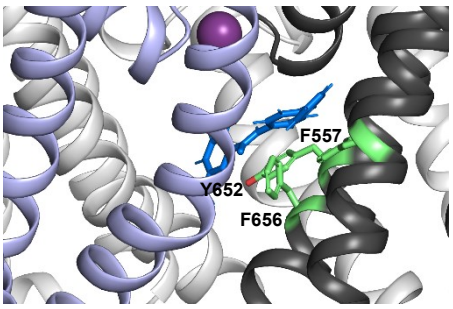

C SKF32802, 73.3478

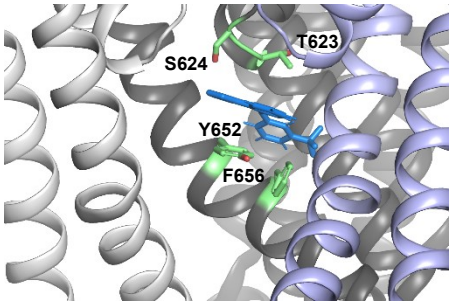

D SKF32802, 73.9940

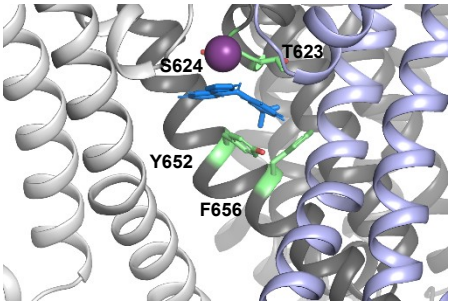

E LUF7346, 84.3023

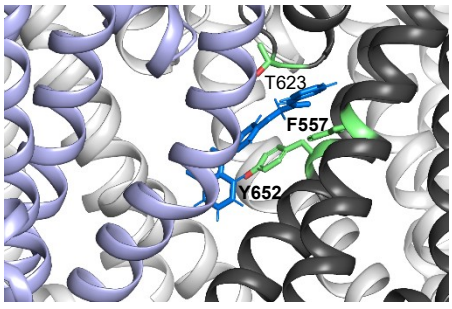

F LUF7346, 68.5454

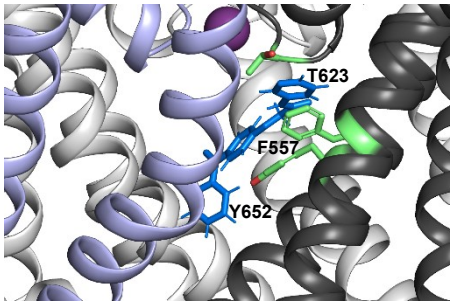

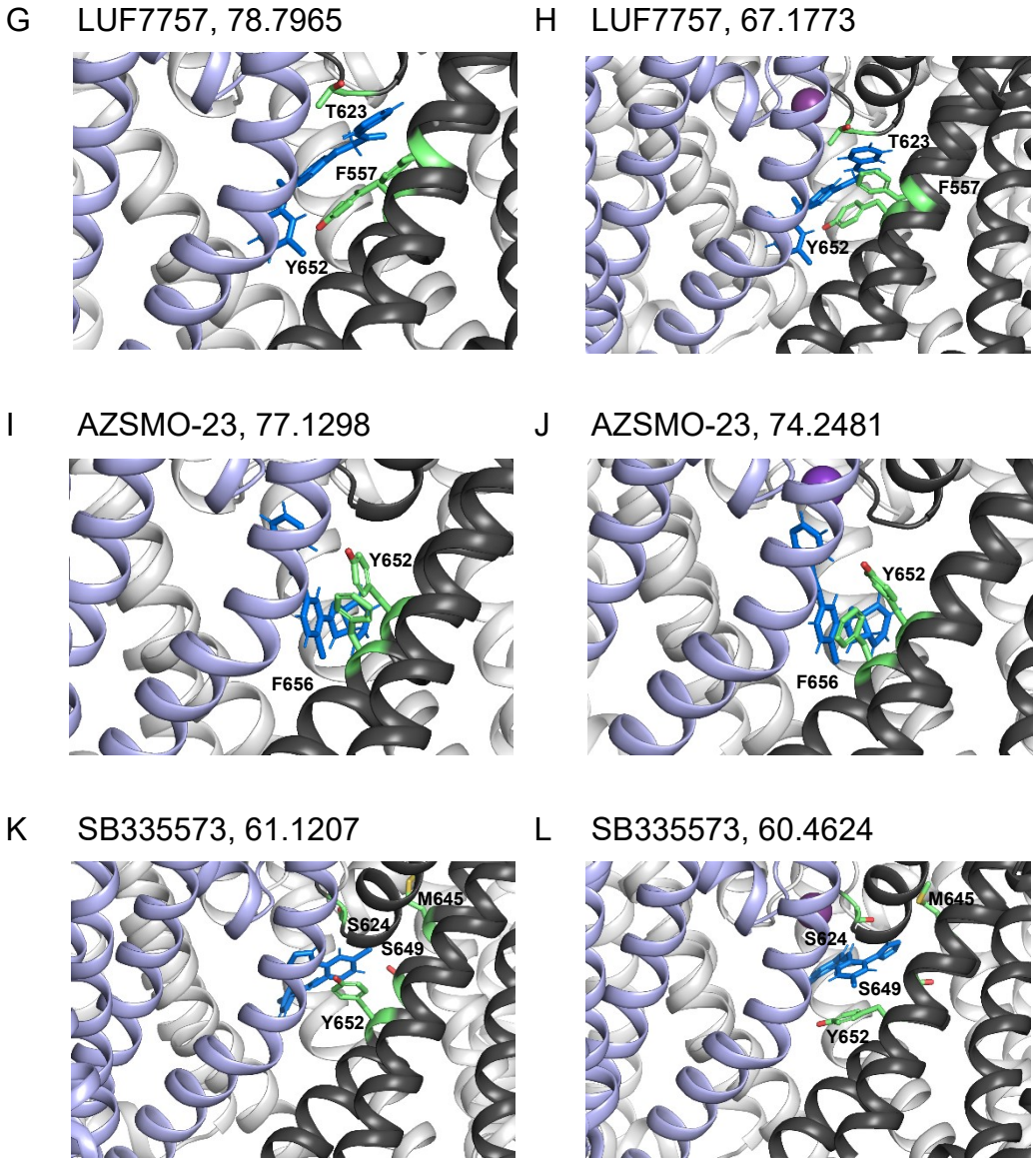

Figure 50: Activators docking in GOLD (Hermes 2024.2.0) shows subunits contributing to the binding sites colored in light blue and dark grey. The specific binding residues, known from experimental data, are highlighted in green. Best docking scores, calculated using the CHEMPLP scoring function in GOLD, are also displayed, providing a quantitative measure of binding affinity. A: ICA105574 in the activated state with the binding residues F557, Y652 and F656; B: ICA105574 in the inactivated state with the binding residues F557, Y652 and F656; C: SKF32802 in the activated state with the binding residues T623, S624, Y652 and F656; D: SKF32802 in the inactivated state with the binding residues T623, S624, Y652 and F656; E: LUF7346 in the activated state with the binding residues F557, T623 and Y652; F: LUF7346 in the

inactivated state with the binding residues F557, T623 and Y652; G: LUF7757 in the activated state with the binding residues F557, T623 and Y652; H: LUF7757 in the inactivated state with the binding residues F557, T623 and Y652; I: AZSMO-23 in the activated state with the binding residues Y652 and F656; J: AZSMO-23 in the inactivated state with the binding residues Y652 and F656; K: SB335573 in the activated state with the binding residues S624, M645, S649 and Y652; L: SB335573 in the inactivated state with the binding residues S624, M645, S649 and Y652

Activated state **Inactivated state**

A ICA105574

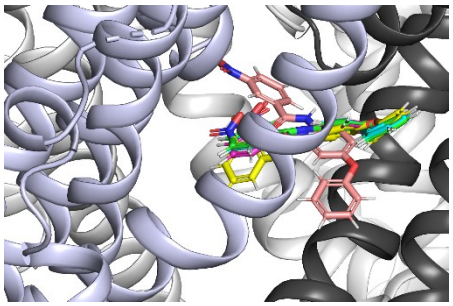

B ICA105574

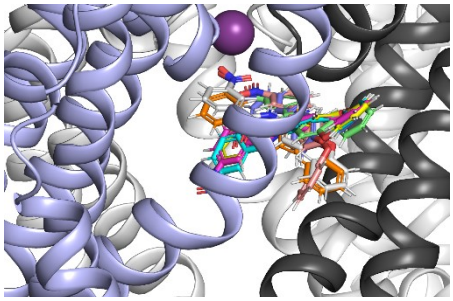

C MABE 146

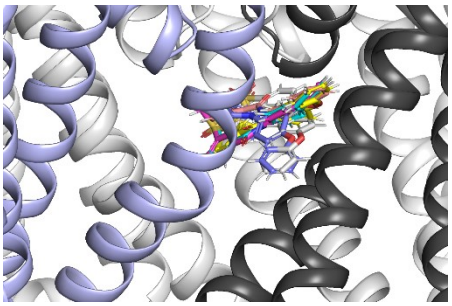

D MABE 146

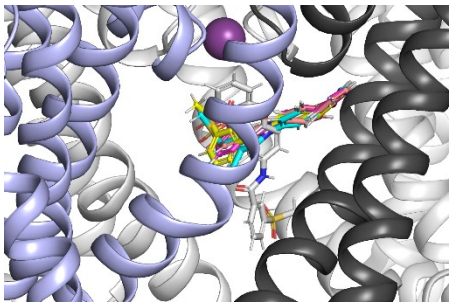

E MABE 170

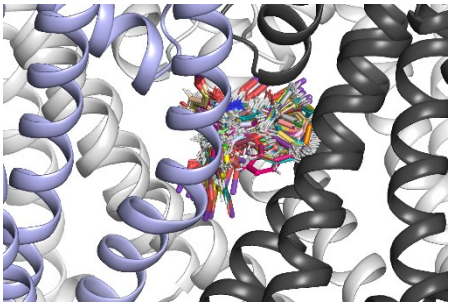

F MABE 170

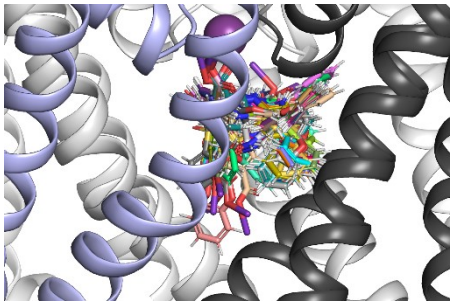

G MABE 171

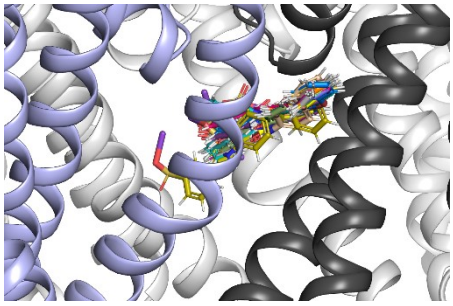

H MABE 171

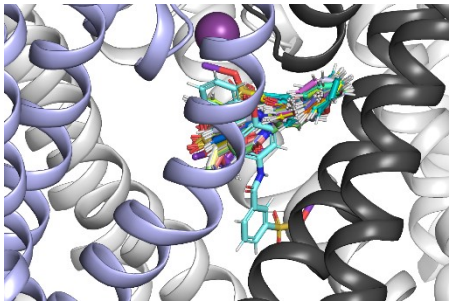

I YOCH 145

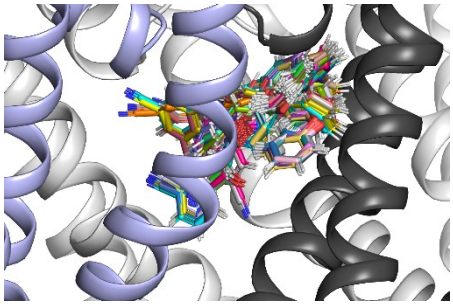

J YOCH 145

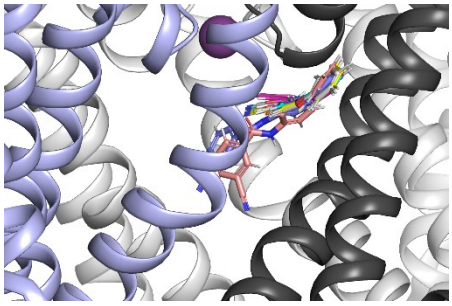

K YOCH 167

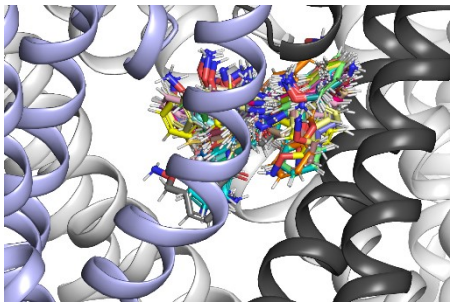

L YOCH 167

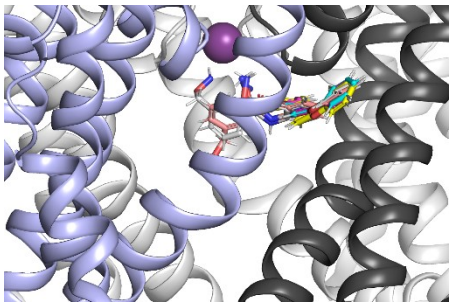

M YOCH 503

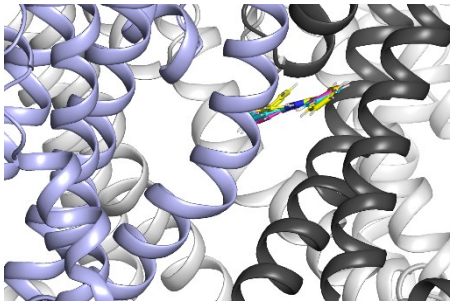

N YOCH 503

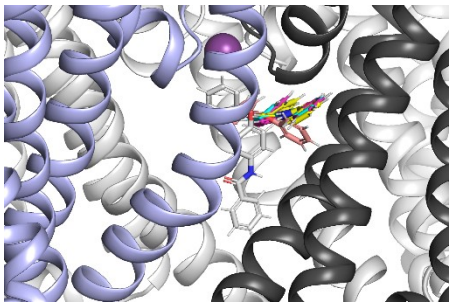

O YOCH 504

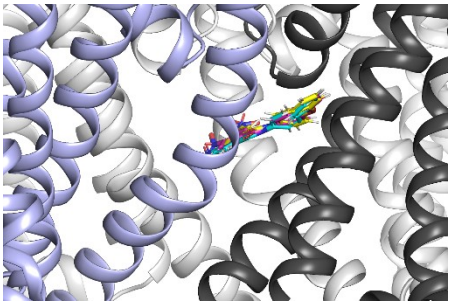

P YOCH 504

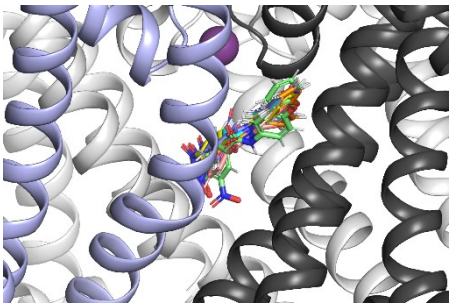

Figure 51: Activators docking in GOLD (Hermes 2024.2.0) shows subunits contributing to the binding sites colored in light blue and dark grey. A: ICA105574 in the activated state; B: ICA105574 in the inactivated state; C: MABE 146 in the activated state; MABE 146 in the inactivated state; E: MABE 170 in the activated state; F: MABE 170 in the inactivated state; G: MABE 171 in the activated state; H: MABE 171 in the inactivated state; I: YOCH 145 in the activated state; J: YOCH 145 in the inactivated state; K: YOCH 167 in the activated state; L: YOCH 167 in the inactivated state; M: YOCH 503 in the activated state; N: YOCH in the inactivated state; O: YOCH 504 in the activated state; P: YOCH 504 in the inactivated state

Activated state **Inactivated state**

A LUF7346

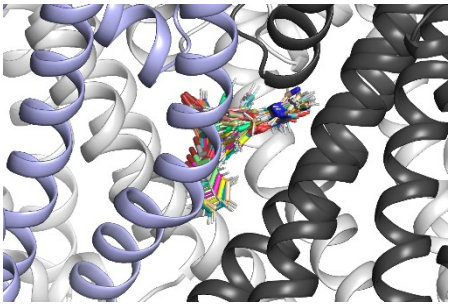

B LUF7346

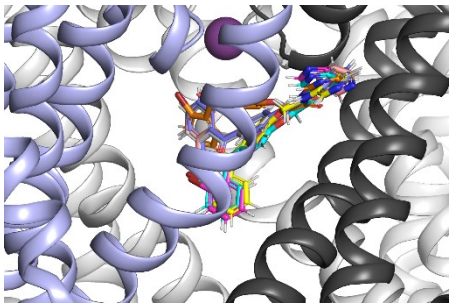

C LUF7757

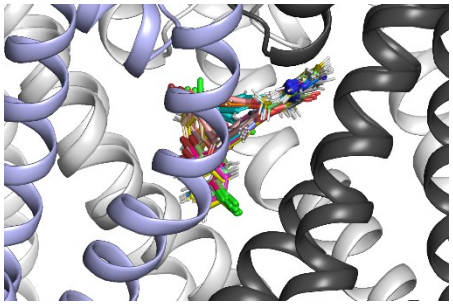

D LUF7757

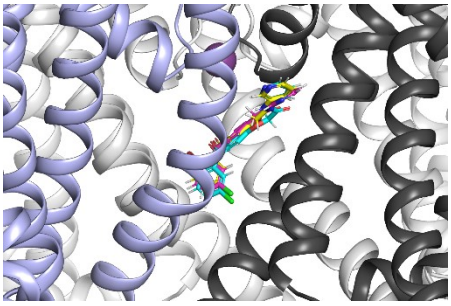

E Inhibitor 5e

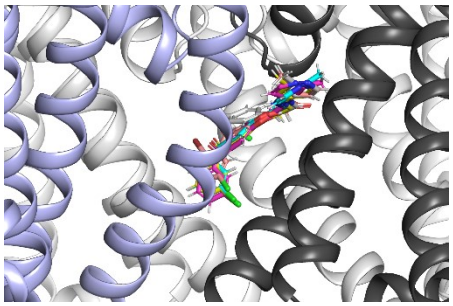

F Inhibitor 5e

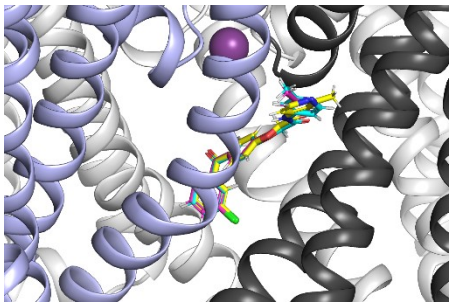

G Inhibitor 6k

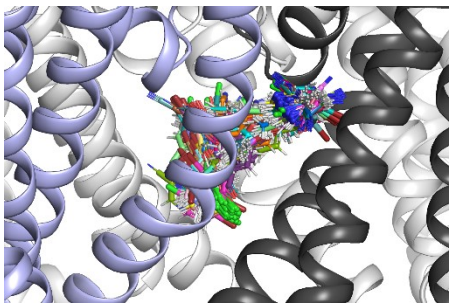

H Inhibitor 6k

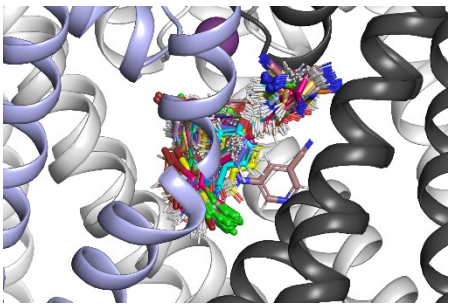

I Inhibitor 9k

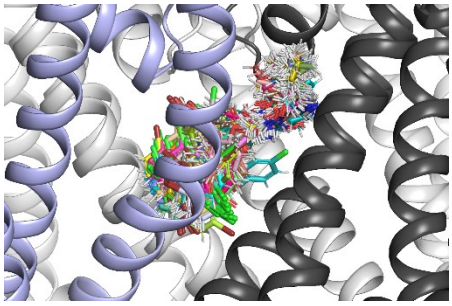

J Inhibitor 9k

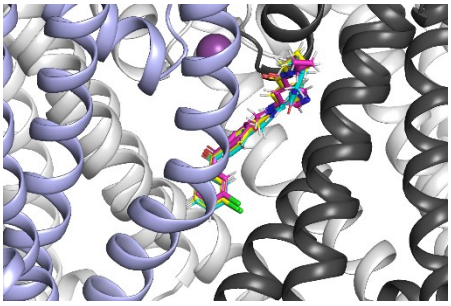

Figure 52: Activators docking in GOLD (Hermes 2024.2.0) shows subunits contributing to the binding sites colored in light blue and dark grey. A: LUF7346 in the activated state; B: LUF7346 in the inactivated state; C: LUF7757 in the activated state; D: LUF7757 in the inactivated state; E: Inhibitor 5e in the activated state; F: Inhibitor 5e in the inactivated state; G: Inhibitor 6k in the activated state; H: Inhibitor 6k in the inactivated state; I: Inhibitor 9k in the activated state; J: Inhibitor 9k in the inactivated state

Activated state **Inactivated state**

A GSK960257A

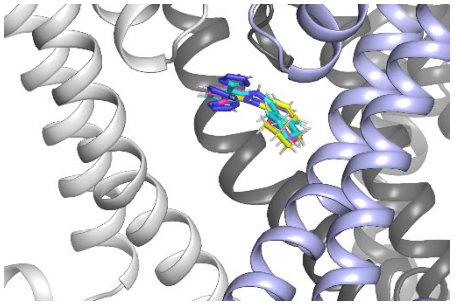

B GSK960257A

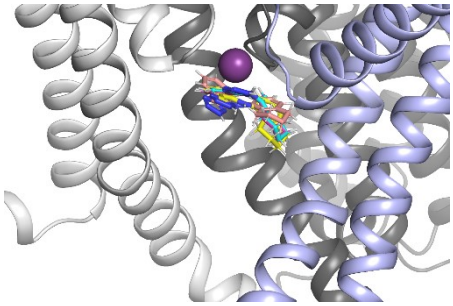

C SKF28458

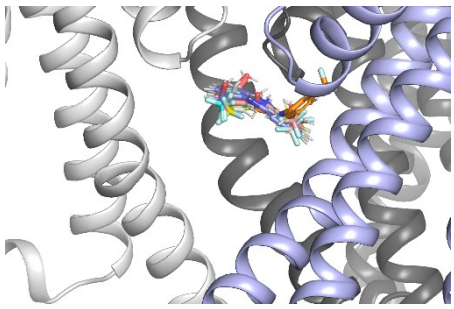

D SKF28458

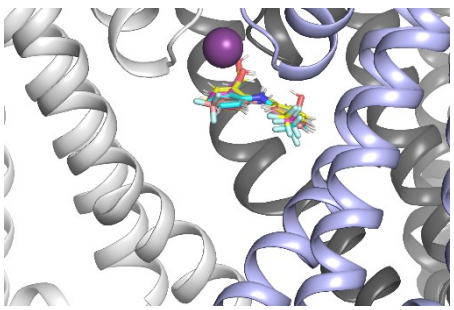

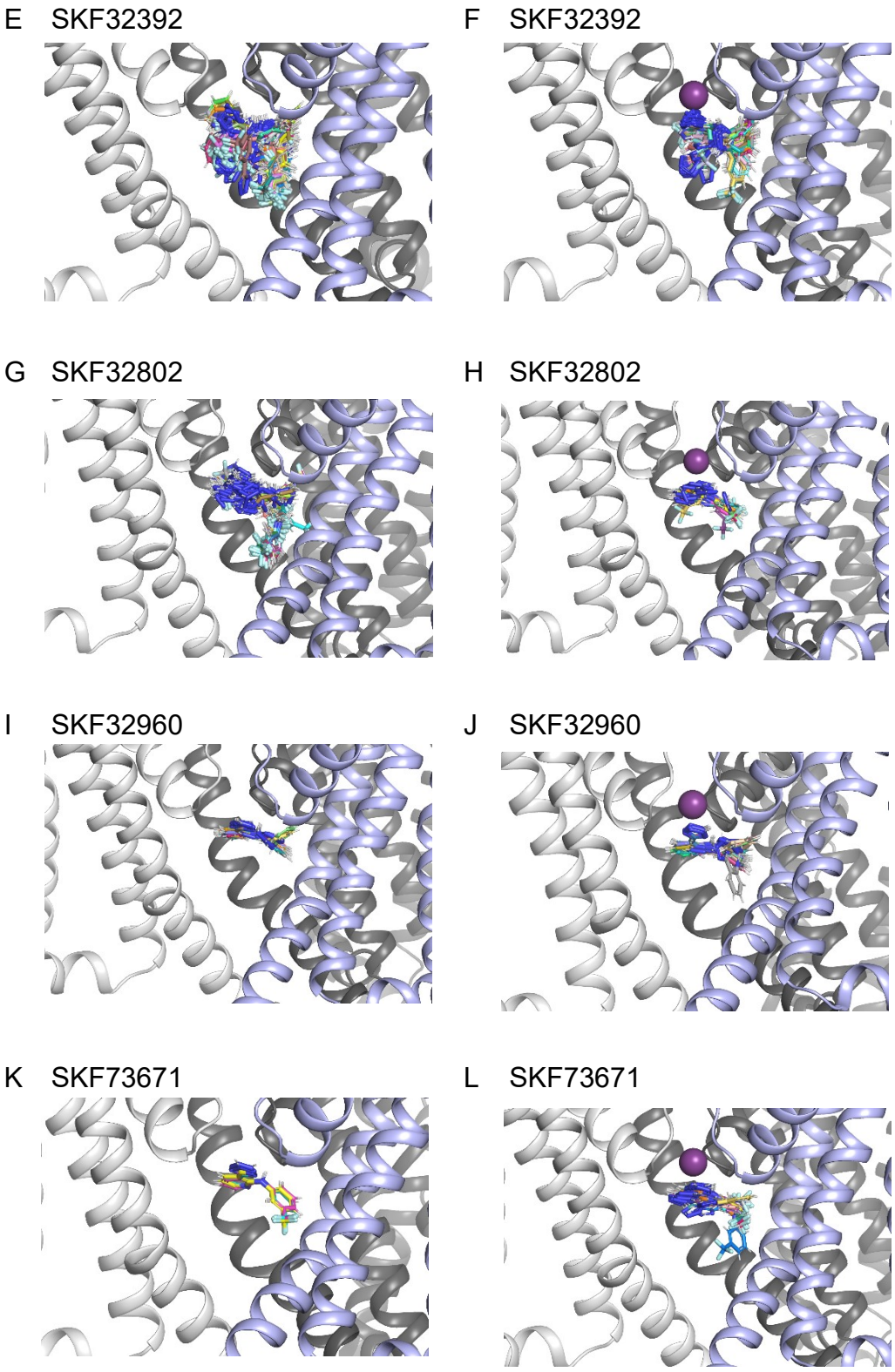

Figure 53: Activators docking in GOLD (Hermes 2024.2.0) shows subunits contributing to the binding sites colored in light blue and dark grey. A: GSK960257A in the activated state; B: GSK960257A in the inactivated state; C: SKF28458 in the activated state; D: SKF28458 in the inactivated state; E: SKF32393 in the activated state; F: SKF32393 in the inactivated state; G:

SKF32802 in the activated state; H: SKF32802 in the inactivated state; I: SKF32960 in the activated state; J: SKF32960 in the inactivated state; K: SKF73671 in the inactivated state

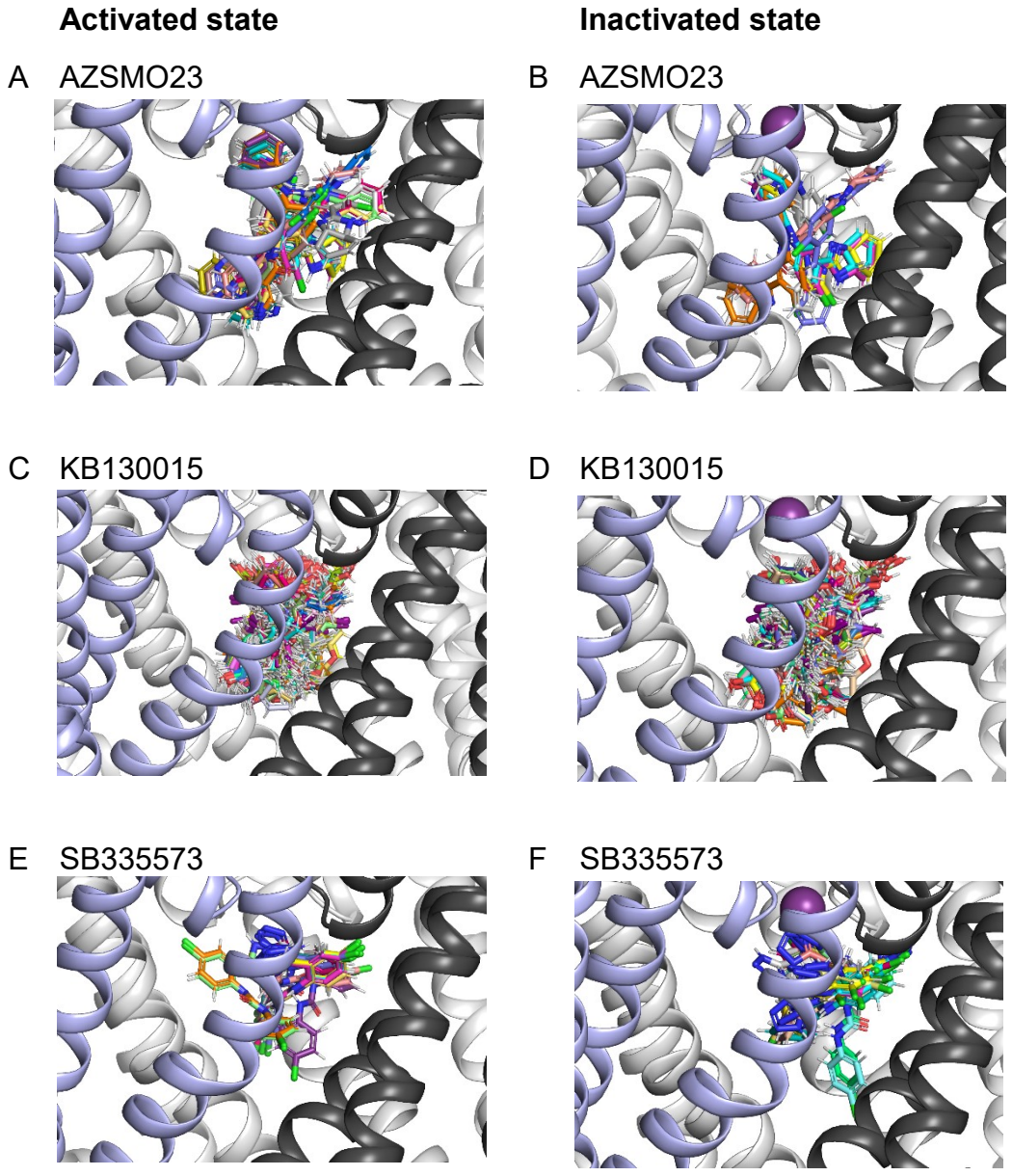

Figure 54: Activators docking in GOLD (Hermes 2024.2.0) shows subunits contributing to the binding sites colored in light blue and dark grey. A: AZSMO23 in the activated state; B: AZSMO23 in the inactivated state; C: KB130015 in the activated state; D: KB130015 in the inactivated state; E: SB335573 in the activated state; F: SB335573 in the inactivated state

8 Discussion

The hERG channel is a voltage-gated potassium channel that plays a crucial role in the repolarization of the cardiac action potential. Its unique properties, especially its quick inactivation and slow deactivation, make it a key regulator of heart rhythm. Problems with hERG channel function, whether from genetic mutations or drug effects, can lead to dangerous heart rhythm issues, particularly Long QT Syndrome.

Given how serious hERG channel inhibition can be and how often drugs can cause LQTS, hERG activators could be a promising treatment option. These compounds might not only help treat inherited LQTS but also protect against unwanted drug side effects. Developing specific and potent hERG activators could therefore be a big step forward in cardiology and drug safety.

The docking studies we performed with the cryo-EM structure of hERG gives us some insights into how activators and inhibitors might bind. But they also show some limitations of this method, which makes it hard to fully explain what is seen in experiments.

A big issue is that a cryo-EM structure only shows one state of the hERG channel. Recent studies suggest that the channel probably goes through several dynamic changes in shape during activation and inactivation. Static docking simulations cannot capture this movement. For example, Perissinotti et al. (2019) had to use molecular dynamics simulations to see changes in the channels shape that matter for how the blocker Ivabradine binds (20). Similarly, Negami et al. found that MD simulations were needed to correctly predict how different blockers bind (20). Therefore, it is plausible that a single state might not be sufficient to explain why a compound might be able to bind to one but not the other state.

Another important point is that the state captured in the cryo-EM structure might not be the fully activated or inactivated state. Cheng et al. could only explain their experimental data on the blocker Sarizotan by using a homology model that represents a different channel state. This is another example that

shows that the cryo-EM structure alone might not be enough to show all the important shapes the channel can take (20).

In our docking studies, we found several possible binding poses for the ligands we looked at consistent with already available mutagenesis data, but we did not see clear differences between the binding modes in the supposedly activated and inactivated states - This does not match up with the experimental data, which show no effects for some substances like ICA and slight inhibitory effects for other like LUF. We cannot explain this mismatch just from docking, which shows more research needs to be conducted.

Even though the GOLD docking program we used takes charges into account (93) we did not see significant differences in binding modes that would explain what we see in experiments. This might be a limitations of the program itself.

In summary, this work shows that docking studies with the cryo-EM structure of hERG can give valuable first insights into possible binding modes and sites. However, they are not sufficient on their own to fully explain the complex ways the channel is modulated. Future studies should use additional methods like molecular dynamics simulations to better capture the channels movement and its interactions with ligands. Looking at more channel states through homology modeling or additional structural data could also help to gain a more complete picture of how hERG is modulated.

Developing activators for hERG could be a big step forward in treating LQTS and preventing drug-induced arrhythmias. However, this requires a deeper understanding of how the channels structure relates to its function and how it interacts with ligands. Combining structural, functional and computer-based approaches will be crucial to reach this goal and ultimately develop safer and more effective treatments for patients with heart rhythm problems.

9 List of Figures

Figure 1: Overview of the classification of voltage-gated potassium channels (5) 1
Figure 2: Side view of the full hERG cryo-EM structure (20)..... 5
Figure 3: Structure of the voltage sensor domain, illustrating the distribution of positive and negative charges across the individual segments (19) 5
Figure 4: Structure of the hERG channel with a detailed depiction of the pore domain (21)..... 7
Figure 5: Conformation changes during the channel transitions between close and open (22)..... 9
Figure 6: Transitions between the different states, C--> closed, O--> open, I--> inactivate (4) 9
Figure 7: Left: Crystal structure in an open state (22); Right: Crystal structure in a closed state (22)..... 10
Figure 8: Cellular control mechanisms of hERG channel production (44).... 15
Figure 9: Top: Cardiac action potential with the different phases; Bottom: Individual ion currents with their respective time courses (47)..... 18
Figure 10: Overview of LQT2 mutations; Yellow: Represents amino acids; Purple, orange and blue dots show various mutations (44) 20
Figure 11: Image (a, left): a normal action potential in humans, (a, right): a prolonged action potential simulated by reducing hERG current by 80%; Image (b, left): standard ECG recording for one cardiac cycle, (b, right): irregular ECG recording showing a prolonged QT interval (22) 21
Figure 12: A single heartbeat depicted by an electrocardiogram and the corresponding cardiac action potential trace (5) 22
Figure 13: Chemical structure of agonists classified by their mechanisms (2) 25
Figure 14: Chemical structure of agonists with uncategorized mechanisms (2) 25
Figure 15: Binding residues of RPR260243; Yellow: RPR260243; Pink: Prolongation of deactivation; Green: Attenuation of deactivation (66) 26
Figure 16: Research was conducted with and without RPR260243. The results using the potentiometric dye RH 237 are represented by red for high and blue

for low signal intensity (A). The difference is evident in B, which shows that RPR shortened the ADP. Picture C illustrates a boxplot of the impact of RPR260243 on the ADP measured at 30% and 90% repolarization. Effects on the Triangulation index are shown in D (65). 28
Figure 17: RPR260243 effects on hERG currents: Slow deactivation, produces persistent currents at room temperature (A, B) and 37°C (D). Effects are reversible and voltage-dependent (C). Chemical structure shown in A (68). 29
Figure 18: Impact of Compound K on hERG K+ Channel Currents (69) 33
Figure 19: Impact of Protopanaxatriol on hERG K+ Channel Currents (69) . 34
Figure 20: Impact of Protopanaxadiol (PPD) on hERG channels (69) 35
Figure 21: This Figure from Sala et al. shows the effect of the allosteric modulator LUF7346 on the IKr current in HEK293-hERG cells (77) 38
Figure 22: Effect of ICA-105574 on hERG currents in HEK293 cells (80) 42
Figure 23: AZSMO-23 effects on the hERG channel (85) 44
Figure 24: Mallotoxin enhances hERG channel currents; Dofetilide blocks this effect. The effect is reversible in inside-out patch experiment (86). 46
Figure 25: Overview how Mallotoxin enhances hERG channel acitivity by making the channels open at lower voltages and increasing current flow with the effect increasing as the concentration of Mallotoxin rises (86) 47
Figure 26: Representation of the activation kinetics of SKF-32802 (87) Comparison of voltage dependence of activation samples for SKF-32802 (B) and its corresponding control (A) (87) 49
Figure 27: Comparison of voltage dependence of activation samples for SKF-32802 (B) and its corresponding control (A) (87) 49
Figure 28: Illustration of activation and blocking by KB130016 and the concentration dependent effect (88) 50
Figure 29: Overview that the activation of hERG1 channels by KB130015 depends on hERG1 gating (88) 51
Figure 30: Figure from Mao et al. shows the effect of PD-118057 on the voltage-dependent activation of the hERG channel (89) 54
Figure 31: Figure from Sanguinetti, M. gives an overview of the mechanisms of hERG1 channel agonists (31) 55

Figure 32: Calibration of the binding models and their RMSDs for Dofetilide, Terfenadine and Verapamil including comparison of the percentage current data with the calibrated models and the RMSD of the bootstrap samples compared to the reference model CiPA v1.0 (82) 57
Figure 33: Overview of the binding models that were used (82) 58
Figure 34: (A): The hERGT construct removes certain amino acid residues from the hERG primary structure to facilitate cryo-EM structure determination at a 3,8 Å resolution. (B): Voltage recordings show the electrical properties of wild type hERG (hERGWT) in transfected HEK293T cells. (C): Similar voltage recordings for the modified hERGT construct demonstrate its electrophysiological properties. (D): The normalized tail current curves show differences in voltage sensitivity and activation between hERGWT and hERGT. (E): Dose-response curves demonstrate the response of the hERGT cahnnel to the drugs astemizole and dofetilide, including IC50 values (1)… 60
Figure 35: (A): The sequence alignment shows conserved amino acid residues and those associated with drug binding, with relevant residues highlighted in yellow. (B): The EM density map of the putative drug binding site is displayed as a blue mesh, while the molecular model shows the relevant residues in yellow. (C): The overlay of hERG and KvChim shows the position of drug-binding related residues near the central cavity. (D): The inner molecular surface around the central cavity of hERG is represented in terms of electrostatic potential, with relevant residues highlighted. (E): The inner molecular surface of KvChim is represented similarly to that of hERG to illustrate structural similarities (1). 61
Figure 36: (A-C): The side view of the cryo-EM density maps shows the selectivity filters of hERGT, EAG1 and the non-inactivating mutant hERGTs S631A, highlighting the positions of the aromatic residues. (D): The overlay of the aromatic residues in the selectivity filter illustrates the differences between hERGT, hERGTs S631, EAG1, KcsA and KvChim. (E): The density maps of F627 in hERGT and F439 in EAG1, viewed from the extracellular side, show a counterclockwise rotation of the residue. (F): The overlay of the density maps and models of F627 in hERGT and hERGTs S631A highlights the structural differences between the two variants. (G-H): Representative whole-cell voltage

recordings demonstrate the electrical properties of hERGT and the non-inactivating mutant hERGT S631A in HEK293T cells (1). 62
Figure 37: Figure from Lau et al. shows (D): The overlay of structures shows that a low K+ concentration, the backbone of F627/G628 and the V625 carbonyl experience significant displacements. (E): The selectivity filter profile shows an expansion at V625 and constrictions at S624 and G626 at low K+ concentration compared to the high-K+ structure (90).....63
Figure 38: Figure from Lau et al. represents the structures with high (blue) and low (orange) K+ concentrations exhibit different hydrogen bonding patterns, particularly regarding the interactions of the S620 side chain (90). 64
Figure 39: Figure from Lau et al. demonstrates: The free energy profile derived from umbrella sampling of the V625-Gly626 linkages Ψ angle rotation reveals energy minima at Ψ= -50° and +70° for V625 backbone carbonyls pointing towards and away from the central axis, respectively, when ions are held in S0/S2/S4 (blue) or S1/S3/cavity (orange) configurations (90). 64
Figure 40: Figure from Lau et al. shows: Illustration of the transition between conducting and non-conducting states of the hERG potassium channel selectivity filter using cryo-EM maps and protein structures. It depicts a five-stage process, from the conducting state where S620 interacts with F627/G626 amides, through a transition state where S620 interacts with the Y616 backbone, to the non-conducting state where S620 interacts with the flipped V625 backbone carbonyl. Energy diagrams accompany each stage, showing the relative energies of conductive, transition and non-conductive states. The figure also demonstrates changes in energy barriers for ion movement and shows how potassium concentration influences the flavored state of the channel (90).....65
Figure 41: These show the hydrophobic pockets of the hERG channel that are potential binding sites for inhibitors (91). 66
Figure 42: These display the binding affinity curves of astemizole to hERGT, demonstrating its comparability to the wild-type hERG channel (91).....66
Figure 43: These show the cryo-EM structure of the hERG channel with K+ ions in the selectivity filter (91).....67

Figure 44: These illustrate the structure with astemizole and K+, showing the additional densities in the hydrophobic pockets (91)..... 67
Figure 45: These provide a close-up view of the selectivity filter with and without astemizole, helping to visualize the proposed inhibition mechanism (91). 68
Figure 46: Comparison of hERG particles in different detergents (92)..... 69
Figure 47: Showing the structures of the transmembrane domain of hERGT with and without bound astemizole, including overview and close-up images of the selectivity filter in different states (92). 70
Figure 48: This figure likely shows the binding modes of astemizole, including the two possible binding models and the role of piperidine (92). 71
Figure 49: This image illustrates the similarities and differences in how E-4031 and pimozide interact with and bind to the hERG channel (92). 72
Figure 50: Activators docking in GOLD (Hermes 2024.2.0) shows subunits contributing to the binding sites colored in light blue and dark grey. The specific binding residues, known from experimental data, are highlighted in green. Best docking scores, calculated using the CHEMPLP scoring function in GOLD, are also displayed, providing a quantitative measure of binding affinity. A: ICA105574 in the activated state with the binding residues F557, Y652 and F656; B: ICA105574 in the inactivated state with the binding residues F557, Y652 and F656; C: SKF32802 in the activated state with the binding residues T623, S624, Y652 and F656; D: SKF32802 in the inactivated state with the binding residues T623, S624, Y652 and F656; E: LUF7346 in the activated state with the binding residues F557, T623 and Y652; F: LUF7346 in the inactivated state with the binding residues F557, T623 and Y652; G: LUF7757 in the activated state with the binding residues F557, T623 and Y652; H: LUF7757 in the inactivated state with the binding residues F557, T623 and Y652; I: AZSMO-23 in the activated state with the binding residues Y652 and F656; J: AZSMO-23 in the inactivated state with the binding residues Y652 and F656; K: SB335573 in the activated state with the binding residues S624, M645, S649 and Y652; L: SB335573 in the inactivated state with the binding residues S624, M645, S649 and Y652 77
Figure 51: Activators docking in GOLD (Hermes 2024.2.0) shows subunits contributing to the binding sites colored in light blue and dark grey. A:

ICA105574 in the activated state; B: ICA105574 in the inactivated state; C: MABE 146 in the activated state; MABE 146 in the inactivated state; E: MABE 170 in the activated state; F: MABE 170 in the inactivated state; G: MABE 171 in the activated state; H: MABE 171 in the inactivated state; I: YOCH 145 in the activated state; J: YOCH 145 in the inactivated state; K: YOCH 167 in the activated state; L: YOCH 167 in the inactivated state; M: YOCH 503 in the activated state; N: YOCH in the inactivated state; O: YOCH 504 in the activated state; P: YOCH 504 in the inactivated state.....80
Figure 52: Activators docking in GOLD (Hermes 2024.2.0) shows subunits contributing to the binding sites colored in light blue and dark grey. A: LUF7346 in the activated state; B: LUF7346 in the inactivated state; C: LUF7757 in the activated state; D: LUF7757 in the inactivated state; E: Inhibitor 5e in the activated state; F: Inhibitor 5e in the inactivated state; G: Inhibitor 6k in the activated state; H: Inhibitor 6k in the inactivated state; I: Inhibitor 9k in the activated state; J: Inhibitor 9k in the inactivated state.....82
Figure 53: Activators docking in GOLD (Hermes 2024.2.0) shows subunits contributing to the binding sites colored in light blue and dark grey. A: GSK960257A in the activated state; B: GSK960257A in the inactivated state; C: SKF28458 in the activated state; D: SKF28458 in the inactivated state; E: SKF32393 in the activated state; F: SKF32393 in the inactivated state; G: SKF32802 in the activated state; H: SKF32802 in the inactivated state; I: SKF32960 in the activated state; J: SKF32960 in the inactivated state; K: SKF73671 in the inactivated state 83
Figure 54: Activators docking in GOLD (Hermes 2024.2.0) shows subunits contributing to the binding sites colored in light blue and dark grey. A: AZSMO23 in the activated state; B: AZSMO23 in the inactivated state; C: KB130015 in the activated state; D: KB130015 in the inactivated state; E: SB335573 in the activated state; F: SB335573 in the inactivated state.....84

10 Bibliography

1. *Cryo-EM structure of the open human ether-a-go-go related K+ channel hERG.* **Wang, W., MacKinnon, R.** Cell 169 (3): 422-430 : s.n., 2017, Cell. 169(3): 422-430.e10.

2. *Pharmacological activation of the hERG K+ channel for the management of the long QT: syndrome: A review.* **Harchi, A. E., Brincourt, O.** Journal of Arrhythm. 38 (4): 554-569 : s.n., 2022, Journal of Arrhythm 38(4): 554-569.

3. *Long QT Syndrome Type 2: Emerging Strategies for Correcting Class 2 KCNH2 (hERG) Mutations and Identifying New Patients.* **Ono, M., Burgess, D. E., Schroder, E. A., Elayi, C. S., Anderson, C. L., January, C. T., Sun, B., Immadisetty, K., Kekenes-Huskey, P. M., Delisle, B. P.** Biomolecules 10 (8): 1144 : s.n., 2020.

4. *hERG K+ Channels: Structure, nction. and clinical significance.* **Vandenberg, J. I., Perry, M. D., Perrin, M. J., Mann, S. A., Ke, Y. & Hill, A. P.** Physiol Rev. 92 (3): 1393-478 : s.n., 2012.

5. *Role of hERG potassium channel assays in drug development.* **Priest, B., Bell, I. M., Garcia, M.** Channels (Austin) 2 (2): 87-93 : s.n., 2008, Channels 2:2, 87-93.

6. *Currents Carried by Sodium and Potassium Ions through the Membrane of the Giant Axon of Lolligo.* **Hodgkin, A. L., Huxley, A. F.** Journal of Physiol. 116 (4): 449-472 : s.n., 1952, The Journal of Physiology 116: 449-72.

7. *Cloning of genomic and complementary DNA from Shaker, a putative potassium channel gene from Drosophila.* **Papazian, D. M., Schwarz, T. L., Tempel, B. L., Jan, Y. N., Jan, L. Y.** Science 237 (4816): 749-53 : s.n., 1987, Science 237(4816):749-753.

8. *The behavior of four neurological mutants of Drosophila.* **Kaplan, W. D., Trout, W. E.** Genetics 61 (2): 399-409 : s.n., 1969, Genetics vol. 61,2: 399-409.

9. *Evidence for Two Components of Delayed Rectifier K+ Current in Human Ventricular Myocytes.* **Li, G. R., Feng, J., Yue, L., Carrier, M., Nattel, S.** Circulation Research Vol. 78 (4): 689-696 : s.n., 1996.

10. *A family of potassium channel genes related to eag in Drosophila and mammals.* **Warmke, J. W., Ganetzky, B.** Proc Natl Acad Sci U S A. 91 (8): 3438-3442 : s.n., 1994, Proc. Natl. Acad. Sci. USA Vol. 91, pp, 3438-3442.

11. *HERG-like K+ channels in microglia.* **Zhou, W., Cayabyab, F. S., Pennefather, P. S., Schlichter, L. C., DeCoursey, T. E.** Journal Gen Physiol. 111 (6): 781-94 : s.n., 1998, J Gen Physiol. 111(6):781-94.

12. *A Mechanistic Link between an Inherited and an Acquired Cardiac Arrhythmia: HERG Encodes the IKr Potassium Channel.* **Sanguinetti, M. C., Jiang, C., Curran, M. E., Keating, M. T.,.** Cell, Vol. 81, 299-307 : s.n., 1995, Cell 81, no 2: 299-307.

13. *A Molecular Basis for Cardiac Arrhythmia: HERG Mutations Cause Long QT Syndrome.* **Curran, M. E., Splawski, I., Timothy, K. W., Vincent, G. M., Green, E. D., Keating, M. T.** Cell 80 (5): 795-803 : s.n., 1995, Cell, Vol. 80, 795-803.

14. *Five years of the CiPA project (2013-2018): what did we learn?* **Yim, D. S.** Translational and Clinical Pharmacology 26 (4): 145-149 : s.n., 2018.

15. *Revealing the structural basis of action of hERG potassium channel activators and blockers.* **Perry, M., Sanguinetti, M., Mitcheson, J.** Journal of Physiol. 588 (Pt 17): 3157-3167 : s.n., 2010, The Journal of Physiology, 588 (Pt 17), 3157-3167.

16. *hERG S4-S5 linker acts as a voltage-dependent ligand that binds to the activation gate and locks it in a closed state.* **Malak, O. A., Lamoureux, Z. E. S., Loussouarn, G.** Scientific Reports 7, Article number: 113 : s.n., 2017.

17. *Molecular dynamics simulations suggest possible activation and deactivation pathways in the hERG channel.* **Costa, F., Guardiani, C., Giacomello, A.** Communications Biology 5, Article number: 165 : s.n., 2022.

18. *Activation of human ether-a-go-go related gene (hERG) potassium channels by small molecules.* **Zhou, P. Z., Babcock, J., Liu, L. Q., Li, M., Gao, Z. B.** Acta Pharmacologica Sinica) 32: 781–788 : s.n., 2011, Acta Pharmacologica Sinica 32: 781-788.

19. *Interactions Between Charged Residues in the Transmembrane Segments of the Voltage-sensing Domain in the hERG Channel.* **Zhang, M., Liu, J., Jiang, M., Wu, D. M., Sonawane, K., Guy, H. R., Tseng, G. N.** Journal of Membr Biol. 207 (3): 169-81 : s.n., 2005, The Journal of Membrane Biology 207, 169-181.

20. *An Update on the Structure of hERG.* **Butler, A., Helliwell, M. V., Zhang, Y., Hancox, J. C., Dempsey, C. E.** Front Pharmacol. 10: 1572 : s.n., 2020.

21. *The voltage-gated potassium channels and their relatives.* **G., Yellen.** Nature 419, 35-42 : s.n., 2002, Nature 419, 35-42.

22. *hERG potassium channels and cardiac arrhythmia.* **Sanguinetti, M., Tristani-Firouzi, M.** Nature 440, 463-469 : s.n., 2006, Nature 440, 463-469.

23. *Crystal Structure and Functional Analysis of the HERG Potassium Channel N Terminus: A Eukaryotic PAS Domain.* **Cabral, J. H. M, Lee, A., Cohen, S. L., Chait, B. T., Li, M., Mackinnon, R.** Cell 95 (5): 649-55 : s.n., 1998, Cell 95:649–655.

24. *Modulation of hERG K+ Channel Deactivation by Voltage Sensor Relaxation.* **Shi, Y. P., Thouta, S., Claydon, T. W.** Front Pharmacol 11:139 : s.n., 2020, Front. Pharmacol. 11:139.

25. *hERG Potassium Channel Regulation by the N-terminal eag Domain.* **Gustina, A. S., Trudeau, M. C.** Cell Signal 24 (8): 1592-1598 : s.n., 2012.

26. *hERG potassium channel gating is mediated by N- and C-terminal region interactions.* **Gustina, A. S., Trudeau, M. C.** Journal of Gen Physiol. 137 (3): 315-25 : s.n., 2011, J Gen Physiol. 137(3):315-325.

27. *The hERG potassium channel intrinsic ligand regulates N- and C-terminal interactions and channel closure.* **Codding, S. J, Trudeau, M. C.** Journal of Gen Physiol. 151 (4): 478-488 : s.n., 2019, J Gen Physiol. 151(4): 478-488.

28. *FRET with multiply labeled HERG K(+) channels as a reporter of the in vivo coarse architecture of the cytoplasmic domains.* **Miranda, P., Manso, D. G., Barros, F., Carretero, L., Hughes, T. E., Alonso-Ron, C., Dominguez, P., Pena, De la Pena, P.** Biochim Biophys Acta 1783 (10): 1681-99 : s.n., 2008.

29. *HERG, a human inward rectifier in the voltage-gated potassium channel.* **Trudeau, M. C., Warmke, J. W., Ganetzky, B., Robertson, G. A.** Science 269 (5220): 92-5 : s.n., 1995, Science 269:92-95.

30. *The inward rectification mechanism of the hERG cardiac potassium channel.* **Smith, P. L.. Baukrowitz, T., Yellen, G.** Nature 379 (6568): 833-6 : s.n., 1996, Nature 379, 833-836.

31. *HERG1 Channel Agonists and Cardiac Arrhythmia.* **Sanguinetti, M.** Curr Opin Pharmacol. 0: 22-27 : s.n., 2014, Curr Opin Pharmacol. 0:22-27.

32. *Interactions between S4-S5 linker and S6 transmembrane domain modulate gating of hERG K+ channels.* **Firouzi, M. T., Chen, J., Sanguinetti, M. C.** Journal Biol Chem. 277 (21): 18994-9000 : s.n., 2002, Biol Chem 277 (21): 18994-9000.

33. *Fast and Slow Voltage Sensor Movements in HERG Potassium Channels.* **Smith, P. L., Yellen, G.** Journal of Gen Physiol. 119 (3): 275-93 : s.n., 2002, Journal of General Physiology 119:275-293.

34. *Coupling between Voltage Senors and Activation Gate in Voltage-gated K+ Channels.* **Lu, Z., Klem, A. M., Ramu, Y.** Journal Gen Physiol. 120 (5): 663-676 : s.n., 2002, Journal of General Physiology 120:663-676.

35. *Structure-function studies of the outer mouth and voltage sensor domain of hERG.* **Tseng, G. N., Guy, H. R.** Novartis Found Symp. 266: 19-35 : s.n., 2005, Novartis Found Symp 266:19-35; discussion 35-45.

36. *Voltage sensor of Kv1.2: structural basis of electromechanical coupling.* **Long, S. B., Campbell, E. B., Mackinnon, R.** Science 309 (5736): 903-8 : s.n., 2005, Science 309(5736):903-908.

37. *Molecular determinants for activation and inactivation of HERG, a human inward rectifier potassium channel.* **Schönherr, R., Heinemann, S. H.** Journal of Physiol. 493.3, pp.635-642 : s.n., 1996, The Journal of Physiology 493:635-642.

38. *An intracellular hydrophobic nexus critical for hERG1 channel slow deactivation.* **Stevens-Sostre, W. A., Flores-Aldama, L., Bustos, D., Li, J., Morais-Cabral, J. H., Delemotte, L. Robertson, G. A.** Biophys J. 123 (14): 2024-2037 : s.n., 2024.

39. *hERG1 channel activators: A new antiarrhythmic principle.* **Grunnet, M., Hansen, R. S., Olesen, S. P.** Prog Biophys Mol Biol. 98 (2-3): 347-62 : s.n., 2008, ScienceDirect 98:347-362.

40. *Molecular Insights Into the Gating Kinetics of the Cardiac hERG Channel, Illuminated by Structure and Molecular Dynamics.* **Zequn, Z., Jiangfang, L.** Front. Pharmacol Vol. 12: 687007 : s.n., 2021.

41. *Negative Charges in the Transmembrane Domains of the HERG K+ Channel Are Involved in the Activation- and Deactivation-gating Processes.* **Liu, J., Zhang, M., Jiang, M., Tseng, G. N.** Journal of Gen Physiol. 121 (6): 599-614 : s.n., 2003, Journal of General Physiology 121:599-614.

42. *Mechanism for the effects of extracellular acidification on HERG-channel function.* **Jiang, M. Q., Jogini, V., Borhani, D. W., Leffler, A. E., Dror, R. O., Shaw, D. E.** Am J Physiol. 277 (4): H1283-92 : s.n., 1999, American Journal of Physiology-Heart and Circulatory Physiology 277:1283-1292.

43. *Extracellular protons accelerate hERG channel deactivation by destabilizing voltage sensor relaxation.* **Shi, Y. P., Thouta, S., Cheng, Y. M., Claydon, T. W.** Journal of Gen Physiol. 151 (2): 231-246 : s.n., 2019.

44. *Translational toxicology and rescue strategies of the hERG channel dysfunction: biochemical and molecular mechanistis aspects.* **Zhang, K. P., Yang, B. F., Li, B. X.** Acta Pharmacologica Sinica 35, 1473-1484 : s.n., 2014, Acta Pharmacologica Sinica 35: 1473-1484.

45. *N-linked glycosylation sites determine HERG channel surface membrane expression.* **Petrecca, K., Atanasiu, R., Akhavan, A., Shrier, A.** Journal of Physiol. 515 (Pt 1): 41-48 : s.n., 1999.

46. *Novel roles for hERG K+ channels in cell proliferation and apoptosis.* **Jehle, J., Schweizer, P.A., Katus, H.A., Thomas, D.** Cell Death Dis. 2 (8): e193 : s.n., 2011, Cell Death and Disease 2, e193.

47. *Developmental Basis for Electrophysiological Heterogeneity in the Ventricular and Outflow Tract Myocardium As a Substrate for Life-Threatening Ventricular Arrhythmias.* **Boukens, B. J. D., Christoffels, V. M., Coronel, R., Moorman, A. F. M.** Circ Res 104 (1): 19-31 : s.n., 2009, Circulation Research 104, no. 1: 19-31.

48. *Initiation of ventricular arrhythmia in the acquired long QT syndrome.* **Alexander, C., Bishop, M. J., Gilchrist, R. J., Burton, F. L., Smith, G. L., Myles, R. C.** Cardiovascular Research Vol. 119 (2): 465-476 : s.n., 2023.

49. *Spectrum of HERG K+ Channel Dysfunction in an Inherited Cardiac Arrhythmia.* **Sanguinetti, M. C., Curran, M. E., Spector, P. S., Keating, M. T.** Proc Natl Acad Sci U S A 93 (5): 2208-12 : s.n., 1996, Proceedings of the National Academy of Sciences 93, no. 5: 2208-12.

50. *Rescue of protein expression defects may not be enough to abolish the pro-arrhythmic phenotype of long QT type 2 mutations.* **Perry, M. D., Ng, C. A., Phan, K., David, E., Steer, K., Hunter, M. J., Mann, S. A., Imtiaz, M., Hill, A. P., Ke, Y., Vandenberg, J. I.** Journal of Physiol. 594 (14): 4031-4049 : s.n., 2016, The Journal of Physiology 594, no. 14: 4031-49.

51. *Genetics of Long QT Syndrome.* **Tester, D. J., Ackermann, M. J.** Methodist Debakey Cardiovasc J. 10 (1): 29-33 : s.n., 2014.

52. *A Structural Basis for Drug-induced Long QT Syndrome.* **Mitcheson, J. S., Chen, J., Lin, M., Culberson, C., Sanguinetti, M. C.** Proc Natl Acad Sci U S A 97 (22): 12329-33 : s.n., 2000, Proceedings of the National Academy of Sciences 97, no. 22: 12329-33.

53. *Interactions between S4-S5 Linker and S6 Transmembrane Domain Modulate Gating of HERG K+ Channels.* **Tristani-Firouzi, M., Chen, J., Sanguinetti, M. C.** Journal Biol Chem. 277 (21): 18994-9000 : s.n., 2002, Journal of Biological Chemistry, Vol. 277, Issue 21, P18994-19000.

54. *The ERG1 K+ Channel and Its Role in Neuronal Health and Disease.* **Sanchez-Conde, F. G., Jimenez-Vazquez, E. N., Auerbach, D. S., Jones, D. K.** Front Mol Neurosci. 15: 890368 : s.n., 2022, Front Mol Neurosci. 15: 890368.

55. *Molecular pathogenesis of long QT syndrome type 2.* **Smith, J. L., Anderson, C. L., Burgess, D. E., Elayi, C. S., January, C. T., Delisle, B. P.** Journal Arrhythm 32 (5): 373-380 : s.n., 2016, Journal of Arrhythmia 32:373-380.

56. *Long QT Syndrome Type 2: Emerging Strategies for Correcting Class 2 KCNH2 (hERG) Mutations and Identifying New Patients.* **Ono, M., Burgess, D. E., Schroder, E. A., Elayi, C. S., Anderson, C. L., January, C. T., Sun, B., Immadisetty, K., Kekenes-Huskey, P. M., Delisle, B. P.** Biomolecules 10 (8): 1144 : s.n., 2020, Biomolecules 10(8):1144.

57. *Sudden Death Associated With Short-QT Syndrome Linked to Mutations in HERG.* **Brugada, R., Hong, K., Dumaine, R., Cordeiro, J., Gaita, F., Borggrefe, M., Menendez, T., M., et al.** Circulation 109 (1): 30-5 : s.n., 2004, Circulation, Vol. 109, no. 1:30-35.

58. *Diagnosis and management of short QT syndrome.* **Bjerregaard, P.** Heart Rhythm 15 (8): 1261-1267 : s.n., 2018, Heart Rhythm 15:1261-1267.

59. *Metabolic and electrolyte abnormalities as risk factors in drug-induced long QT syndrome.* **TeBay, C., Hill, A. P., Windley, M. J.** Biophysical Reviews Vol. 14, 353-367 : s.n., 2022.

60. *Causes and management of drug-induced long QT syndrome.* **Ayad, R. F., Assar, M. D., Simpson, L., Garner, J. B., Schussler, J. M.** Proc (Bayl Univ Med Cent) 23 (3): 250-255 : s.n., 2010.

61. *Mechanism of block and identification of the verapamil binding domain to HERG potassium channels.* **Zhang, S., Zhou, Z., Gong, Q., Makielski, J. C., January, C. T.** Circ Res. 14; 84 (9): 989-98 : s.n., 1999.

62. *Acquired Long QT Syndrome and Electrophysiology of Torsade de Pointes.* **El-Sherif, N., Turitto, G., Boutjdir, M.** Arrhythm Electrophysiol Rev. 8 (2): 122-130 : s.n., 2019.

63. *The cardiac hERG/IKr potassium channel as pharmacological target: structure, function, regulation, and clinical applications.* **Thomas, D. A., Karle, C., Kiehn, J.** Current Pharmaceutical Design 12 (18): 2271-83 : s.n., 2006.

64. *Structural analysis of hERG channel blockers and the implications for drug design.* **AlRawashdeh, S., Chandrasekaran, S., Barakat, K. H.** Journal of Mol Graph Model. 120:108405 : s.n., 2023.

65. *The hERG channel activator, RPR260243, enhances protective Ikr current early in the refractory period reducing arrhythmogenicity in zebrafish hearts.* **Shi, Y. P, Pang, Z. K., Venkateshappa, R., Gunawan, M., Kemp, J., Truong, E., Chang, C., Lin, E., Shafaattalab, S., Faizi, S., Rayani, K., Tibbits, G. F., Claydon, V. E., Claydon, T. W.** Am J Physiol. Heart Circ Physiol. 319 (2): H251-H261 : s.n., 2020, American Journal of Physiology Vol. 319 (2): H251-H261.

66. *Binding of RPR260243 at the intracellular side of the hERG1 channel pore domain slows closure of the helix bundle crossing gate.* **Zangerl-Plessl, E. M., Wu, W., Sanguinetti, M. C., Stary-Weinzinger, A.** Front. Mol. Biosci. Vol. 10 : s.n., 2023, Journal Frontiers in Molecular Biosciences Vol. 10.

67. *Tg(Δ113p53:cmyc) Transgene Upregulates glut1 Expression to Promote Zebrafish Heart Regeneration.* **Tang, Z., Wang, K., Lo, L., Chen, J.** Journal Cardiovasc Dev Dis 10 (6): 246 : s.n., 2023.

68. *Discovery of a Small Molecule Activator of the Human Ether-a-go-go-Related Gene (HERG) Cardiac K+ Channel.* **Kang, J. Ji, J., Wang, H., Tabart, M.** Molecular Pharmacology 67 (3), 827-836 : s.n., 2005.

69. *Differential effects of ginsenoside metabolites on HERG k channel currents.* **Choi, S. H., Shin, T. J., Hwang, S. H., Lee, B. H., Kang, J., Kim, H. J., Oh, J. W., Bae., C. S., Lee, S. H., Nah, S. Y.** Journal Ginseng Res. 35 (2): 191-9 : https://creativecommons.org/licenses/by-nc/3.0/, 2011.

70. *Evaluation of glucosidases of Aspergillus niger strain comparing with other glucosidases in transformation of ginsenoside Rb1 to ginsenosides Rg3.* **Chang, K. H., Jo, M. N., Kim, K. T., Paik, H. D.** Journal of Ginseng Research Vol. 38, Issue 1, Pages 47-51 : s.n., 2014.

71. *Anticancer effects of ginsenoside Rg3.* **Sun, M., Ye, Y., Xiao, L., Duan, X., Zhang, Y., Zhang, H.** Int J Mol Med. 39 (3): 507-518 : s.n., 2017, International Journal of Molecular Medicine 39: 507-518.

72. *Ginsenoside Rg3 attenuates the osimertinib resistance by reducing the stemness of non-small cell lung cancer cells.* **Tan, Q., Lin, S., Zeng, Y., Yao, M., Liu, K., Yuan, H., Liu, C., Jiang, G.** Environ Toxicol. 35 (6): 643-651 : s.n., 2020.

73. *Ginsenoside Rg3 Reduces Epithelial-Mesenchymal Transition Induced by Transforming Growth Factor-β1 by Inactivation of AKT in HMrSV5 Peritoneal Mesothelial Cells.* **Yan, X., Zhang, W., Kong, F., Li, Q., Shan, W., Zhang, C., Han, T., Che, Y., Zhang, Y.** Med Sci Monit 25: 6972-6979 : s.n., 2019.

74. *Antiobesity effect of ginsenoside Rg3 involves the AMPK and PPAR-γ signal pathways.* **Hwang, J. T., Lee, M. S., Kim, H. J., Sung, M. J., Kim, H. Y., Kim, M. S., Kwon, D. Y.** Phytotherapy Research, Vol. 23, Issue 2, p. 262-266 : s.n., 2008.

75. *Effects of R type and S type ginsenoside Rg3 on DNA methylation in human hepatocarcinoma cells.* **Teng, S., Wang, Y., Li, P., Liu, J., Wei, A., Wang, H., Meng, X., Pan, D., Zhang, X.** Mol Med Rep. 15 (4): 2029-2038 : s.n., 2017.

76. *Ginsenoside Rg3 inhibits the senescence of prostate stromal cells through down-regulation of interleukin 8 expression.* **Peng, Y., Zhang, R., Kong, L., Shen, Y., Xu, D., Zheng, F., Liu, J., Wu, Q., Jia, B., Zhang, J.** Oncotarget 8 (39): 64779-64792 : s.n., 2017.

77. *A new hERG allosteric modulator rescues genetic and drug-induced long-QT syndrome phenotypes in cardiomyocytes from isogenic pairs of patient induced pluripotent stem cells.* **Sala, L., Yu, Z., Oostwaard, D. W., Veldhoven, J., Moretti, A., Laugwitz, K. L., Mummery, C. L., Ijerzman, A. P., Bellin, M.** EMBO Mol Med 8 (9): 1065-81 : s.n., 2016, EMBO Mol Med. 8 (9): 1065-1081.

78. *LUF7244 an allosteric modulator/activator of Kv11.1 channels, counteracts dofetilide-induced torsades de pointes arrhythmia in the chronic atrioventricular block dog model.* **Qile, M., Beekman, H. D. M., Sprenkeler, D. J., Houtman, M. J. C., Ham, W. B., Stary-Weinzinger, A.., Beyl, S., Hering, S., Van den Berg, D. J., Lange, E. C. M., Heitman, L. H., Ijerzman, A. P., Vos, M. A., Van der Heyden, M. A. G.** Br J Pharmacol. 176 (19): 3871-3885 : s.n., 2019.

79. *ICA-105574 interact with a common binding site to elicit opposite effects on inactivation gating of EAG and ERG potassium channels.* **Garg, V., Stary-Weinzinger, A., Sanguinetti, M. C.** Mol Pharmacol. 83 (4): 805-13 : s.n., 2013.

80. *Effects of an hERG Activator, ICA-105574, on Electrophysiological Properties of Canine Hearts.* **Asayama, M., Kurokawa, J., Shirakawa, K., Okuyama, H., Kagawa, T., Okada, J. I., Sugiura, S., Hisada, T., Furukawa, T.** Journal Pharmacol Sci 121, 1-8 : s.n., 2013.

81. *Characterization of A-935142, a hERG enhancer, in the presence and absence of standard hERG blockers.* **Liu, X., Limberis, J. T., Su, Z., Houseman, K., Diaz, G. J., Gintant, G. A., Cox, B. F., Martin, R. L.** Life Sci. 90 (15-16): 607-11 : s.n., 2012.

82. *The impact of uncertainty in hERG binding mechanism on in silico predictions of drug-induced proarrhythmic risk.* **Lei, C. L., Whittaker, D. G., Mirams, G. R.** Br. J. Pharmacol. Vol. 181 (7): 987-1004 : s.n., 2023.

83. *Pharmacological and electrophysiological characterization of AZSMO-23, an activator of the hERG K+ channel.* **Mannikko, R., Bridgland-Taylor, M. H.,**

Pye, H., Swallow, S., Abi-Gerges, N., Morton, M. J., Pollard, C. E. British Journal of Pharmacology 172 (12): 3112-3125 : s.n., 2015.

84. *Toward a Structural View of hERG Activation by the Small-Molecule Activator ICA-105574.* **Zangerl-Plessl, E. M., Berger, M., Drescher, M., Chen, Y., Wu, W., Maulide, N., Sanguinetti, M., Stary-Weinzinger, A.** J. Chem. Inf. Model. 60, 1, 360-371 : s.n., 2020.

85. *Pharmacological and electrophysiological characterization of AZSMO-23, an activator of the hERG K(+) channel.* **Mannikko, R., Bridgland-Taylor, M. H., Pye, H., Swallow, S., Abi-Gerges, N., Morton, M. J., Pollard, C. E.** British Journal of Pharmacol. 172 (12): 3112-25 : s.n., 2015.

86. *Mallotoxin is a novel human ether-a-go-go-related gene (hERG) potassium channel activator.* **Zeng, H., Lozinskaya, I. M., Lin, Z., Willette, R. N., Brooks, D. P., Xu, X.** Jorunal Pharamcol Exp Ther. 19 (2): 957-62 : s.n., 2006.

87. *Discovery and electrophysiological characterization of SKF-32802: A novel hERG agonist found through a large-scale structural similarity search.* **Donovan, B. T., Bandyopadhyay, D., Duraiswami, C., Nixon, C. J., Townsend, C. Y., Martens, S. F.** Eur Journal Pharmacol 818:306-327 : s.n., 2018.

88. *The amiodarone derivative KB130015 activates hERG1 potassium channels via a novel mechanism.* **Gessner, G., Macianskiene, R., Starkus, J. G., Schönherr, R., Heinemann, S. H.** Eur J Pharmacol. 632 (1-3): 52-59 : s.n., 2010.

89. *Pharmacologic Approach to Defective Protein Trafficking in the E637K-hERG Mutant with PD-118057 and Thapsigargin.* **Mao, H., Lu, X., Karush, J. M., Huang, X., Yang, X., Ba, Y., Wang, Y., Liu, N., Zhou, J., Lian, J.** PLoS ONE 8(6): e65481 : s.n., 2013.

90. *Potassium dependent structural changes in the selectivity filter of hERG potassium channels.* **Lau, C. H. Y., Flood, E., Hunter, M. J., Williams-Noonan, B. J., Corbett, K. M., Ng, C. A., Bouwer, J. C., Stewart, A. G., Perozo, E., Allen, T. W., Vandenberg, J. I.** Nature Communication 15, Article number: 7470 : s.n., 2024.

91. *Cryo-EM Structure of K+-Bound hERG Channel Complexed with the Blocker Astemizole.* **Asai, T., Adachi, N., Moriya, T., Oki, H., Maru, T., Kawasaki, M., Suzuki, K., Chen, S., Ishii, R., Yonemori, K., Igaki, S., Yasuda, S., Ogasawara, S., Senda, T., Murata, T.** Structure, Volume 29, Issue 3, 203-212.e4 : s.n., 2021.

92. *Improved higher resolution cryo-EM structures reveal the binding modes of hERG channel inhibitors.* **Miyashita, Y., Moriya, T., Kato, T., Kawasaki, M., Yasuda, S., Adachi, N., Suzuki, K., Ogasawara, S., Saito, T., Senda, T., Murata, T.** Structure, Volume 0, Issue 0 : s.n., 2024.

93. **(CCDC), Cambridge Crystallographic Data Centre.** Cambridge Crystallographic Data Centre (CCDC). [Online] [Cited: October 01, 2024.] https://www.ccdc.cam.ac.uk/.

94. *Targeting the Kv11.1 (hERG) channel with allosteric modulators. Synthesis and biological evaluation of three novel series of LUF7346 derivatives.* **Veldhoven, J. P. D., Campostrini, G., Gessel, C. J. E., Oostwaard, D. W., Liu, R., Mummery, C. L., Bellin, M., Ijzerman, A. P.** European Journal of Medicinal Chemistry Vol. 212, 113033 : s.n., 2021.

95. *Biophysical Characterization of the New Human Ether-A-Go-Go-Related Gene Channel Opener NS3623 [N-(4-Bromo-2-(1H-tetrazol-5-yl)-phenyl)-N'-(3'-trifluoromethylphenyl)urea].* **Hansen, R. S., Diness, T. G., Christ, T., Wettwer, E.** Molecular Pharmacology 70 (4): 1319-29 : s.n., 2006.

96. **Kemp, J. M., Whittaker, D. G., Venkateshappa, R., Pang, Z., Johal, R., Sergeev, V., Tibbits, G. F., Mirams, G. R., Claydon, T. W.** *Electrophysiological characterization of the hERG R56Q LQTS variant and targeted rescue by the activator RPR260243.* 2021 : s.n., Journal of Gen Physiol. 153 (10): e202112923.

97. *Excellent response to β-1 adrenergic receptor blockade (metoprolol) and exercise restriction in high-risk type 1 long QT syndrome. A 22-year follow up.* **Tejeda-Mollinedo, W., Diaz-Tostado, S., Gomez-Flores, J., Nava-Townsend, S., Levinstein-Jacinto, M., Marquez, M. F.** HeartRhythm Case Report, Vol. 8, Issue 3, P191-194 : s.n., 2022.

98. *Structural implications of hERG K+ channel block by a high-affinity minimally structured blocker.* **Helliwell, M. V., Zhang, Y., Harchi, A. E., Du, C., Hancox, J. C., Dempsey, C. E.** J Biol Chem 293 (18): 7040-7057 : s.n., 2017.

99. *Structural determinants for high-affinity block of hERG potassium channels.* **Mitcheson, J., Perry, M., Stansfeld, P., Sanguinetti, M. C., Witchel, H., Hancox, J.** Novartis Found Symp 266:136-150; discussion 150-138 : s.n., 2005.

100. *Molecular determinant of high-affinity dofetilide binding to HERG1 expressed in Xenopus oocytes: involvement of S6 sites.* **Lees-Miller, J. P., Duan, Y., Teng, G. Q., Duff, H. J.** Mol Pharmacol 57 (2): 367-374 : s.n., 2000.

101. *Open channel block of HERG K+ channels by vesnarinone.* **Kamiya, K., Mitcheson, J. S., Yasui, K., Kodama, I., Sanguinetti, M. C.** Mol Pharmacol 60 (2): 244-253 : s.n.

102. *Structural modeling of the hERG potassium channel and associated drug interactions.* **Maly, J., Emigh, A. M., DeMarco, K. R., Furutani, K., Sack, J. T., Clancy, C. E., Vorobyov, I., Yarov-Yarovoy, V.** Front. Pharmacol. Vol. 13 : s.n., 2022.

103. *Stereoselective Inhibition of the hERG1 Potassium Channel.* **Grilo, L. S., Carrupt, P. A., Abriel, H.** Front Pharmacol. 1:137 : s.n., 2010.

104. *hERG toxicity assessment: Useful guidelines for drug design.* **Garrido, A., Lepailleur, A., Mignani, S. M., Dallemagne, P., Rochais,C.** HAL open science : s.n., 2022.

105. *The impact of uncertainty in hERG binding mechanism on in silico predictions of drug-induced proarrhythmic risk.* **Lei, C. L., Whittaker, D. G., Mirams, G. R.** British Journal of Pharmacology Vol. 181, Issue 7, p. 987-1004 : s.n., 2023.